THE UNIVERSITY
of EDINBURGH

Investigating the Role of Interferon—γ Signalling for Malaria Dyserythropoiesis

Eze Nwoke

A thesis submitted for the degree of

Doctor of Philosophy—Immunology and Infection Research

University of Edinburgh

August 2019

History merely repeats itself. Nothing is truly new; it has all been done or said before. What can you point to that is new? How do you know it didn't exist long ages ago? We don't remember what happened in those former times, and in the future generations no one will remember what we have done back here.

Ecclesiastes 1:9-11 (TLB)

Abstract

In innate and adaptive immunity, the proinflammatory type 1 cytokine interferon gamma (IFN-γ), is well known for its protective role particularly against intracellular pathogens. However, this type 2 interferon has been implicated in the pathology of several diseases. In malaria, it has been demonstrated that IFN-γ exerts both protective and pathological roles. In humans and in mouse models, the acute infection results in aberrant erythroid differentiation termed dyserythropoiesis which contributes to the development of severe malarial anaemia. The mechanism that drives this process is poorly understood. However, recent data from our lab suggests a role for IFN-γ as the one candidate to mediate the manifestation of early dyserythropoiesis. This study aimed to determine the stages of erythropoiesis in the bone marrow (BM) and spleen that are perturbed by malaria, and investigate if IFN-γ signalling in the haematopoietic compartment alone, is sufficient to promote suppression of erythropoiesis during malaria.

To address the first aim, I used three murine models of experimental malaria which differ in virulence, parasite burden, proinflammatory cytokine induction and elicited immune response. In all malaria models, I observed an expansion of the erythroid progenitors in the bone marrow and spleen, nevertheless, this expansion failed to reflect in the number of downstream precursors. Early in infection, there was no change in the absolute number of erythroid precursors in infected mice, in comparison to naive gender and age matched controls, but at peak parasitaemia at the time points sampled, there was a significant contraction in the number of all erythroid precursor stages, from the proerythroblast to the orthochromatic erythroblast. Furthermore, I observed that this aberration of erythropoiesis in the BM and spleen manifests independently of the degree of peripheral parasite burden, suggesting a role for proinflammatory cytokines, in particular, IFN-γ in mediating this process.

To further decipher the role of IFN-γ for malaria dyserythropoiesis, I made use of the *Vav1::iCre/Ifngr2*$^{fl/fl}$ mice, which are deficient in IFN-γ signalling specifically in haematopoietic cells. I observed that the absolute number of BM lineage negative

(LIN$^-$) cells, erythroid progenitors and erythroid precursors was significantly higher in *Vav1::iCre/Ifngr2*$^{fl/fl}$ mice, in comparison to control mice. Interestingly, the absolute number of basophilic and polychromatic erythroblasts in infected *Vav1::iCre/Ifngr2*$^{fl/fl}$ mice was significantly higher than in naive mice which was not the case for infected control mice.

Based on these observations, my results suggest that IFN-γ plays a key role in malaria dyserythropoiesis by inhibiting the expansion and differentiation of erythroid progenitors and precursors, through a direct signalling in haematopoietic cells. In this study, I have demonstrated a novel and unpublished method for the identification and isolation of erythroid progenitor subsets at high purity and showed for the first time in an *in vivo* setting, that IFN-γ signalling in the haematopoietic compartment alone is crucial for malaria dyserythropoiesis.

Lay summary

Malaria is a disease that kills more than 400,000 people annually (1). The malaria parasite multiplies in red blood cells and destroys these cells. It has been reported that people who have malaria are not able to produce sufficient red blood cells to replace the ones that are being destroyed by the parasite. This is because their bone marrow (BM), which is where the production of red blood cells occurs, has problems in producing new cells. People with this condition could become severely anaemic.

There are cells in the body that produce a protein called interferon gamma which helps other cells fight the malaria parasite. Several studies have demonstrated that interferon gamma can suppress the production of red blood cells in the BM. This production of red blood cells in the bone marrow occurs in several stages beginning with the immature haematopoietic stem cell, which develops through a series of intermediate cells to give rise to mature red blood cells in a process called erythropoiesis. This process is divided into early and terminal erythropoiesis.

In my thesis, I investigated what stages of red blood cell production are affected by malaria. At early time points during experimental malaria in mouse, I observed an increase in the number of cells involved in early erythropoiesis, and a contraction in the number of cells involved in terminal erythropoiesis. This indicated a block in erythropoiesis that is, the cells at the early stage were not developing to become the cells at the terminal stage.

To understand if interferon-gamma might be responsible for this, I performed experiments in mice that contain a unique class of cells which do not respond to the protein. I observed that when I infected these mice with the malaria parasite, the number of cells involved in early and terminal erythropoiesis was higher than in infected mice in which all the cells could respond to interferon gamma. Interestingly, I observed that the number of some of the cells involved in terminal erythropoiesis was significantly higher in infected mice that do not respond to interferon gamma, than in mice that did not have malaria.

These observations suggest that interferon-gamma plays a role in preventing sufficient production of red blood cells during malaria, by preventing early-stage erythroid cells from developing to red blood cells. It does this by acting on a unique class of cells in the BM, the haematopoietic cells.

Acknowledgements

My sincere gratitude goes to my primary supervisor Dr. Alexandre Potocnik for the opportunity to do a PhD in his lab. I thank Prof. Alexandra Rowe, for her support and guidance throughout my PhD, ensuring all experiments proceeded as planned. I am particularly grateful to my committee members Dr Joanne and Prof. Rose Zamoyska for their constructive input during my PhD.

I am thankful to Kasia Gawron, Ed Marr and the BVS staff, especially Craig Watt, Christopher Flockhart, Lynn, Jamie and David for all the training and assistance you provided during my PhD. I would like to thank Dr. Dietmar Zaiss in particular, for accommodating my project needs, without your help, the animal experiments in genetically engineered mice would not have been possible.

I am highly indebted to Sir Kenneth Murray and the Darwin Trust of Edinburgh for funding my PhD and taking care of my living costs. I am grateful to the Spence laboratory for providing the malaria parasite strain used in this study. To my African colleagues at the university of Edinburgh, thank you for all your support and friendship.

To my family, who have always been there for me: I am grateful in more ways than I can express for your support and encouragement over the years**.** To Anne and Richard, you demonstrated that one does not have to be related by blood to be family, thank you for your support and care. To my sisters, Chioma and Amarachi, thank you for your love, understanding and words of wisdom. To my mum, you're the reason I am the man I am today. To my late dad, thank you for raising a champion. To my partner and best friend Fiona, thank you for your unwavering love, support and understanding, you light up my world.

Finally, to the one who sits on the throne, my King and father, thank you for this life.

Abbreviations

^{0}C	Degree Celsius
bp	Base pair
BM	Bone marrow
BFU—e	Burst forming unit erythroid
CD	Cluster of differentiation
CFU-e	Colony forming unit erythroid
CI	Confidence interval
CLP	Common lymphoid progenitor
CMP	Common myeloid progenitor
DC	Dendritic cell
DNA	Deoxyribonucleic acid
dNTP	deoxyribonucleotide triphosphate
DPI	Days post-infection
EDTA	Ethylenediaminetetraacetic acid
EKLF/KLF1	Erythroid Kruppel-like factor
ELISA	Enzyme-Linked Immunosorbent assay
EpoR	Erythropoietin receptor
ETP	Early thymic progenitor
FACS	Fluorescence Activated Cell Sorting

Fc	Fragment crystallisable
FITC	Fluorescein isothiocyanate
fl	Floxed
FSC-A	Forward scatter area
FSC-W	Forward scatter width
g (rcf)	Relative centrifugal force
g/dL	Gram per decilitre
GAS	Gamma activated sequence
GM	Granulocyte-macrophage
GMP	Granulocyte-macrophage progenitor
h	Hour
HPC	Haematopoietic progenitor cell
HRP	Horseradish peroxidase
HSC	Haematopoietic stem cell
HSPC	Haematopoietic stem and progenitor cell
i.p	Intraperitoneal
i.v	Intravenous
IFN-γ	Interferon gamma
IFN-γR	Interferon gamma receptor
IL	Interleukin
IRF1	Interferon regulatory factor 1

JAK1	Janus-activated kinase 1
JAK2	Janus-activated Kinase 2
KSG	Krebs saline with glucose
KO	Knock out
LT-HSC	Long term haematopoietic stem cells
LIN$^-$	Lineage negative
M	Molar
mAb	Monoclonal antibody
MACS	Magnetic-activated cell sorting
MEP	Megakaryocyte-erythroid progenitor
MIF	Macrophage migration inhibitory factor
miRNA	MicroRNA
mL	Millilitre
mM	millimolar
MPP	Multipotent progenitor
ng	Nanograms
NK cells	Natural Killer cells
ns	not significant
ND	Not detectable
p.i	Post-infection
PCR	Polymerase Chain Reaction

pmol	Picomoles
pg	Picogram
RBC	Red Blood Cells
rpm	Revolutions per minute
Sca-1	Stem cell antigen—1
SCF	Stem cell factor
SD	Standard deviation
SEM	Standard error of mean
SLAM	Signalling lymphocytic activation molecule
SMA	Severe Malarial Anaemia
SOCS1	Suppressor of cytokine signalling 1
SSC-A	Side scatter area
ST-HSC	Short term haematopoietic stem cells
STAT1	Signal transducer and activator of transcription 1
TMB	3,3',5,5'-Tetramethylbenzindine
TNF-α	Tumor Necrosis Factor alpha
µg/mL	Micrograms Per Millilitre
µL	Microlitre
WT	Wildtype

List of figures and tables

Table of Contents xv
Figure 1.1 The revised model of steady state haematopoiesis 6
Figure 1.2 Scheme of bone marrow erythropoiesis in steady state 10
Figure1.3 Life cycle of *Plasmodium* parasite in the mosquito and vertebrate hosts 14
Figure 1.4 The IFN- γ receptor and its signalling 20
Figure 1.5 Assembly of IFN-γR2 on cell surface 21
Figure 2.1 PCR for *lox-p* flanked alleles and *Cre* expression 31
Figure 3.1 Haematopoietic progenitor cells in steady state 36
Figure 3.2 CD150, CD27 and CD135 surface expression reveals phenotypic heterogeneity of early BM haematopoietic progenitor cells 42
Figure 3.3 Analysis of $CD150^{+}$ $CD27^{int}$ and $CD150^{-}$ $CD27^{-}$HPC subsets before and after FACS purification 44
Figure 3.4 Lineage commitment fate of $CD150^{+}$ $CD27^{-}$ and $CD150^{-}$ $CD27^{-}$ HPC subsets in vitro 45
Figure 3.5 Characterisation of BM erythroid precursors in steady state 48
Figure 3.6 Quantitation of erythroid progenitors and precursors in murine BM in steady state… 50
Figure 4.1 Contraction of BM cellularity and increase in splenic cellularity during acute malaria infection 59
Figure 4.2 Infection induced upregulation of Sca-1 on HPCs 61
Figure 4.3. Identification of erythroid and myeloid progenitors during malaria 62
Figure 4.4 Infection induced expansion of erythroid progenitors and contraction of myeloid progenitors in three malaria models 64
Figure 4.5 Infection induced increase in number of MEP analogue in spleen of mice with *P. c. chabaudi* AS malaria 66
Figure 4.6 Contraction of erythroid precursors in BM of mice infected with *P. c. chabaudi* AS 69
Figure 4.7 Absence of increased extramedullary erythropoiesis during *P. c. chabaudi* malaria 71
Figure 4.8 Kinetics of IFN-γ and TNF-α during *P. c. chabaudi* AS malaria 72

Figure 5.1 *Vav1::iCre/Ifngr2*$^{fl/fl}$, *Ifngr2*$^{fl/fl}$ and *Vav1::iCre* mice exhibit no difference in absolute number of HPC subsets in steady state 80
Figure 5.2 *Vav1::iCre/Ifngr2*$^{fl/fl}$ mice do not upregulate Sca-1 during malaria.....81
Figure 5.3 IFN-γ signalling in haematopoietic cells is crucial for malaria parasite control…… 83
Figure 5.4 Loss of LIN$^-$ BM cells during *P. chabaudi* malaria is dependent on IFN-γ signalling in haematopoietic cells 85
Figure 5.5 Suppression of erythroid progenitor expansion in the BM during malaria is dependent on IFN-γ signalling in haematopoietic cells.....88
Figure 5.6 Contraction of erythroid precursors in the BM during malaria is dependent on IFN-γ signalling in haematopoietic cells 91
Figure 5.7 Contraction of erythroid precursors in the spleen during malaria is dependent on IFN-γ signalling in haematopoietic cells 95
Table 2.1 mAb clones and suppliers……33
Table 2.2 Primer sequences……..……..34
Table 3.1 CD150$^+$ CD27^{int} HPC is a direct precursor of CD150$^-$CD27$^-$HPC……45
Table 3.2 CD150$^-$CD27$^-$ HPC differentiate to Ter119$^+$ erythroblasts *in vitro*…… 46

Table of Contents

Declaration ii

Abstract iv

Lay summary vi

Acknowledgements viii

Abbreviations ix

List of figures and tables xiii

CHAPTER 1 1

1.1 HAEMATOPOIESIS 2

1.1.1 STEADY STATE HAEMATOPOIESIS 3

1.1.2 ERYTHROID PROGENITORS AND PRECURSORS 6

1.1.3 KEY REGULATORS OF ERYTHROPOIESIS. 8

1.1.4 STRESS INDUCED HAEMATOPOIESIS 10

1.2 MALARIA 12

1.2.1 THE BIOLOGY OF PLASMODIUM PARASITES 13

1.2.2 CLINICAL SYNDROMES OF SEVERE MALARIA 14

1.2.3 DYSERYTHROPOIESIS IN MALARIA 17

1.3 MECHANISMS OF ERYTHROPOIESIS INHIBITION BY IFN-γ 18

1.4 AIMS OF THE STUDY 22

CHAPTER 2 23

2.1 MICE 24

2.2 INFECTION MODELS 24

2.2.1 SERIAL BLOOD PASSAGE MODEL 24

2.2.2 MOSQUITO TRANSMISSION MODEL 25

2.2.3 SPOROZOITE INOCULATION MODEL 25

2.3 PREPARATION OF SINGLE CELL SUSPENSION 26

2.4 PHYSICAL DEPLETION OF LINEAGE POSITIVE BONE MARROW CELLS. 26
2.5 PREPARATIVE AND ANALYTICAL FLOW CYTOMETRY 27
2.6 ELECTRONIC EXCLUSION OF LINEAGE POSITIVE CELLS 27
2.7 *IN VITRO* ERYTHROID DIFFERENTIATION ASSAY 27
2.8 BLOOD COLLECTION AND SERUM PREPARATION 28
2.9 ENZYME LINKED IMMUNOSORBENT ASSAY (ELISA) 28
2.10 DNA EXTRACTION 28
2.11 POLYMERASE CHAIN REACTION (PCR) 29
2.12 SCREENING FOR *LOX-P (LOCUS OF CROSSOVER IN PHAGE P1)*-FLANKED ALLELES AND *CRE* EXPRESSION 29
2.13 STATISTICAL ANALYSIS 32

CHAPTER 3 35

3.1 INTRODUCTION 36
3.2 DEFINING HAEMATOPOIETIC PROGENITORS IN THE ADULT BM IN STEADY STATE 37
3.3 ANALYSIS OF THE FUNCTIONAL POTENTIAL OF $CD150^{+}$ $CD27^{INT}$ AND $CD150^{-}CD27^{-}$ HPCS 42
3.4 DEFINING ERYTHROID PRECURSORS IN THE ADULT BM IN STEADY STATE 46
3.5 QUANTITATION OF HAEMATOPOIETIC PROGENITOR CELLS AND ERYTHROID PRECURSORS IN STEADY STATE 49
3.6 DISCUSSION 51

CHAPTER 4 54

4.1 INTRODUCTION 55
4.2 IMPACT OF ACUTE MALARIA INFECTION ON BM AND SPLENIC CELLULARITY 56
4.3 CHANGES IN BM HAEMATOPOIETIC PROGENITOR CELL POOL IN BM AND SPLEENS OF MICE WITH *P. C. CHABAUDI* AS MALARIA 59
4.4 CHANGES IN ERYTHROID PRECURSORS IN BM AND SPLEEN OF MICE WITH *P. CHABAUDI* MALARIA 66
4.5 SERUM LEVELS OF PROINFLAMMATORY CYTOKINES POTENTIALLY MEDIATING DYSERYTHROPOIESIS 72
4.6 DISCUSSION 73
4.7 CONCLUSION 76

CHAPTER 5 77

5.1 INTRODUCTION 78
5.2 ABLATION OF IFN-γ SIGNALLING IN HAEMATOPOIETIC CELLS DOES NOT ALTER THE NUMBER OF ERYTHROID AND MYELOID PROGENITORS IN STEADY STATE 79

5.3 UPREGULATION OF SCA-1 ON HPCS DURING MALARIA IS DIRECTLY DEPENDENT ON IFN-γ SIGNALLING IN HAEMATOPOIETIC CELLS 80

5.4 IFN-γ SIGNALLING IN HAEMATOPOIETIC CELLS IS CRUCIAL FOR MALARIA PARASITE CONTROL 82

5.5 CONTRACTION OF LINEAGE NEGATIVE BONE MARROW CELLS DURING ACUTE MALARIA IS DEPENDENT ON IFN-γ SIGNALLING IN HAEMATOPOIETIC CELLS. 83

5.6 IFN-γ SIGNALLING IN HAEMATOPOIETIC CELLS IS CRUCIAL FOR MALARIA DYSERYTHROPOIESIS IN BONE MARROW AND SPLEEN 85

5.7 DISCUSSION 95

5.6 CONCLUSION 97

CHAPTER 6 99

6.1 STEADY STATE ERYTHROPOIESIS 101

6.2 ERYTHROID DEVELOPMENT DURING MALARIA 102

6.3 ERYTHROID DEVELOPMENT DURING MALARIA IN TISSUE SPECIFIC ABSENCE OF IFN-γ SIGNALLING. 103

6.4 FUTURE DIRECTION 105

Appendix A: *Ifngr2*$^{wt/wt}$ locus 107

Appendix B: *Ifngr2*$^{fl/fl}$ locus 108

BIBLIOGRAPHY 109

CHAPTER 1

INTRODUCTION

1.1 Haematopoiesis

The advancement of single cell technologies in the past decades, and identification of novel cell surface markers have facilitated the study and understanding of mammalian haematopoiesis. Multiparameter flow cytometry and cell sorting, *in vitro* and *in vivo* clonal assays for haematopoietic stem and progenitor cell functions and single cell sequencing, together have allowed the systematic functional characterisation and transcriptional profiling of rare and highly purified cells (2). Furthermore, the use of conditional gene deletion technologies has permitted lineage specific approach in studying various aspects of haematopoiesis in steady state, and under inflammatory conditions.

Haematopoiesis, the step-wise process by which blood cells are formed, has been studied extensively for over a century. Haematopoietic cells were first detected in the aorta of the developing pig more than 80 years ago (3). Haematopoiesis is highly conserved in vertebrates and most of our knowledge of this process has come from the use of various animal models, such as the mouse and zebrafish. Haematopoiesis occurs in two sequential waves which can be divided into primitive and definitive haematopoiesis.

In primitive haematopoiesis which occurs in the yolk sac, the haemangioblast gives rise to myeloid cells and primitive erythrocytes via an erythroid progenitor intermediate (4). The primitive wave is transitory and its primary aim is to generate erythrocytes to facilitate tissue oxygenation for the rapidly developing embryo (3). This wave is characterised by the production of large nucleated erythrocytes that express embryonic globins. The switch from primitive to definitive haematopoiesis coincides with the switch of the principal site of haematopoiesis from the yolk sac to the foetal liver. During the definitive wave in humans, haematopoietic stem cells arise in the aorta-gonad-mesonephros (AGM) then seed the foetal liver and bone marrow (BM), generating all blood lineages (5).

The BM, the principal site of definitive haematopoiesis in adults, has a central role in maintaining immune homeostasis, and being able to generate and mobilise immune cells in response to infection is one of its pivotal function. Haematopoiesis is a tightly

regulated process, which is under the control of several transcription factors and haematopoietic cytokines. Microbial infection can result in the production of systemic cytokines such as type I and type II interferons at distal sites that could cause profound changes in the BM, resulting in aberrant haematopoiesis (6).

1.1.1 Steady state haematopoiesis

Haematopoiesis is a complex but well-ordered process in which long term repopulating haematopoietic stem cells (LT-HSCs) proliferate (self-renew) and differentiate to give rise to all mature blood cell lineages via intermediate progenitor populations. Under normal physiological conditions, this process occurs primarily in the BM of an adult organism.

Transplantation studies in mice have shown that a single LT-HSC is able to reconstitute and maintain all haematopoietic lineages in lethally irradiated mice throughout their life-time. Under homeostatic conditions, LT-HSCs are thought to be largely quiescent (7–10). Quiescence has been postulated to prevent HSCs from exhaustion (7) and to protect against the acquisition of mutations (11). LT-HSCs are rare cells and in mice constitute ~ 0.005% of BM mononuclear cells. Their location at the apex of the haematopoietic hierarchy and their ability for indefinite self-renewal and multilineage differentiation makes these cells the foundation pillars of haematopoiesis.

Akashi *et al*. proposed a model describing this multilineage differentiation of LTHSC to terminally differentiated blood cells in what is now known as the “classical” model of haematopoiesis (12). Since then, several alternative models of haematopoiesis have been proposed using different surface markers and techniques, and to date, there exists no general consensus on the “true” model of haematopoiesis.

In the classical model of haematopoiesis, LTHSCs differentiate first into highly proliferative short-term repopulating HSCs (STHSCs). Both the LTHSCs and STHSCs express the tyrosine kinase receptor c-Kit (CD117) and the membrane glycoprotein stem cell antigen 1 (Sca-1), but are lineage negative (LIN^-), that is, they lack markers of terminal differentiation (CD4, CD8, CD11c, CD11b, CD19, B220, Gr1, NK1.1 and

Ter119). Despite these cells being part of the LIN^- $Sca1^+$ c-Kit^{hi} (LSK) fraction of the BM, the STHSCs differ from the LTHSCs both functionally and phenotypically. STHSCs are capable of limited self-renewal and short-term reconstitution of lethally irradiated recipients. In mice, STHSCs also express the cell surface marker CD34 which is absent on LTHSCs (13). Oguro and colleagues showed that LTHSC (HSC1) are $CD229^{-/low}$ whereas STHSC (HSC2) are $CD229^+$(10). No single specific marker is known by which HSCs can be identified. Kiel *et al*. (14) demonstrated that single HSCs (LSK, $CD150^+$, $CD48^-$) competitively reconstituted into irradiated mice gave rise to long term reconstitution whereas HSCs isolated as LSK $Thy1^{lo}$ did not. In conjunction with the LSK definition, LTHSCs are identified by four members of the signalling lymphocytic activation molecule (SLAM) family namely, SLAMF1 (CD150), SLAMF2 (CD48), SLAMF3 (CD229) and SLAMF4 (CD244) and are LSK $CD150^+$, $CD48^-$ $CD229^{-/low}$ $CD244^-$ (10).

STHSCs irreversibly lose their self-renewal potential, giving rise to a population termed multipotent progenitors (MPPs) (15). MPPs are also part of the LSK fraction of the BM. Expression of CD135 in MPPs is associated with loss of long term myeloid reconstituting potential (16). A recent model of haematopoiesis shows that STHSCs also branch out early to give rise to the megakaryocytic/erythroid pathways via an intermediate population termed pre-MEP (17). The pre-MEP undergoes further differentiation steps to give rise to platelets and erythrocytes via several intermediate progenitor populations.

Several subsets of MPPs have been described in the literature, with each subset exhibiting some bias towards specific lineage commitments (15,18). In general, MPPs irreversibly commit to three differentiation pathways namely the myeloid pathway via the common myeloid progenitor, the lymphoid pathway via the common lymphoid progenitor and the megakaryocytic/erythroid pathway via the pre-MEP (15). The myeloid pathway gives rise to granulocytes, monocytes and dendritic cells, while the lymphoid pathway gives rise to B cells and NK cells in the BM.

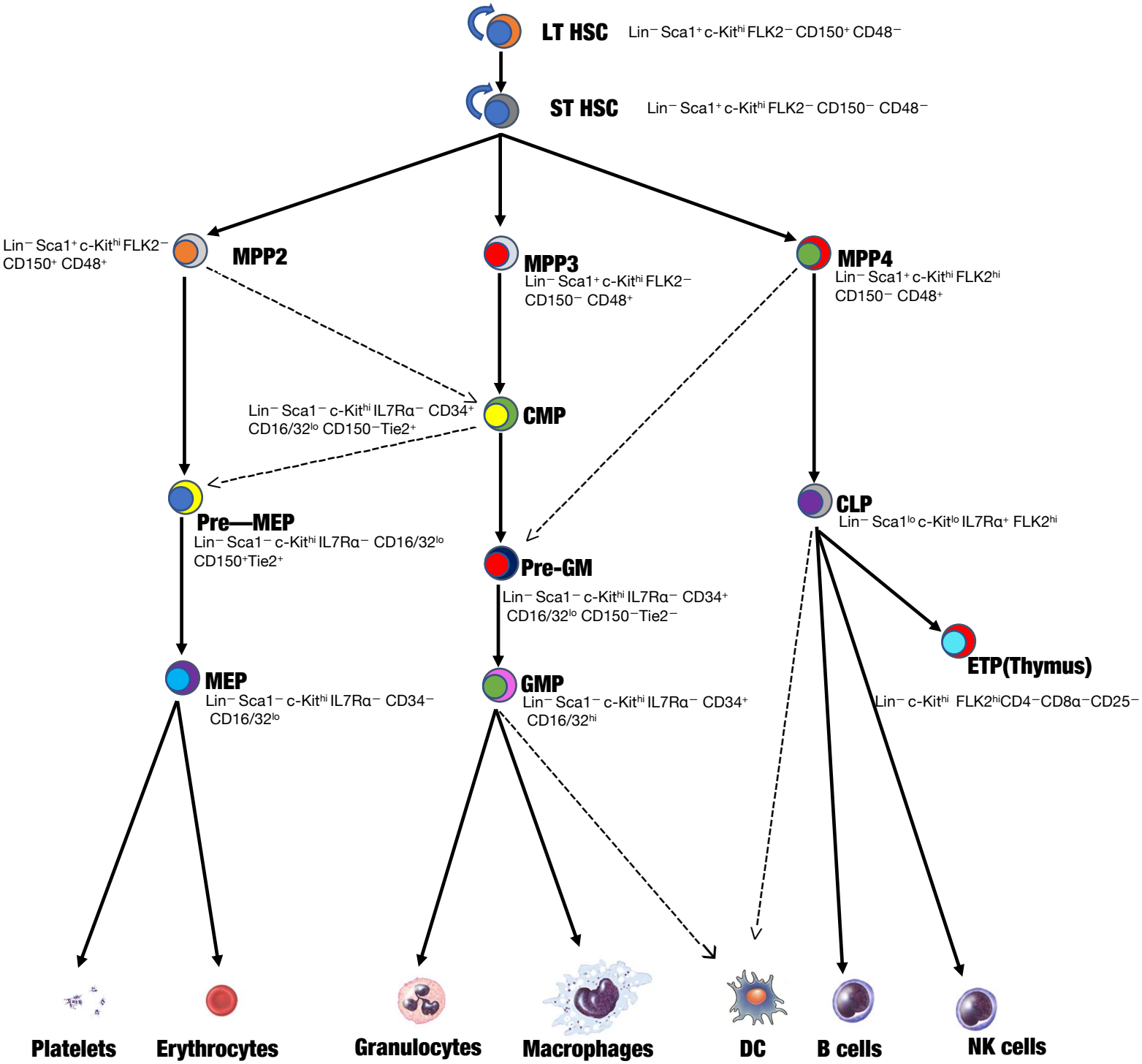
LT HSC
Lin⁻ Sca1⁺ c-Kit^hi FLK2⁻ CD150⁺ CD48⁻
ST HSC
Lin⁻ Sca1⁺ c-Kit^hi FLK2⁻ CD150⁻ CD48⁻
MPP2
Lin⁻ Sca1⁺ c-Kit^hi FLK2⁻ CD150⁺ CD48⁺
MPP3
Lin⁻ Sca1⁺ c-Kit^hi FLK2⁻ CD150⁻ CD48⁺
MPP4
Lin⁻ Sca1⁺ c-Kit^hi FLK2^hi CD150⁻ CD48⁺
CMP
Lin⁻ Sca1⁻ c-Kit^hi IL7Rα⁻ CD34⁺ CD16/32^lo CD150⁻Tie2⁺
Pre—MEP
Lin⁻ Sca1⁻ c-Kit^hi IL7Rα⁻ CD16/32^lo CD150⁺Tie2⁺
Pre-GM
Lin⁻ Sca1⁻ c-Kit^hi IL7Rα⁻ CD34⁺ CD16/32^lo CD150⁻Tie2⁻
CLP
Lin⁻ Sca1^lo c-Kit^lo IL7Rα⁺ FLK2^hi
ETP(Thymus)
Lin⁻ c-Kit^hi FLK2^hiCD4⁻CD8α⁻CD25⁻
MEP
Lin⁻ Sca1⁻ c-Kit^hi IL7Rα⁻ CD34⁻ CD16/32^lo
GMP
Lin⁻ Sca1⁻ c-Kit^hi IL7Rα⁻ CD34⁺ CD16/32^hi
Platelets
Erythrocytes
Granulocytes
Macrophages
DC
B cells
NK cells

Figure 1.1 The revised model of steady state haematopoiesis

Adapted from Pietras *et al*., 2015 (15)

In this revised model of haematopoiesis, LTHSCs give rise to STHSCs and this step is accompanied with some loss of self-renewal potential. The STHSCs produce in parallel, distinct lineage biased MPPs namely MPP2, MPP3 and MPP4 which are biased towards megakaryocytic/erythroid, myeloid and lymphoid commitment respectively. These MPPs are devoid of self-renewal potential. The solid and dashed arrows depict the main and alternative differentiation pathways respectively. Abbreviations: *Long term haematopoietic stem cells (LTHSC), short term haematopoietic stem cells (ST HSC), multipotent progenitors (MPP), common myeloid progenitor (CMP), pre-megakaryocyte` erythroid progenitor (Pre-MEP), pre-granulocyte macrophage progenitor (Pre-GM), common lymphoid progenitor (CLP), megakaryocyte erythroid progenitor (MEP), granulocyte-macrophage progenitor (GMP), early thymic progenitor (ETP), dendritic cells (DC), Natural killer (NK) cells.*

1.1.2 Erythroid progenitors and precursors

In the classical model of haematopoiesis, a bipotent CMP lacking lymphoid potential, gives rise to both a megakaryocyte-erythroid progenitor (MEP) and a granulocyte-macrophage progenitor (GMP). This has been a useful working model but is likely an oversimplification.

Several studies over the last decade have revised this model through the identification of alternative differentiation pathways and subpopulations within the previously defined progenitor stages. Recent studies have suggested that the differentiation into the megakaryocytic/erythroid lineages could be an event upstream or in parallel to the generation of CMP (15).

Downstream of the MPPs, the most primitive population with megakaryocytic and erythroid potential but lacking myeloid potential is the pre- megakaryocytic erythroid progenitor also known as pre-MEP (17,19). In *in vitro* clonal assays, the pre-MEP (Lin^- Sca-1^- c-Kit^{hi} $CD150^+$ $CD105^-$ $CD135^-$) gave rise to megakaryocytic, erythroid and mixed megakaryocytic/erythroid colonies but failed to produce any myeloid colonies (19). Downstream of the pre-MEP is the MEP (Figure 1.2). Using CD150 and Endoglin (CD105), Pronk *et al*. demonstrated that the MEP described by Akashi *et al*.

as Lin^- $Sca\text{-}1^-$ $c\text{-}Kit^{hi}$ $CD34^-CD16/32^-$ (12) is indeed a heterogenous population that contains a $CD150^+$ subset the pre-MEP, which I have mentioned above, and a $CD150^-$ subset (19). This heterogeneity of the MEP has also been demonstrated in human studies (20,21).

The MEP differentiates into the earliest erythroid restricted progenitor, the burst forming unit erythroid (BFU-e) cell. The BFU-e is highly motile and it is hypothesised that it migrates towards $CD169^+$ macrophages located in specialised BM niches called erythroblastic islands, where upon its differentiation to the erythropoietin sensitive colony forming unit erythroid (CFU-e) cell, adheres to the macrophage through a number of different molecules such as β1 integrins, CD44, Lu and ICAM 4 (22–24). The BFU-e and CFU-e have been traditionally identified by their morphology in clonogenic assays (25–29). This differentiation from the LTHSC to the CFU-e is referred to as early erythroid differentiation. Terminal erythroid differentiation involves the differentiation of the CFU-e through four distinct erythroblasts stages (proerythroblast, basophilic erythroblast, polychromatic erythroblast and orthochromatic erythroblast), to the reticulocyte and ultimately terminal red blood cell formation. Socolovsky and colleagues pioneered the identification and isolation of the distinct erythroblast stages in the spleen and foetal liver, on the basis of the expression of the transferrin receptor (CD71) and the red cell membrane protein (Ter119) in these populations (30,31). Another parameter, cell size (FSC) was later included to improve the identification of these populations in the spleen and BM (32). Despite the addition of FSC, the gating strategy employed could only identify three of the four erythroblast populations that express CD71 on their surface, namely proerythroblast ($CD71^{hi}$ $Ter119^{int}$), Ery A ($CD71^{hi}$ $Ter119^{hi}$ FSC^{hi}) and Ery B ($CD71^{hi}$ $Ter119^{hi}$ FSC^{lo}) (32). The Ery A population comprised of basophilic erythroblasts while the Ery B population comprised of late basophilic and polychromatic erythroblasts (32). However, Chen *et al*. using same markers but a different gating strategy, described a more comprehensive breakdown of these erythroid populations that included all four erythroblast populations and reticulocytes (33). Furthermore, Chen *et al*. replaced CD71 with CD44 and isolated erythroblast populations at a higher purity (33).

Terminal erythropoiesis is unique in that proliferation occurs simultaneously with differentiation. It is well established that under physiological conditions, a single proerythroblast undergoes three mitotic divisions to produce sequentially, two basophilic erythroblasts, four polychromatic erythroblasts and eight orthochromatic erythroblasts (34). Thus, the ratio of proerythroblasts: basophilic erythroblasts: polychromatic erythroblasts: orthochromatic erythroblasts follows a 1:2:4:8 pattern (34). This ratio is maintained as a result of the tight regulation of erythropoiesis by an array of transcription factors, haematopoietic cytokines, growth factors, adhesive receptors and miRNAs. How this ratio is altered could identify potential pathology in terminal erythroid differentiation and could provide useful insight into the molecular basis of inherited and acquired anaemias.

1.1.3 Key regulators of erythropoiesis.

The differential expression of transcription factors is considered operational in directing cells towards a particular development fate. Some transcription factors of crucial importance for erythroid lineage commitment are Erythroid Krüppel like factor (EKLF/KLF1), GATA binding factor 1 (GATA-1), friend of GATA-1 (FOG1) and PU.1.

(KLF1/EKLF) is a master regulator of terminal erythroid differentiation, and controls cell division, membrane stability, heme and globin synthesis, and iron metabolism (35–37). KLF1 knock out mice die of anaemia at embryonic day 16 (E16) demonstrating a non-redundant role of KLF1 for erythroid development (35,38). *Klf1*$^{-/-}$ erythroblasts completely fail to enucleate due to a block at the orthochromatic stage of terminal differentiation (39). KLF1 regulates the switch from foetal (gamma) globin to adult (beta) globin through the activation of Bcl11a, which encodes a repressor of gamma globin gene transcription (40,41). *Klf1*$^{-/-}$ primary erythroid cells fail to enter the S phase efficiently (42,43). KLF1 regulates the transcriptional expression of the transferrin receptor (*Tfrc*) as well as a majority of enzymes required for heme synthesis (44).

GATA-1 and GATA-2 are members of the evolutionary conserved GATA transcription factor gene family which bind to the DNA consensus sequence (A/T)GATA(A/G) by two characteristic C_4 (Cys-X_2-Cys-X_{17}-Cys-X_2-Cys) zinc-finger motifs specific to the

GATA family (45,46). GATA-1 is expressed in erythroid cells (47), megakaryocytes (48), eosinophils (49) and mast cells (48). Similar to the phenotype seen in KLF knock out mice, GATA-1 null mice die from severe anaemia between embryonic day 10.5 (E10.5) and E11.5(47). GATA-1 null erythroid cells do not mature beyond the proerythroblast stage (50) and these arrested erythroid precursors die by apoptosis (51). Furthermore, the anti-apoptotic gene *Bcl-$_{XL}$* is a direct target of GATA-1 (52).

GATA-2 is highly expressed in HSCs and MPPs. However its expression decreases with opposing increase in GATA-1 expression (53). It is thought that this incremental expression of GATA-1 is required for the formation of erythroid progenitors. GATA-1 switches off GATA-2 controlled early progenitor genes and activates terminal maturation genes, failure of which promotes megakaryocyte commitment at the expense of erythroid commitment (54).

Using the inducible *myxovirus* resistance -1-Cre (Mx1-Cre) and Poly I:C system, conditional deletion of *Zfmp-1* which encodes FOG-1, was shown to prevent specification of all megakaryocyte and erythroid progenitors while the conditional deletion of *Gata-1* was indispensable for pre-MEP commitment to an erythroid fate but dispensable for commitment towards a megakaryocytic fate (55).

PU.1 encoded by *Spi1* is a member of the ETS family of transcription factors, and is expressed exclusively in haematopoietic cells (56–58) but its role for erythropoiesis still remains controversial. There is experimental evidence suggesting that PU.1 is not essential for erythropoiesis; in two PU.1 deficient mouse lines generated independently, terminally differentiated erythrocytes were present in the foetuses (59,60). However, in one of these lines, the embryos exhibited a reduced number of reticulocytes and erythrocytes (60). This incidence of anaemia was linked to the genetic background of the mice and was abrogated by back crossing the *Spi1*$^{-/-}$ mutation onto a C57BL/6 (61). There is however some evidence of a role of PU.1 for erythroid development. Using PU.1 deficient mice with a knock-in of an enhanced green fluorescent protein (EGFP) in the *Spi1* locus, it was demonstrated that foetal erythroid progenitors undergo proliferation arrest, premature differentiation and apoptosis (62).

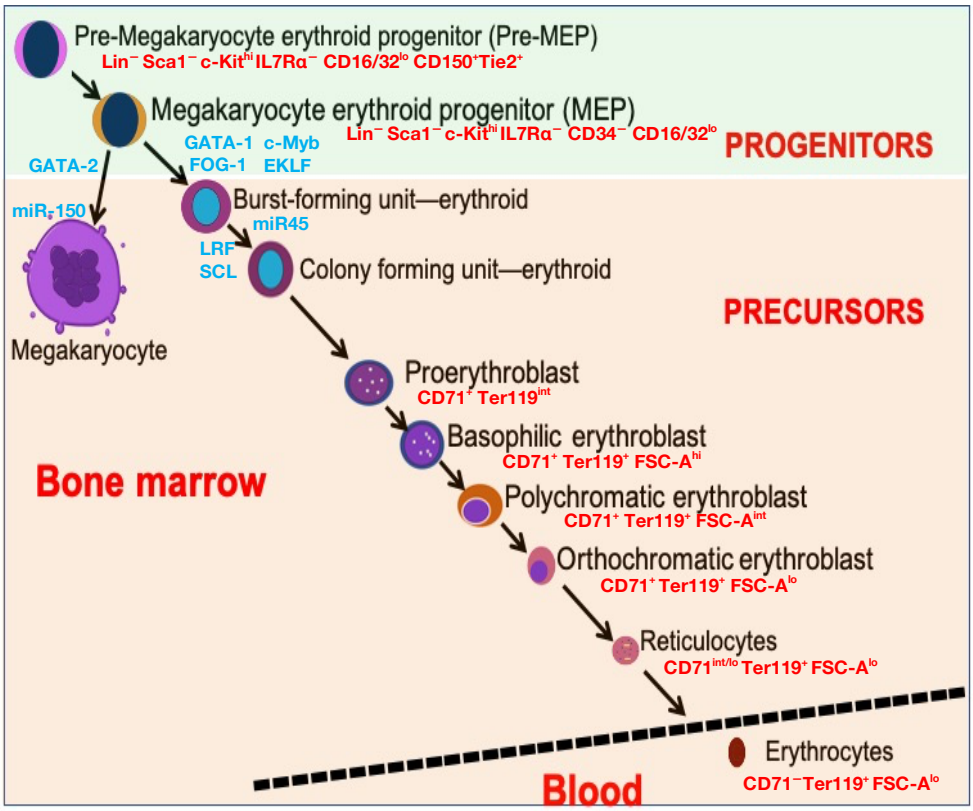

Figure 1.2 Scheme of bone marrow erythropoiesis in steady state

The decision of whether the megakaryocyte-erythroid progenitor should commit to an erythroid or megakaryocytic fate is controlled by an array of transcription factors and microRNAs. GATA-1, FOG-1, EKLF, c-Myb, LRF, SCL and miR451 direct erythroid lineage commitment and progression to erythroblasts while GATA-2 and miR150 direct megakaryocytic lineage commitment. *Abbreviations: GATA-binding factor 1 (GATA-1), friend of GATA-1 (FOG-1), erythroid krüppel like factor (EKLF), leukemia/lymphoma-related factor (LRF), stem cell leukemia (SCL).* Adapted from Chen *et al*., 2019 (33) and Doré *et al*., 2011(63).

1.1.4 Stress induced haematopoiesis

It is well known that systemic infection with a variety of pathogenic microorganisms can result in profound alterations in the phenotype and functional potential of BM haematopoietic stem and progenitor cells (HSPCs). These alterations appear to be part of a conserved host response to microbial challenge.

Systemic challenge often elicits a stress induced haematopoietic response that is characterised by increased BM output of cells of the myeloid lineage and the mobilisation of BM neutrophils to peripheral tissues. This rapid response in which

myeloid progenitors are induced to proliferate under stress conditions is termed emergency granulopoiesis.

In malaria and toxoplasmosis, in addition to emergency granulopoiesis, there is a transient decrease in lymphocytes, megakaryocytes and erythrocytes despite low parasite burden in this site (64–66). The suppression of erythropoiesis and development of anaemia is characteristic of many infections. Studies in our laboratory using a model of *Plasmodium chabaudi* malaria, showed a contraction of the erythroid lineage restricted progenitors, the BFU-e and CFU-e at early time points during infection (67), as well as a decrease in both the frequency and absolute numbers of myeloid progenitors. This contraction of myeloid progenitors was dependent on indirect IFN-γ signalling (68).

Ehrlichia muris infection of C57BL/6 was accompanied by major changes in BM function, with an almost complete loss of the BFU-e, marked reduction in BM erythroid precursors ($Ter119^+$ BM cells), myeloid progenitors and B lymphocytes, and a significant decrease in BM cellularity. This was accompanied by the manifestation of severe anaemia and thrombocytopenia despite an increase in splenic erythroid precursors, (69). These changes were not associated with the presence of the bacteria in the BM.

However, a study in anaemic children under the age of five showed an association between the presence of *Plasmodium falciparum* and hemozoin in BM, with ineffective erythropoiesis (70). Microscopic examination of BM smears from these children revealed dyserythropoietic features such as nuclear pyknosis and irregular nuclei. These features were more prevalent in BM containing hemozoin, while erythroid hyperplasia was more prevalent in BM with parasites. Ineffective erythropoiesis was confirmed by reticulocytopenia (< 0.5% reticulocytes in peripheral blood) and reticulocyte production index (RPI) of less than 1. The RPI is used as a marker in the diagnosis of anaemia and also in the determination of the erythropoietic response to anaemia. It is a standard measure of the production of reticulocytes and takes into consideration both the degree of anaemia and the early release of reticulocytes from the BM into circulation in patients with anaemia. An RPI < 2 indicates an inadequate response to anaemia. In another study in Gabon in which 39

individuals were diagnosed with severe malarial anaemia (SMA) with a mean haematocrit (HCT), haemoglobin (Hb) concentration and parasitaemia of 14.3%, 4.9 g/dL and 1.2 x 10^4 μL^{-1} respectively, the mean RPI was 0.7 indicating a grossly inadequate erythropoietic response to anaemia in these individuals (71)

Toxoplasma gondii infection in WT C57BL/6 mice resulted in decreased red blood cell production that was characterised by a marked reduction in the number of reticulocytes which was completely abolished in IFN-γ KO and IFN-γR KO mice (72).

From these studies, most of the changes that occur in the BM during infection could result from the direct presence of the parasite and/or parasite products in the BM or could be immune mediated as a result of the production of cytokines at distal sites, the latter might perhaps be the most common scenario.

Many infections are characterised by high systemic levels of IFN-γ, IL1 and tumor necrosis factor alpha (TNF-α), and these cytokines have been linked to alterations in BM haematopoiesis. IFN-γ is able to modify myelopoiesis (9,67,68,73) and other aspects of haematopoiesis (74). IFN-γ can activate quiescent HSCs during infection with Mycobacterium avium (75), and together with TNF-α, has been implicated in the suppression of erythropoiesis.

1.2 Malaria

Malaria is the most important parasitic disease of humans (76). The aetiological agent is a unicellular apicomplexan obligate parasite of the genus *Plasmodium*. There are six species of *Plasmodium* that commonly infect man (*P.falciparum, P.vivax, P.malariae, P.ovale curtisi, P.knowlesi and P. ovale wallikeri*), all of which can cause anaemia. This disease is vector borne and is transmitted by *Anopheles* mosquitoes in 108 countries which are inhabited by half the world's population (76).

In 2017, there were an estimated 219 million cases of malaria worldwide, which resulted in 435,000 deaths (WHO 2018). The vast majority of morbidity and mortality is caused by *Plasmodium falciparum* and was implicated in 99.7% of cases in 2017. Children under the age of 5 remain the most vulnerable group and in 2017 accounted for 61% of all malaria deaths world wide (WHO 2018).

1.2.1 The biology of Plasmodium parasites

The life cycle of *Plasmodia* (summarised in Figure 1.3) is characterised by an exogenous sexual phase named sporogony, in which multiplication occurs in several species of *Anopheles* mosquitoes and an endogenous asexual phase named schizogony which takes place in the vertebrate host (77). In the asexual phase, about 15-123 motile sporozoites from the salivary duct of an infected female *Anopheles* mosquito are inoculated into a suceptiible host's subcutaneous tissue during a blood meal (78–81). The sporozoites migrate and enter the parenchymal cells of the liver. In the vertebrate host, the life cycle of *Plasmodium* is characterised by a tissue phase in the liver, and the erythrocytic phase which is responsible for the appearance of clinical manifestations. In hepatocytes, the sporozoites undergo their development and multiplication to become a tissue schizont containing thousands of merozoites in a process known as pre-erythrocytic or exo-erythrocytic schizogony. The mature schizont ruptures together with the infected hepatocytes, releasing merozoites into the blood where they invade erythrocytes. Within infected erythrocytes, the merozoites replicate and mature progressively from ring-stage parasites to trophozoites then to schizonts. The erythrocyte eventually ruptures, releasing between 8 and 32 merozoites, that in turn invade new erythrocytes to repeat the cycle (82). The asexual cycle in the blood takes approximately 48h for *P.falciparum, P.vivax and P.ovale*, 72h for *P.malariae* and 24h for *P.knowlesi* (76).

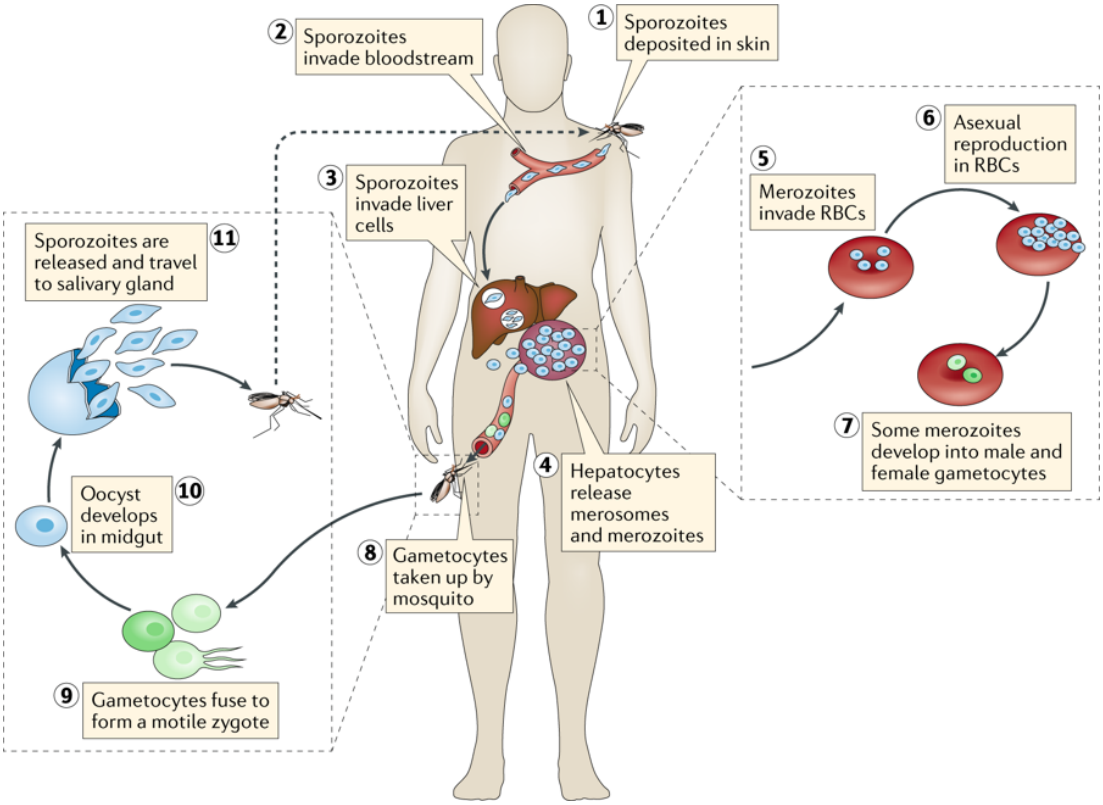

Figure1.3 Life cycle of Plasmodium parasite in the mosquito and vertebrate hosts

Sporozoites from the salivary duct of a *Plasmodium*-infected female *Anopheles* mosquito are deposited into the subcutaneous tissues during blood meal. Motile sporozoites migrate from the dermis to the liver via the blood stream and invade hepatocytes via interactions between *Plasmodium* circumsporozoite protein and heparan sulfate molecules on hepatocytes. Infected hepatocytes release tens of thousands of merozoites and merosomes (membrane-bound packets of merozoites) into the bloodstream which invade red blood cells. Merozoites undergo repeated rounds of asexual replication and a minor proportion of merozoites differentiate into male and female gametocytes. The gametocytes can be ingested by another female *Anopheles* mosquito and in the midgut, the male and female gametocytes fuse and develop into a motile ookinete then into oocyts. Oocyts give rise to sporozoites which migrate to the salivary gland for transmission to a new host. Adapted from Kurup *et al*., 2019 (83).

1.2.2 Clinical syndromes of severe malaria

Malaria disease can be categorised as uncomplicated or severe. Severe malaria occurs when infections are complicated by serious organ failures and abnormalities in patients blood or metabolism. Almost all severe forms and deaths from malaria are caused by *P. falciparum,* nevertheless, non-*falciparum* species such as *P. vivax* and

P. knowlesi are also able to cause severe disease (84,85). The major complications of severe malaria include cerebral malaria, severe anaemia, pulmonary oedema, acute renal failure, metabolic acidosis and hypoglycemia. In sub-Saharan Africa, children with severe malaria typically present with one complication such as respiratory distress, convulsions or severe anaemia (86).

In areas of high *P. falciparum* transmission intensity, the risks of developing severe disease are highest in the first two years of life and decline rapidly thereafter. Conversely, in low to moderate transmission settings, the period of risks is much extended up to the age of five. At the lowest end of the transmission spectrum, the risks of severe disease appear to be spread evenly throughout childhood (87). Furthermore, the presentation of severe disease changes from severe anaemia in children between 1 and 3 years in areas of high transmission intensity to celerbral malaria in older children in areas of lower transmission intensity (87). In malaria-endemic areas where transmission is stable, severe malaria is unlikely to occur after five years of age due to naturally acquired immunity (NAI). Also, infants remain remarkably resistant to severe disease until about 6 months of age. This protection is thought to be associated with the presence of maternal immunoglobulin G antibodies and/or parasite growth-inhibitory factors such as lactoferrin and secretory immunoglobulin A found in breast milk and in maternal and infant sera (88). NAI to severe malaria may be acquired relatively quickly after up to four exposures (88) and mathematical models have suggested that protection against non cerebral severe malaria develops after one or two infections (89).

Severe malarial anaemia (SMA) is the main manifestation of severe malaria in young children in areas of high transmission intensity (90). In holoendemic *P. falciparum* transmission areas, SMA accounts for 30% of the mortality in children under three years of age (91). In a study in 880 young children in Tanzania, transmission season at time of delivery and cord blood levels of IL-1β provided the strongest discrimination of SMA risk during the first three years of life (92).

SMA is an outcome of the perturbation of red blood cell homeostasis either as a result of a reduced erythroid output from the BM or an increased clearance/destruction of erythroid cells. SMA according to the WHO is defined as haemoglobin (Hb)

concentration of < 5 g/dL or haematocrit (HCT) of less than 15% with any degree of parasitaemia. Rapid haemoglobin reductions of 20 to 50% are commonly observed in patients with SMA and they must be rescued by blood transfusion which poses a great risk of HIV acquisition, especially in sub-Saharan countries (93).

According to the literature, patients with SMA have appropriate erythropoietin (Epo) response. A study in Gabonese children showed elevated serum Epo concentration of $15{,}364 \pm 9984$ mU/mL before therapy which declined to basal levels of 144 ± 180 mU/mL, 28 days after initiation of therapy (94). However, the reticulocyte production index (RPI) in these patients remained low considering the degree of anaemia.

The aetiology of SMA is multifactorial and could arise as a result of distinct and overlapping features such as clearance and/or destruction of infected and uninfected erythrocytes, dyserythropoiesis and erythropoietic suppression (95). These mechanishms are present in both humans and mouse models. Destruction of uninfected erythrocytes rather than infected erythrocytes is estimated to account for most of the loss of erythrocytes during malaria and might explain why parasitaemia fails to correlate with SMA.

A desirable feature of mouse models of malaria is that there are four known species of rodent malaria parasites namely *P. chabaudi*, *P. vinckei*, *P. berghei* and *P. yoelii,* and various strains such as *P. yoelii* YM and *P. yoelii* 17XNL, with each displaying unique parasite biology and pathogenicity. *P. berghei* for example infects mature red cells and reticulocytes and is used in the study of experimental cerebral malaria in C57BL/6 and CBA/T6 mice, *P. yoelii* XNL which preferentially invades reticulocytes, has been used extensively in multiple strains of mice to study the pathogenesis of malaria and immune mechanisms of protection and may serve better as a model for *P. vivax*. The lethal strain *P. yoelii* YM that infect both reticulocytes and mature red cells has been used to test vaccine candidates, and various strains of *P. chabaudi* that infect mature erythrocytes and reticulocytes, and *P. vinckei* that infect mature erythrocytes have been used in different mouse strains to study immune mechanisms, pathogenesis and susceptibility to drugs. The course of infection and

the immune response are variable among the various mouse models but specific for each host-parasite combination (96).

In acute disease, the imbalance between proinflammatory and anti-inflammatory mediators may be the main cause of dyserythropoiesis and mouse models able to reflect this are those that use *P. chabaudi* and *P. yoelii* (96). The *P. chabaudi* model of malaria mirrors many of the pathological and immunological aspects of human malaria infections, making it an excellent tool to expand our knowledge of human malaria infections and to identify new targets for therapeutic interventions. However there are several limitations to this model such as, the organ of sequestration in mice (the liver rather than the brain), some differences in pathogenic symptoms such as the development of hypothermia rather than fever, and the discrepancy of parasitaemia profiles between mice (97).

Severe anaemia is a feature of all mouse models (98) however, the majority of these mouse models demonstrate acute malaria infection with parasitaemia that often exceeds 20% which is in contrast to SMA in humans in which acute malaria commonly occurs with a lower parasitaemia (96). Despite this difference, SMA in *P. falciparum* and *P. chabaudi* malaria have several features in common. For instance, in *P. falciparum* malaria, patients with SMA and suppressed erythropoiesis as evidenced by their low RPI, have a robust erythropoietin response (94), and this has also been reported in non-lethal *P. chabaudi experimental* malaria in C57BL/6 mice (99). The increased levels of erythropoietin fail to correct the deficit in haematocrit caused by haemolysis and erythrocyte sequestration, which suggests a non-responsiveness of erythroid cells to erythropoietin stimulation during SMA in both *P. falciparum* and *P. chabaudi* malaria, a hallmark of dyserythropoiesis.

1.2.3 Dyserythropoiesis in Malaria

Erythropoietic suppression or dyserythropoiesis is known to occur in humans and in mouse models. Two distinct patterns of dyserythropoiesis are observed in humans. Acute malaria is characterised by a reduction of erythropoieitic activity, normal or

reduced BM cellularity, erythroid hypoplasia and a reduced percentage of erythroblasts, while in chronic malaria, BM cellularity and percentage of erythroblasts are increased, erythroid hyperplasia is evident and these are associated with substantially greater ineffective erythropoiesis than in acute malaria (100). The study of disordered erythropoiesis in mouse models has been restricted to the the acute phase of the disease and there is paucity of data on dysplastic changes in murine erythoid cells during the chronic phase of the disease. Unlike in SMA in humans in which no change in BM CFU-e has been reported (98), a transient 50% decrease in BM CFU-e was reported in *P. chabaudi malaria* in C57BL/6 mice (101). This remarkable decrease in BM CFU-e was further confirmed by Belyaev and colleagues (102).

In individuals with dyserythropoiesis, erythropoietic suppression could persist for weeks after the commencement of drug therapy and well after clearance of the parasite (100). This suggests that this phenomenon is not directly driven by the parasite itself but rather could be as a result of by-products of parasite metabolism such as haemozoin (70,103,104) and/or host derived factors.

Dyserythropoiesis is characterised by non-responsiveness of erythroid cells to erythropoietin (EPO) stimulation (105), this is supported by the low reticulocyte production index (106) despite a robust erythropoietin response in children with SMA (94). Miller *et al*. performed experiments demonstrating that an unknown soluble factor inhibited erythropoiesis during malaria (105). A number of host derived factors, in particular, proinflammatory cytokines namely TNF-α, IFN-γ and macrophage migration inhibitory factor (MIF), produced during the immune response to malaria, have been implicated as mediators of malaria dyserythropoiesis (107,108). Most of these studies have focussed on MIF and TNF-α with only a few on the role of IFN-γ for ineffective erythropoiesis during malaria.

1.3 Mechanisms of erythropoiesis inhibition by IFN-γ

The proinflammatory cytokine IFN-γ is produced predominantly by natural killer cells, natural killer T cells, type 3 innate lymphoid cells, innate B cells and macrophages as part of the innate immune response, and by Th1 CD4 and CD8 T cells once

antigen-specific immunity develops (109–111). IFN-γ secretion by these cells is essential for the control of intracellular pathogens and tumours, however, aberrant production of IFN-γ contributes to autoimmunity and inflammation in certain disease settings. These divergent roles of IFN-γ are well illustrated in the context of malaria. IFN-γ is a central cytokine in controlling *Plasmodium* infection in both the liver and blood stages (112), but depending on its temporal and spatial production, IFN-γ might exacerbate the severity of malarial disease, one of such pathological roles of IFN-γ in malaria is in mediating anaemia via erythropoiesis suppression.

There are knowledge gaps in our understanding of the molecular mechanisms by which IFN-γ inhibits erythropoiesis during malaria. In a murine model of sterile chronic immune activation, IFN-γ induced the expression of PU.1 in MEPs (113) and PU.1 is able to interact antagonistically with GATA-1 inhibiting its role in erythroid development (114). In this model also, IFN-γ was implicated in the contraction of BFU-e colonies and late stage erythroid precursor (113).

Studies in which IFN-γ induced apoptosis of erythroid cells have been so far only performed *in vitro*. These erythroblast populations alone, deplete of the nourishment and survival signals provided by “nurse cells” in erythroblastic islands, are arguably more sensitive to IFN-γ ultimately leading to their apoptosis. In one of such studies, IFN-γ mediated dyserythropoiesis by induction of Fas (CD95) on highly purified human erythroid colony forming cells which constitutively express FasL (115), leading to their apoptosis. The concentration of IFN-γ used in this study was extremely high (2.5 $ngml^{-1}$) and might not be obtainable under physiological conditions.

The downregulation of stem cell factor (SCF) and EpoR on human erythroid colony forming cells treated with IFN-γ have been linked to apopotosis in these cells (116). IFN-γ upregulated the expression of TNF-related weak inducer of apoptosis (TWEAK) and TNF-related apoptosis inducing ligand (TRAIL) in human erythroblasts and these death ligands directly mediated programmed cell death, and inhibited the expansion and differentiation of these cells (117).

It would be interesting to investigate if similar changes in the expression of key transcription factors, death receptors and ligands, and growth factor receptors occur during malaria.

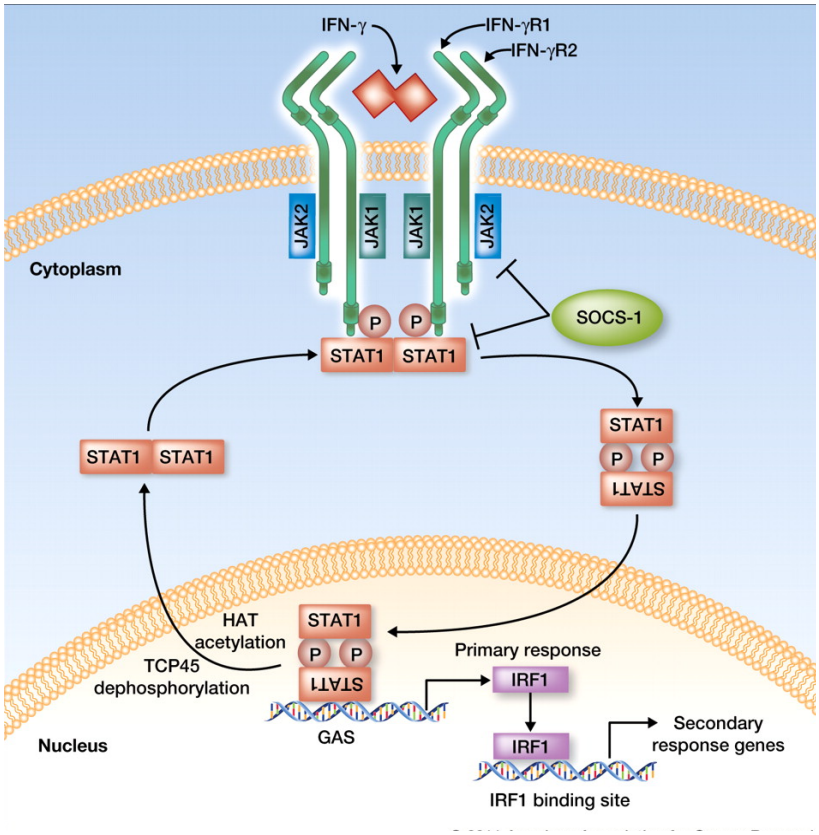

Figure 1.4 The IFN- γ receptor and its signalling

Adapted from Zaidi and Merlino, 2011 (118)

The IFN-γ receptor is made up of two alpha chains and two beta chains. Two kinases Janus kinase 1(JAK1) and Janus kinase 2 (JAK2) associate with the intracellular domains of IFN-γ receptor alpha chains (IFN-γR1) and IFN-γ receptor beta chains (IFN-γR2) respectively. IFN-γ exists as a homodimer and binds solely to IFN-γR1, this binding causes IFN-γR2 to associate strongly with IFN-γR1 bringing JAK1 and JAK2 into close juxtaposition such that they cross-phosphorylate each other and phosphorylate a tyrosine residue on IFN-γR1 creating a docking site for STAT1. Two parallel STAT1 homodimers are recruited to the docking site and their Tyr^{701}phosphorylation by JAK1 and JAK2 converts the homodimers into an antiparallel configuration. The reoriented STAT1 homodimers dissociate from the receptor and translocate to the nucleus. In the nuclues they bind to gamma activated sequence (GAS) sites on the primary response genes and mediate the transcription of primary genes including Interferon regulatory factor-1 (IRF1). IRF1 subsequently activates a large number of secondary response genes with a wide range of immunomodulatory functions. Acetylation

and subsequent dephosphorylation of STAT1 homodimers change their orientation to parallel configuration and cause their exit from the nucleus. Suppressor of cytokine signalling (SOCS-1) is a major negative regulator of IFN-γ signalling and inhibits the phosphorylation of JAKs and STAT1.

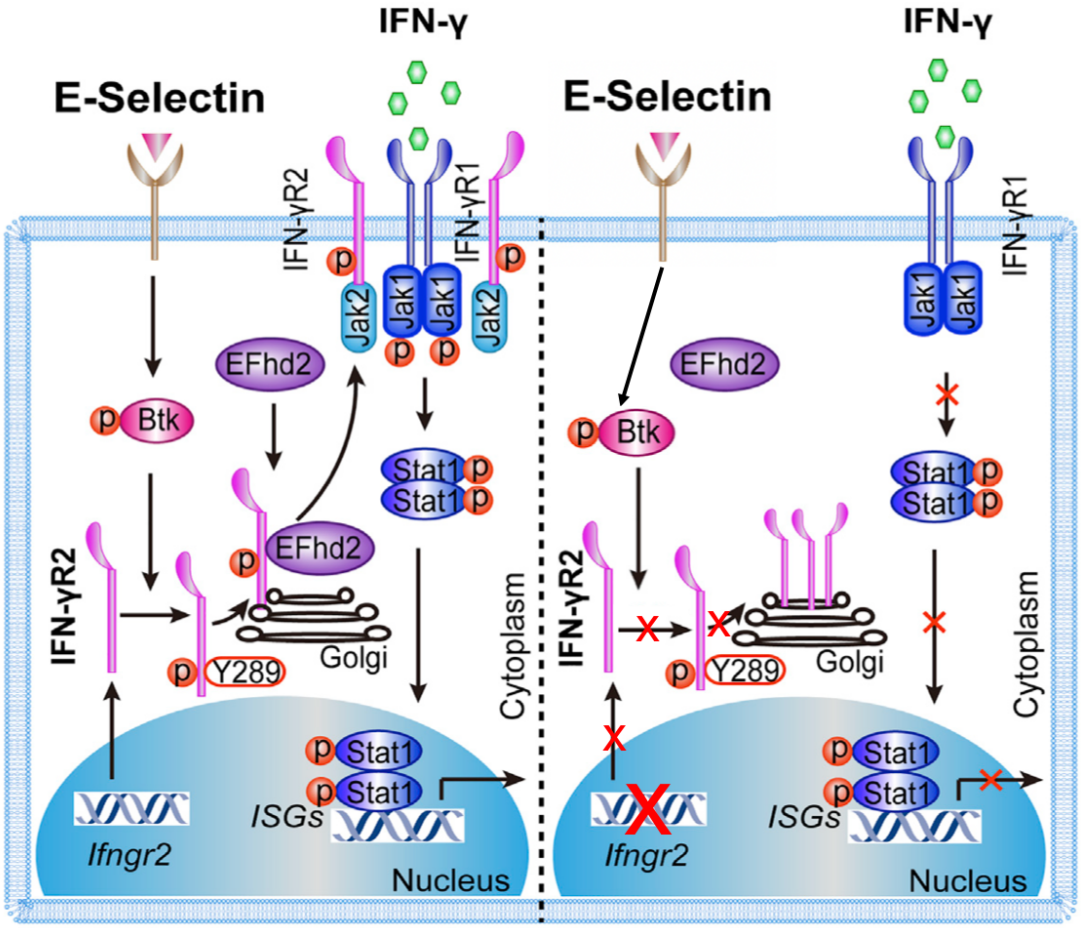

Figure 1.5 Assembly of IFN-γR2 on cell surface

Adapted from Xu *et al*., 2018 (119)

IFN-γR1 is constitutively expressed on the surface of all nucleated cells and is responsible for binding IFN-γ. However, IFN-γR2 is induced after inflammation and translocates to the cell membrane. The engagement of E-selectin to its ligand provides the initial signal for this translocation. Following its engagement, E-selectin activates Bruton's tyrosine kinase (BTK), which phosphorylates tyrosine 289 of IFN-γR2 in the cytoplasm. EFhd2 then binds to the phosphorylated receptor to promote its membrane translocation. In the absence of *Ifngr2* gene, IFN-γR1 is able to bind IFN-γ but downstream signalling is abolished.

1.4 Aims of the study

The primary aim of this PhD work is to investigate the role of IFN-γ signalling on the aberration of erythropoiesis during malaria. To understand the role of IFN-γ signalling for malaria dyserythropoiesis, the accurate identification and isolation of erythroid cells at high purity is pivotal. The erythroid and myeloid progenitors are in the same developmental subset ($LIN^{-}Sca\text{-}1^{-}CD117^{hi}$), and the surface markers currently in use to identify these progenitor populations within the HPC pool, only poorly resolve these progenitors and yields low purity of FACS sorted populations. To address this problem, I aimed to define novel surface markers that could clearly distinguish the myeloid and erythroid progenitors, and yield high purity of FACS sorted populations.

Having defined novel surface markers that could identify the most primitive and least characterised erythroid progenitor, the Pre-MEP, as well as the MEP with a high degree of accuracy, I aimed to investigate the exact stages of erythropoiesis that are impacted by malaria. Previous studies on malaria dyserythropoiesis had focused on stages downstream of the MEP, as the MEP and Pre-MEP were only identified by flow cytometry in the recent years. I used three murine models of infection namely, the serial blood passage, the mosquito transmission and sporozoite inoculation models and observed significant erythroid suppression at multiple stages of erythropoiesis in the BM and spleen.

This led to the final aim to investigate if IFN-γ signalling in the haematopoietic compartment alone, is sufficient to promote suppression of erythropoiesis during malaria. Studies on dyserythropoiesis have focused mainly on MIF and TNF-α, and there is a paucity of data on the *in vivo* role of IFN-γ for dyserythropoiesis during malaria. Furthermore, it remains unknown if the suppression of erythropoiesis by IFN-γ is a consequence of a direct signalling in haematopoietic cells or whether it is a consequence of IFN-γ signalling in non-haematopoietic compartments. Adopting a refined genetic approach, I demonstrated that IFN-γ signalling in the haematopoietic compartment alone is crucial for malaria dyserythropoiesis in the BM and spleen.

CHAPTER 2

MATERIALS AND METHODS

2.1 MICE

Inbred mouse strains used were C57BL/6Jcrl, *Vav1::iCre/Ifngr2*$^{fl/fl}$, *Ifngr2*$^{fl/fl}$ and *Vav1::iCre* mice. *Vav1::iCre* transgenic mice have the mouse HS21/45 control regions directing expression of an optimized variant of *Cre* recombinase (iCre; improved with mammalian codon usage, removed putative cryptic splice sites, altered stop codon, and reduced CpG content to limit the chances of epigenetic silencing in mammals) to hematopoietic cells and their progenitors (120). The *Vav1::iCre/Ifngr2*$^{fl/fl}$ mice were generated by crossing *Vav1::iCre* mice with *Ifngr2*$^{fl/fl}$ mice. *Vav1::iCre* mouse which has a *Cre* insert in the *Vav1* locus was created by de Boer and colleagues(121) and was maintained as heterozygous, considering that homozygosity results in developmental abnormalities and intraembryonic death around E14.5—16.5. *Ifngr2*$^{fl/fl}$ mice were generated by Anne Fleige and Werner Müller (122). Mice were housed under specific pathogen free conditions in the animal facility at the University of Edinburgh and were provided with mouse breeder diet and water *ad libitum*. These mice were maintained either under normal light conditions (light 07.00—19.00 : dark 19.00—07.00) or reverse light conditions (dark 07.00—19.00 : light 19.00—07.00) at 22^{0}C and 50% relative humidity. Mice aged 8 to 12 weeks were used for experiments and all experimental mice were back crossed for at least ten generations onto a C57BL/6 background. All animal experiments were done in accordance with United Kingdom Home Office guidelines.

2.2 INFECTION MODELS

Malaria was established in mice using three models of malaria namely, serial blood passage, mosquito transmission and sporozoite inoculation models.

2.2.1 SERIAL BLOOD PASSAGE MODEL

Frozen stocks of serially blood passaged *Plasmodium chabaudi chabaudi* AS (*Pcc* AS) up to the 30th passage were kind gifts from Dr. Philip J Spence (Institute of Immunology and Infection Research, Ashworth Laboratories, University of Edinburgh) and were maintained in liquid nitrogen. Equal volume of Krebs saline + glucose (KSG)

was added to frozen stock of *Pcc* AS, rapidly thawed and 200 μL was injected intraperitoneally (i.p) into a single donor mouse. Parasitaemia was monitored by examination of thin blood films. At 2-5% parasitaemia, which corresponds to day 7 post infection, donor mouse was euthanised with 50 μL of Euthatal, 200μL of prewarmed heparinized KSG was transferred into the thoracic cavity, the aorta was cut and blood was collected using a sterile pastette (123). Blood stage infection was established in experimental mice by i.p injection of 1×10^5 *Pcc AS* parasitised erythrocytes isolated from the donor mouse. Parasitaemia was determined by counting the number of parasitised erythrocytes in 50 fields of view of approximately 200 erythrocytes each, which were distributed in a monolayer. The number of parasitised erythrocytes was then expressed as a percentage of total erythrocytes.

2.2.2 MOSQUITO TRANSMISSION MODEL

Serial blood passaged parasites were transmitted through the mosquito vector *Anopheles stephensi* and donor mice were infected by mosquito bite, with an estimated nine infective bites per mouse to establish both liver and blood stages of malaria. Vector transmission is assumed to "reset" *Plasmodium* to its original character, regulate gene expression of probable variant antigens in the erythrocytic cycle, modify elicited immune response and regulate parasite virulence (124).

To bypass the pre-erythrocytic stages and control the dose initiating blood-stage infection, experimental mice were injected i.p with 1×10^5 *Pcc AS* parasitised erythrocytes obtained from donor mouse.

2.2.3 SPOROZOITE INOCULATION MODEL

The isolation of *Pcc* AS sporozoites and intravenous (IV) injection of sporozoites into donor mice were performed by Dr. Wiebke Nahrendorf (Institute of Immunology and Infection Research, Ashworth Laboratories, University of Edinburgh). 200 sporozoites teased out of the salivary gland of *Pcc* AS parasitised mosquito vector *Anopheles stephensi,* were injected intravenously into donor mice to establish both pre-erythrocytic and erythrocytic stages of malaria. Similar to the mosquito model, to bypass the pre-erythrocytic stages and control the dose initiating blood-stage

infection, experimental mice were injected i.p with 1×10^5 *P. c. chabaudi AS* parasitised erythrocytes obtained from donor mouse.

2.3 Preparation of single cell suspension

Intact femur and tibia free of attached tissue were obtained from culled mice and placed in Iscove's Modified Dulbecco's Medium (IMDM). Both ends of the bones were cut off and the marrow was flushed out using a 5ml syringe fitted with a 27G-needle. The flow through was collected and passed through a 27G-needle and through a 70μm nylon mesh. In other instances, the bone was gently crushed to expose the marrow and passed through a 70μm nylon mesh. Spleens were passed through a 70μm nylon mesh. Cell number per millilitre (mL) was determined using a Casy cell counter (Roche Innovatis AG).

2.4 Physical depletion of lineage positive bone marrow cells.

Single cell suspension of bone marrow (BM) cells were incubated with Mouse Seroblock FcR (BIO-RAD) according to manufacturer's instructions (10μl of 1/10 dilution per 1 million cells for 10 minutes at 4^0C), after which cells were washed with Fluorescence Activated Cell Sorting (FACS) buffer which is made up of 1x phosphate buffered saline (PBS), 2% fetal calf serum (FCS) and 2mM Ethylenediaminetetraacetic acid (EDTA). Cells were labelled with a cocktail of biotinylated antibodies against lineage antigens (CD3ε, CD8α, CD11b, CD11c, CD19, CD45RB, Gr1, NK1.1, Ter119) at 4^0C for 15 minutes in the dark. After washing the cells with FACS buffer, the cells were labelled with streptavidin paramagnetic microbeads (Miltenyi Biotec), resuspended in degassed magnetic activated cell sorting (MACS) buffer (1x PBS, 2% FCS, 1mM EDTA) and passed through an LD separation column (Miltenyi Biotec) attached to a varioMACS separation unit. The eluate (LIN^- cells) was collected for further staining. To identify and/or isolate erythroid precursors, biotinylated monoclonal antibodies against Ter119 was excluded from the lineage cocktail.

2.5 Preparative and Analytical flow cytometry

All antibodies used in this study were titrated and used at optimised dilutions. 7-Amino-Actinomycin D was used to exclude dead cells. Erythroid progenitors and myeloid progenitors in bone marrow and spleen were identified by staining of LIN^- cells with monoclonal antibodies against CD117, Sca-1, CD150, CD27 CD16/32 and CD34. To identify erythroid precursors, bone marrow cells and splenocytes depleted of lineage positive cells with the exclusion of $Ter119^+$ cells, were stained with CD71 and Ter119. Cell labelling was done at 4^0C for 15 minutes in the dark in all cases. Samples were acquired on an LSRII Fortessa (BD Biosciences) with BDFACSDiVa™ Software (BD Biosciences). FlowJo (v9.9.6; Tree Star, Ashland, OR) was used for data analysis.

2.6 Electronic exclusion of lineage positive cells

Single cells from BM were stained with Fc receptor blocking antibody, after which the cells were labelled with a cocktail of FITC conjugated monoclonal antibodies against lineage antigens. On FlowJo (v9.9.6; Tree Star, Ashland, OR), FITC positive cells were gated as lineage positive (LIN^+) cells and excluded from further analysis. In other instances, biotin conjugated monoclonal antibodies against lineage antigens was used to label LIN^+ cells. Streptavidin-PerCP-Cy5.5 was then used to electronically exclude these cells from further analysis.

2.7 *In vitro* erythroid differentiation assay

$CD150^+$ $CD27^{int}$ and $CD150^-$ $CD27^-$ haematopoietic progenitor cells were sorted using a FACS Aria IIb (Beckton Dickinson) into 5 mL Falcon® round bottom tubes containing 1 mL heat inactivated fetal calf serum (Sigma-Aldrich), then centrifuged at 300xg for 10 minutes at room temperature and resuspended in erythroid differentiation medium (EDM), which is Iscove's Modified Dulbecco's medium (Sigma-Aldrich) supplemented with 10% foetal calf serum (Sigma-Aldrich), stem cell factor (50 ng/ml, PeproTech), erythropoietin (40 ng/ml, R&D Systems), thrombopoietin (10 ng/ml, PeproTech), interleukin 3 (10 ng/ml, PeproTech),

transferrin (0.1 mg/ml, Merck), α monothioglycerol (10^{-4} M, Merck), insulin (5 μg/ml, Sigma-Aldrich) and Dexamethasone (10^{-8} M, Sigma-Aldrich). Sorted cells were seeded at a density of 1 x 10^4 cells in independent wells of a 24-well flat-bottom plate (Costar®) containing 500 μL EDM for erythroid differentiation. Post sort purity was ≥ 98%. Plates were kept in an incubator at 37^0C, 5% $C0_2$ and 95% humidity.

2.8 Blood collection and serum preparation

Mice were euthanised by inhalation of $C0_2$, after which 500-800 μL of blood was drawn from the posterior vena cava using a 25G- needle. The blood was allowed to coagulate, then centrifuged at 11000 x g for 5 minutes. The yellow supernatant (serum) was collected and frozen at -20^0C.

2.9 Enzyme linked immunosorbent assay (ELISA)

Serum samples were analysed for IFN-γ and TNF-α using the mouse IFN-γ and Mouse TNF-α ELISA Ready-SET-Go kits (eBioscience, San Diego, CA). Two-fold dilutions of samples or standards were incubated with IFN-γ or TNF-α capture antibody coated plates. IFN-γ and TNF-α were detected with the provided detection antibodies and Avidin-HRP/TMB substrate solution. The reaction was stopped with 2N sulphuric acid and plates were read on a 96-well ELISA plate reader at 450nm wavelength. The data was converted to concentration (pg. mL^{-1}) using the IFN-γ and TNF-α standard curves.

2.10 DNA extraction

Mouse tail sample was suspended in 500 μL tail lysis buffer (100mM Tris-HCl, pH8.8; 5mM EDTA pH8.0; 0.2%SDS; 200mM NaCl; proteinase K 100 μg/mL) and incubated overnight on an Eppendorf Thermomixer® at 55^0C with agitation at 300rpm. Sample was then vortexed and centrifuged at 20800 x g for 10 minutes, after which 475 μL supernatant was resuspended in new tube containing 950 μL of ice-cold ethanol (neat) to precipitate DNA. Sample was centrifuged at 20800 x g for 10 minutes, supernatant was discarded and mouse DNA was air-dried for at least 1 hour. Mouse

DNA was then resuspended in 50 µL molecular biology grade water (Merck) for PCR analysis.

2.11 Polymerase chain reaction (PCR)

Hot start PCR was used solely for genotyping animals. Reactions were carried out in 0.2 mL PCR tubes (Axygen), each reaction consisted of 4 µL of 5X PCR buffer (Promega), 1.6 µL of 25mM magnesium chloride (Promega), 0.4 µL 10mM dNTP mix, 0.2 µL Taq DNA polymerase (5 U/µL, Promega), 1 µL of template DNA (50-100 ng),1 µL each of forward and reverse primers at 10 pmol/µL for iCre PCR or 1 µL each of *loxP*1*, loxp*2 and *lox*p-site primers at 10 pmol/ µL for *Ifngr2*$^{fl/fl}$ PCR. Molecular biology grade water (Merck) was added to a final volume of 20 µL.

Tubes were placed in a PTC-200 DNA engine thermal-cycler (BIO-RAD) and run on a PCR programme based around the following: Reactions were initially denatured at 94^{0}C for 3 minutes and 30 seconds, after which GoTaq® flexi DNA polymerase (Promega) was added to reaction tubes. They were then cycled 31 times through a programme of denaturing at 94^{0}C for 40 seconds, then annealing at 62^{0}C for 30 seconds, then an extension of 30 seconds at 72^{0}C. After 31 cycles, there was a final extension step of 5 minutes at 72^{0}C. The reaction was stopped by a rapid cooling to 4^{0}C. 12 µL of PCR products were analysed by agarose gel electrophoresis at 100 V for 1 hour.

2.12 Screening for *lox-p (locus of crossover in phage P1)*-flanked alleles and *Cre* expression

In generating the *Ifngr2*$^{fl/fl}$ mice, two *loxP* sites were inserted in the *Ifngr2* locus. One *loxP* site was inserted between exons 3 and 4 and the other between exons 6 and 7 using a pBluescript II SK targeting vector (Figure 2.1A). In detail, the targeting vector for *Ifngr2* was constructed using the RED/ET cloning system (Gene Bridges). A *loxP* flanked neomycin cassette and an xho1 site was inserted between exons 3 and 4 by ET cloning. Then an 8 kb long fragment of the *Ifngr2* gene, containing the region from exon 2 to exon 7 was subcloned into pBluescript II SK. The plasmid was then

transfected into *Cre* recombinase expressing bacteria. The neomycin resistance marker gene was removed, leaving one *loxP* site with an xho1 site in the modified gene. Subsequently a FRT (flippase recognition target)-flanked neomycin gene with one *loxP* site was inserted after exon 6. After verification, the targeting vector was transfected into IDF32F1 embryonic stem (ES) cells (C56BL/6 × 129S1). The ES cell clones were screened by southern blotting with a probe of exon 7 of the *Ifngr2* gene after xho1 restriction digest. One clone, F5, was selected and used to generate chimeric mice. Germline transmission was obtained and the FRT flanked neomycin gene was removed by breeding the mice to FLP (flippase) deleter mice (122). Primers were designed to anneal in such a manner that yields 392 bp and 191bp PCR products in *Ifngr2*$^{fl/fl}$ mice and a 276bp PCR product in *Ifngr2*$^{wt/wt}$ mice (Figure 2.1B and Appendix A and B).

Vav1::iCre mice were bred to heterozygosity as recommended (125), and primers were designed to amplify a 236bp sequence unique to *Cre* recombinase. After PCR, genomic DNA from *Vav1::iCre* mice yielded the expected product of 236 bp while genomic DNA from C57BL/6 mice yielded no PCR product (Figure 2.1C).

A

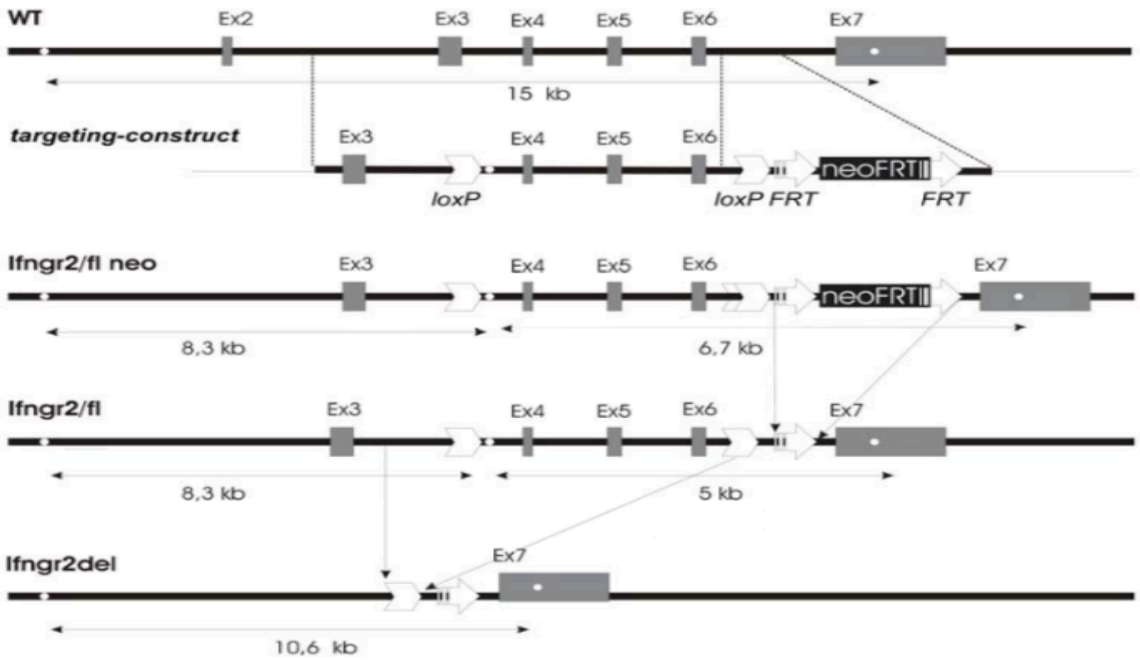

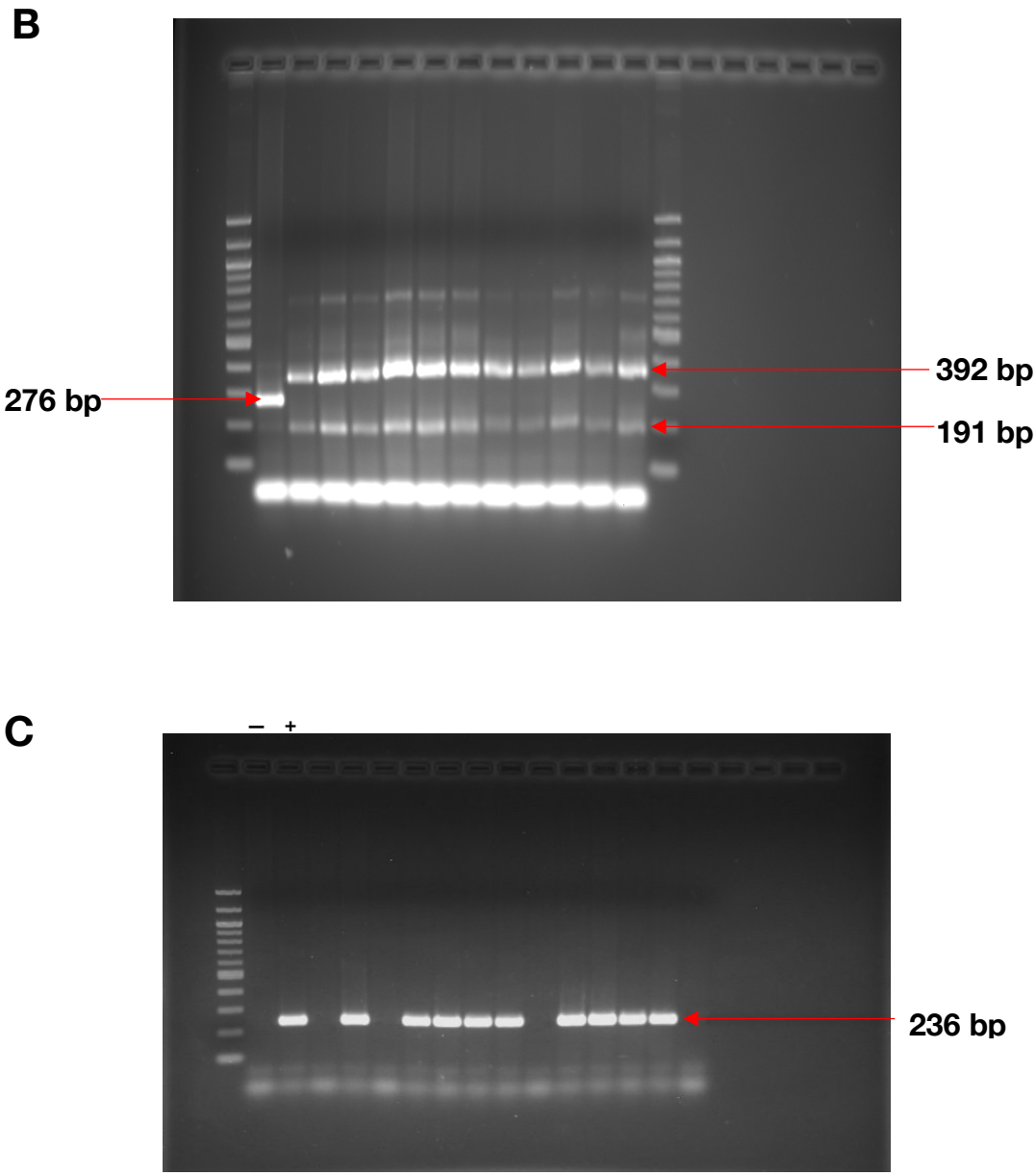

Figure 2.1 PCR for lox-p flanked alleles and Cre expression

(A) Schematic representation of the *Ifngr2* targeting strategy. Agarose gels showing **(B)** 276bp PCR product which represents Ifngr2$^{wt/wt}$ mice (lane 2), and 392bp and 191bp PCR products which represent Ifngr2$^{fl/fl}$ mice (lanes 3-13). **(C)** 236bp PCR product which represents *Vav1::iCre* mice. Negative and positive controls are shown in lanes 2 and 3 respectively. 100bp ladder (lane 1) was used in B and C.

2.13 Statistical analysis

Statistical analysis was performed using the GraphPad Prism software. Means between two groups were compared using two-tailed unpaired Student's t-test. Groups of three or more means were compared using one-way analysis of variance and the Tukey multiple comparisons test. Normal distribution of data was tested using the Shapiro-Wilk test. P values ≤ 0.05 were considered statistically significant.

Table 2.1: mAb clones and suppliers

Antigen	Name	Dilution	Clone	Fluorochrome	Supplier
CD3ε		1:200	145-2C11	FITC, Biotin	eBioscience
CD8α	Ly2	1:200	53-6.7	FITC, Biotin	eBioscience
CD11b		1:200	M1/70	FITC, Biotin	eBioscience
CD11c	Integrin aX	1:200	N418	FITC, Biotin	eBioscience
CD16/32	FcγII/III receptor	1:400	93	PE-Cy7	eBioscience
CD19		1:200	1D3	FITC, Biotin	eBioscience
CD27		1:500	LG.7F9	PE, APC	eBioscience
CD34		1:100	RAM34	FITC	eBioscience
CD45R	B220	1:200	RA3-6B2	FITC, Biotin	eBioscience
CD71	Transferrin receptor	1:2000	R17217	PE	eBioscience
CD117	c-Kit	1:200	2B8	APC-eFluor 780	eBioscience
CD127	IL-7Rα	1:200	A7R34	FITC, Biotin	eBioscience
CD135	Flk-2	1:50	A2F10	PE	eBioscience
CD150	SLAM	1:500	TC15-12F12.2	APC, PE-Cy7	BioLegend
Gr-1	Ly6G	1:200	RB6-8C5	FITC, Biotin	eBioscience
NK1.1	Ly55	1:200	PK136	FITC, Biotin	eBioscience
Ter-119	Ly76	1:200	TER-119	FITC, Biotin	eBioscience

Antigen	Name	Dilution	Clone	Fluorochrome	Supplier
Ter-119	Ly76	1:200	TER-119	APC	BioLegend
Sca-1	Ly6A/E	1:200	D7	Pacific Blue, BV 421	BioLegend
Streptavidin		1:1000		PerCP-Cy5.5	eBioscience
Mouse Seroblock FcR		1:10	FCR4G8		BIO RAD

Table 2.2 Primer sequences

Primer name	Sequence
iCre forward	5'-AGA TGC CAG GAC ATC AGG AAC CTG-3'
iCre reverse	5'-ATC AGC CAC ACC AGA CAC AGA GAT C-3'
LoxP1	5'-TGA GTT CCA AGC AAG ACA GA-3'
LoxP site	5'-AAG TTA TGG TCT GAG CTC GC-3'
LoxP2	5'-CAG GGT AGA AAA GAT GTG CA-3'

CHAPTER 3

ERYTHROPOIESIS IN STEADY STATE

3.1 Introduction

The pool of haematopoietic progenitor cells (HPC) act as a critical population for lineage specification between the haematopoietic stem cells (HSCs)/multipotent progenitors (MPPs), and more mature erythroid, megakaryocytic and myeloid cells. The HPCs are defined as lineage negative (LIN^-) and have a high surface expression of CD117/c-KIT but unlike the HSCs and MPPs, they do not express Sca-1 on their surface in steady state (12). The HPC compartment contains at least three different progenitor populations, which are the CMP ($CD16/32^{lo}$ $CD34^+$), MEP ($CD16/32^{lo}$ $CD34^-$) and GMP ($CD16/32^{hi}$ $CD34^+$) (12) and are the progeny of MPPs (Figure 3.1).

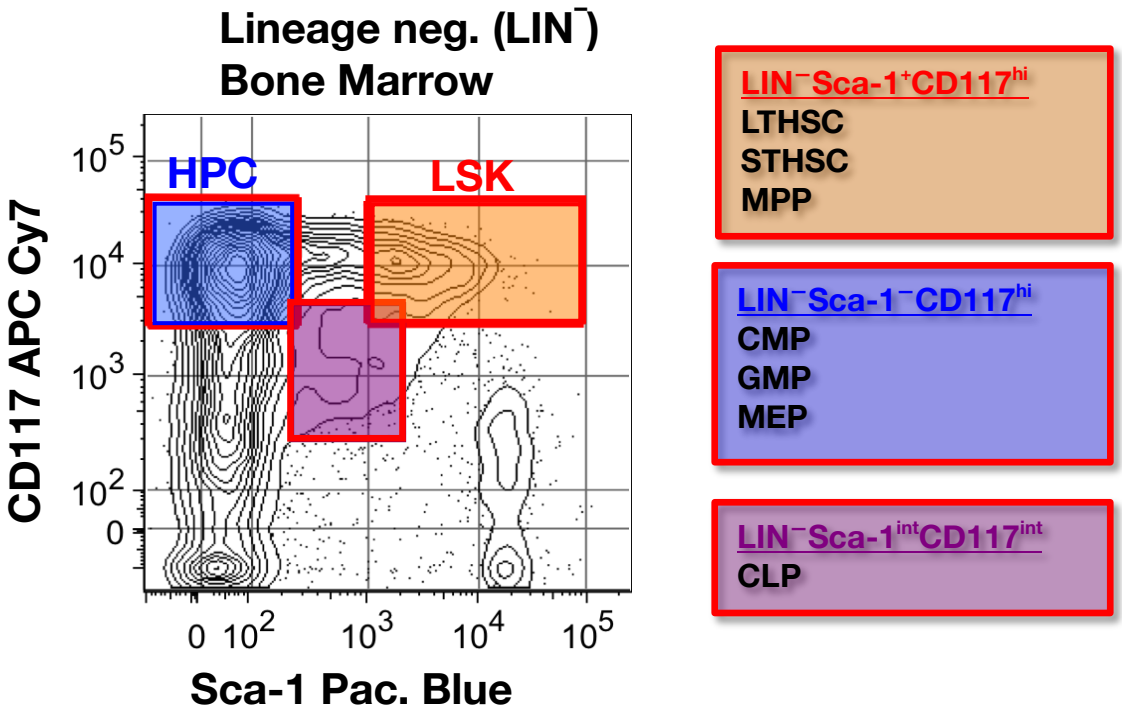

Figure 3.1 Haematopoietic progenitor cells in steady state

The pool of haematopoietic progenitor cells is made up of CMP, GMP and MEP and arise from the differentiation of multipotent progenitors which reside in the LSK pool. This differentiation is coupled with loss of surface expression of stem cell antigen 1 (Sca-1). Abbreviations: LSK; $LIN^-Sca\text{-}1^+c\text{-}KIT^{hi}$, HPC; haematopoietic progenitor cells, LTHSC; long-term haematopoietic stem cell, STHSC; short-term haematopoietic cells, MPP; multipotent progenitors, CMP; common myeloid progenitor, GMP; granulocyte-macrophage progenitor, MEP; megakaryocyte-erythroid progenitor, CLP; common lymphoid progenitor.

The surface markers currently in use to identify the erythroid and myeloid progenitors within the HPC, namely CD16/32 and CD34 only poorly resolve these populations with no clear-cut demarcation of myeloid progenitors that express CD34 on their surface from erythroid progenitors that do not, resulting in an operational problem of how to separate successfully overlapping subpopulations. The inability to isolate erythroid progenitors at a high purity has limited the study of erythropoiesis to more mature erythroid populations such as the BFU-e and CFU-e which are identified based on their morphology in clonogenic assays.

To address this problem, I aimed to find novel surface marker combinations that could better resolve the HPC pool into distinct myeloid and erythroid progenitors. In addition, the surface expression of such markers would have to be stable during infection. Next, I confirmed using *in-vitro* functional assays that the erythroid progenitors I identified using these novel marker combinations are *bona fide* erythroid progenitors.

In this chapter, I performed phenotypic profiling of BM erythroid and myeloid progenitors in steady state, using markers known from literature to be connected to erythroid and myeloid commitment. I also characterised and quantified BM erythroid precursors using the most recent gating strategy (34), to confirm that the 1:2:4:8 ratio of erythroblast maturation is maintained in steady state, which reflects the physiological progression of terminal erythroid differentiation in mice.

3.2 Defining haematopoietic progenitors in the adult BM in steady state

The HPC constitutes a rare pool of LIN^- BM progenitors and identifying them requires the physical depletion or electronic exclusion of LIN^+ cells. In this experiment, naïve female C57BL/6 mice aged 8 to 12 weeks were used. A pair of femur and tibia was isolated from each of three mice and single-cell suspensions of BM cells were prepared and pooled. Next, I performed a physical depletion of LIN^+ BM cells to obtain LIN^- cells as described in the Materials and Methods. Results show that after the depletion protocol, there was a loss of most of the granulocytes which have a

high side scatter and most of the reticulocytes which have a low forward scatter (Figure 3.2A). To ascertain the efficiency of the depletion of LIN^+ cells, the frequency of residual LIN^+ cells after the depletion protocol was determined and the $Gr1^+$ cells were the major contaminants (Figure 3.2B). Considering that the physical depletion of LIN^+ BM cells is not 100% efficient, I further excluded residual LIN^+ cells which were biotinylated during the depletion step, using streptavidin (Figure 3.2C).

To identify BM HPC subsets using the classical scheme pioneered by Akashi and colleagues (12), LIN^- cells were labelled with fluorochrome conjugated monoclonal antibodies against CD117, Sca-1, CD16/32 and CD34. The gating strategy involved selecting live LIN^-cells, excluding doublets, selecting the $CD117^{hi}$ $Sca\text{-}1^-$population and resolving this population into the MEP, CMP and GMP based on surface expression of CD16/32 and CD34 (Figure 3.2D). 7-Amino-Actinomycin D (7AAD) was used to distinguish live from dead cells in all experiments. Consistent with published works (12,68,102), the use of CD16/32 and CD34 only poorly resolved these populations and would present enormous difficulties in sorting these populations at a high purity, thus justifying the need to identify novel marker combinations.

The surface expression of CD27 on cells within the HPC compartment is associated with myeloid potential while the lack thereof is associated with megakaryocytic/erythroid potential (68). Using this marker, I would be able to segregate the MEPs which are $CD27^-$ from the myeloid progenitors (CMP and GMP) which are $CD27^+$. I incorporated as second marker the SLAM family member CD150, to resolve the heterogeneity in the megakaryocytic/erythroid pool, which had been identified by Pronk *et al*. using CD150 and CD105 (19). Next, I determined the CD150 and CD27 surface expression in classically defined MEP, CMP and GMP. LIN^- cells were labelled with fluorochrome conjugated monoclonal antibodies against CD117, Sca-1, CD16/32, CD34, CD150 and CD27. Anti-CD150 and Anti-CD27 cell labelling revealed heterogeneity in the classically defined MEP and CMP. Both progenitors had $CD150^-$ and $CD150^+$ subpopulations, in addition, the MEP had $CD27^-$ and $CD27^{Int}$ subpopulations while the CMP had $CD27^+$ and $CD27^{int}$ subpopulations. The GMP remained homogenous and was $CD150^-$ and $CD27^+$ (Figure 3.2E). In contrast to the $CD150^-$ CMP and GMP that express CD27, the $CD150^-$MEP did not express CD27.

Interestingly, both the CD150^{+} fractions of the MEP and CMP were CD27^{int} and made up 15.5 ± 2.1% and 31.8 ± 5.3% of the cells respectively.

I super-imposed these populations derived from the CD150/CD27 break down of the MEP, CMP and GMP, and identified three distinct populations which were CD150^{-} CD27^{-} (megakaryocytic/erythroid), CD150^{-}CD27^{+} (myeloid) and a unique population that was CD150^{+}CD27^{int} (Figure 3.2F). CD150 is expressed by cells higher up the haematopoietic pathway such as the LTHSCs and MPP2 which is an erythroid biased multipotent progenitor (15), and its expression in subpopulations of MEP and CMP suggest that these subpopulations might be more primitive than their respective CD150^{-} fractions and might constitute a population of their own.

To further confirm phenotypically, the identity of these populations resolved using the novel marker combination of CD150 and CD27, I incorporated an additional marker CD135. also known as foetal liver kinase 2 (FLK2) or fms-like tyrosine kinase 3 (FLT3). CD135 is not expressed on MEPs and HSCs but is present on CMPs, GMPs and MPP4 (126). LIN^{-} cells were labelled with fluorochrome conjugated monoclonal antibodies against CD117, Sca-1, CD150, CD27 and CD135. Within the HPC pool, the CD150^{-}CD27^{-} and CD150^{+} CD27^{int} populations were both CD135^{-}, whereas 59.5 ± 3.5% of the CD150^{-}CD27^{+} population expressed CD135 on their surface (Figure 3.2G).

A

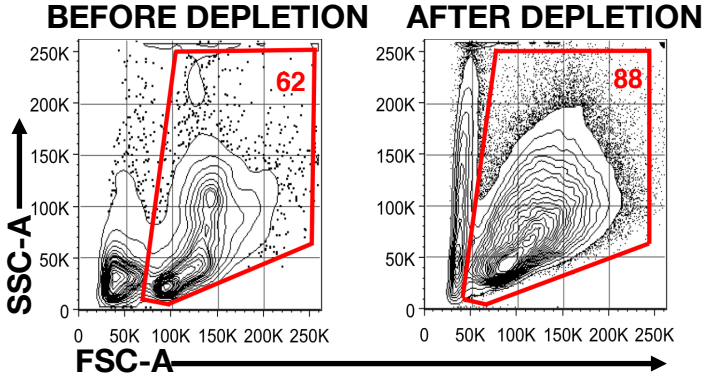

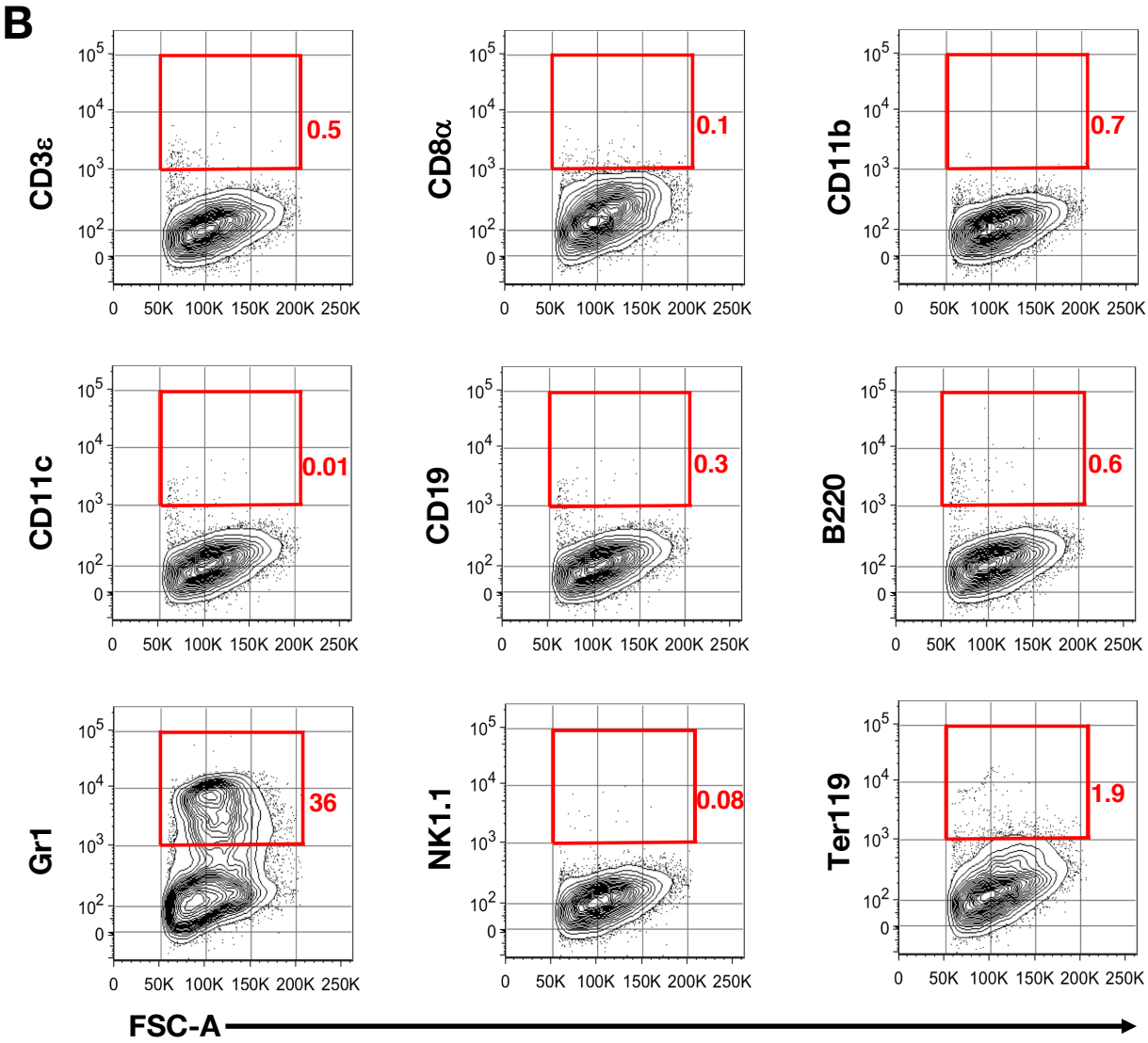
B
CD3ε
0.5
CD8α
0.1
CD11b
0.7
CD11c
0.01
CD19
0.3
B220
0.6
Gr1
36
NK1.1
0.08
Ter119
1.9
0 50K 100K 150K 200K 250K
FSC-A
C
Cell number
32
STREPTAVIDIN
PerCP-Cy5.5
Gr1 FITC
4
FSC-A

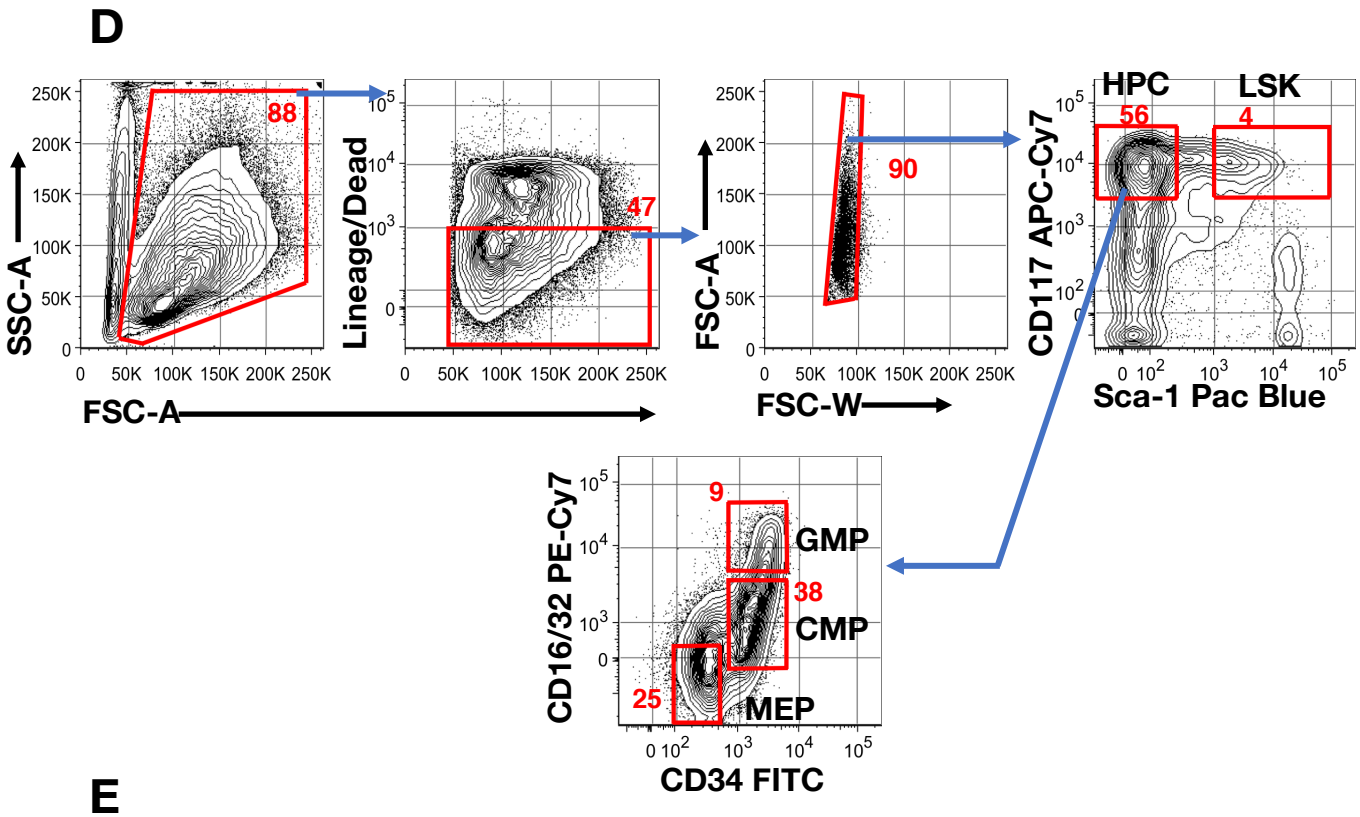
D
SSC-A
FSC-A
88
Lineage/Dead
47
FSC-A
FSC-W
90
HPC
LSK
56
4
CD117 APC-Cy7
Sca-1 Pac Blue
CD16/32 PE-Cy7
CD34 FITC
9
GMP
38
CMP
25
MEP

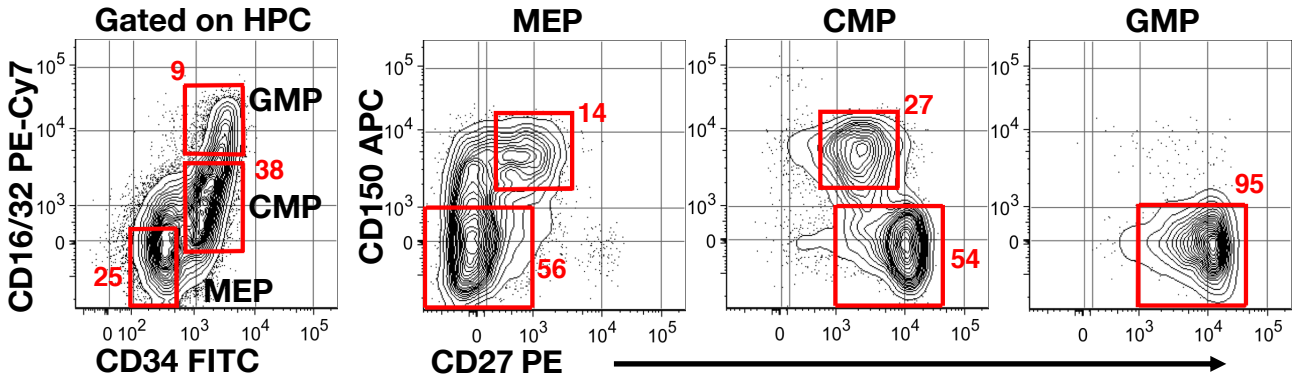
E
Gated on HPC
MEP
CMP
GMP
CD16/32 PE-Cy7
CD34 FITC
CD150 APC
CD27 PE
9
GMP
38
CMP
25
MEP
14
56
27
54
95

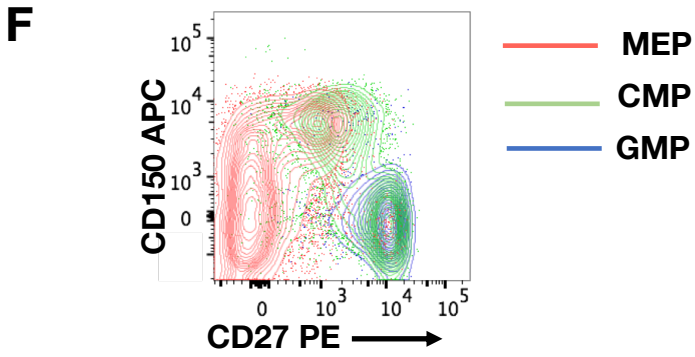
F
CD150 APC
CD27 PE
MEP
CMP
GMP

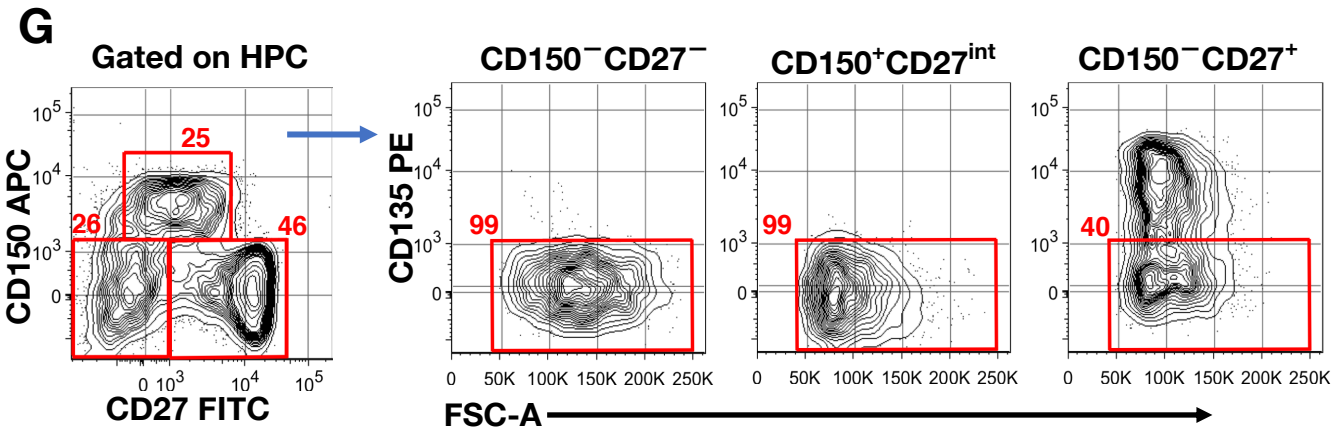

Figure 3.2 CD150, CD27 and CD135 surface expression reveals phenotypic heterogeneity of early BM haematopoietic progenitor cells

(A-B) BM cells isolated from femur and tibia of WT mice were physically depleted of LIN$^+$ cells by magnetic activated cell sorting (MACS), and the frequency of residual LIN$^+$ cells was determined. Representative FACS plots illustrating **(A)** the cell size (FSC-A) and granularity (SSC-A) of BM cells, before and after depletion of LIN$^+$ cells. **(B)** the frequency of residual CD3ε$^+$ CD8α$^+$, CD11b$^+$, CD11c$^+$, CD19$^+$, B220$^+$, Gr1$^+$, NK1.1$^+$ and Ter119$^+$ cells after physical depletion protocol. Monoclonal antibodies against lineage antigens were conjugated to FITC. **(C-G)** Residual LIN$^+$ cells were electronically excluded using streptavidin and LIN$^-$ cells were labelled with fluorochrome conjugated monoclonal antibodies against CD117, Sca-1, CD16/32, CD34, CD150, CD27 and CD135. 7-Aminoactinomycin D (7AAD) was used to exclude dead cells. **(C)** Representative FACS plots showing the frequency of LIN$^-$ cells and residual Gr1$^+$ cells after electronic exclusion of LIN$^+$ cells by streptavidin. Of note is the substantial reduction in frequency of Gr1$^+$ cells **(D)** Gating strategy for the identification of HPC subsets; MEP, CMP and GMP. **(E)** CD150 and CD27 surface expression in MEP, CMP and GMP **(F)** Representative FACS plot illustrating how the classically defined CMP, MEP, and GMP align, when stained with CD150 and CD27. **(G)** CD135 surface expression in CD150$^-$CD27$^-$, CD150$^+$CD27^{int} and CD150$^-$CD27$^+$ HPC subsets.

(A-G) Data represents three individual experiments with similar results using three mice in each experiment; n=9.

3.3 Analysis of the functional potential of CD150$^+$ CD27^{int} and CD150$^-$CD27$^-$ HPCs

Having used a novel phenotypic approach to identify a unique population within the HPC pool that is, the CD150$^+$ CD27^{int} HPC, I determined Its functional potential

in vitro. Based on the work of Pronk and colleagues (19), I hypothesised that this population might contain the Pre-MEP owing to the surface expression of CD150, and the absence of CD135 surface expression. The functional potential of the CD150$^-$ CD27$^-$ HPC was also determined *in-vitro* to confirm that this population is a *bona fide* MEP.

Using pooled BM from eight naïve female C57BL/6 mice, both populations were isolated by fluorescence activated cell sorting (FACS) to a purity greater than 95% (Figure 3.3 A-C). After cell sorting, 1 x 10^4 CD150$^+$ CD27^{int} and CD150$^-$ CD27$^-$HPCs were seeded into the wells of a 24-well flat-bottomed plate containing erythroid differentiation medium (described in Materials and Methods).

After 36 hours in culture, the CD150$^+$ CD27^{int} population lost surface expression of both CD150 and CD27 to acquire a MEP-like phenotype (Figure 3.4A and Table 3.1) indicating that this population contains the Pre-MEP. The CD150$^-$ CD27$^-$ population acquired the erythroid marker Ter119 after 6 days in culture (Figure 3.4B and Table 3.2), confirming that this population is the MEP.

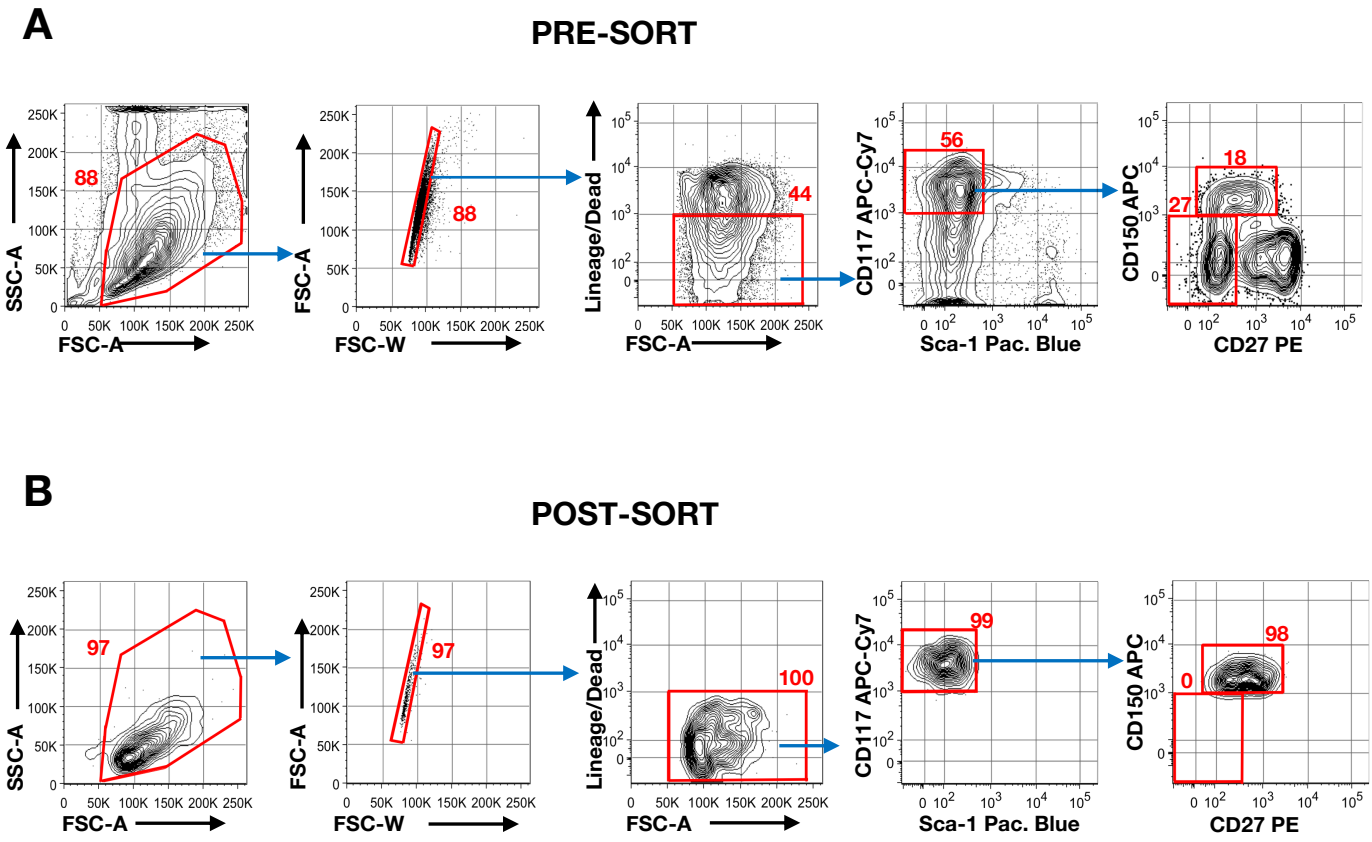

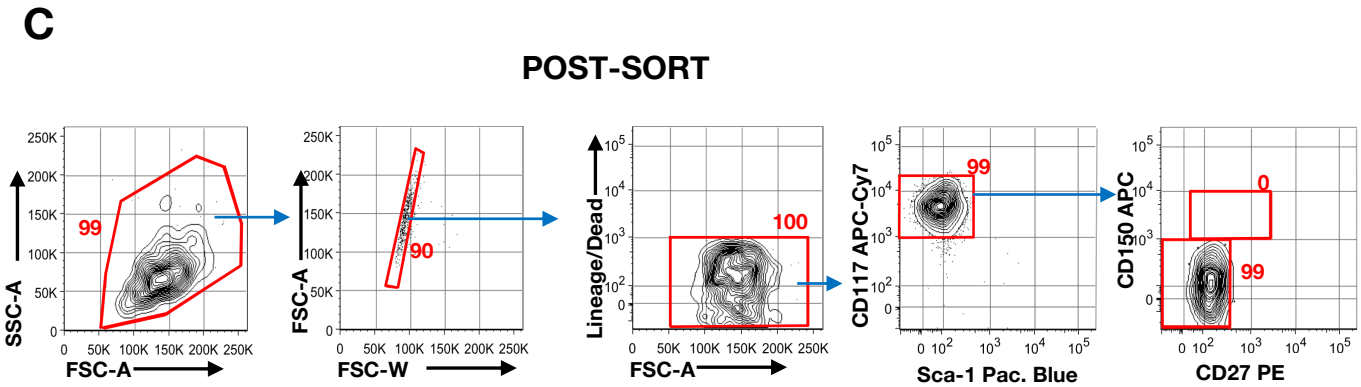

Figure 3.3 Analysis of CD150⁺ CD27^{int} and CD150⁻ CD27⁻ HPC subsets before and after FACS purification

BM from eight naive female C57BL/6 mice were pooled, LIN⁺ cells were physically depleted and both CD150⁺CD27^{int} and CD150⁻CD27⁻ HPC subsets were FACS purified. **(A)** Pre-sort gating strategy for CD150⁺CD27^{int} and CD150⁻CD27⁻ HPC subsets. Post-sort analysis show that both CD150⁺CD27^{int} and CD150⁻CD27⁻ HPC subsets were sorted to over 95% purity in **(B)** and **(C)** respectively.

(A-C) Data represents three individual experiments with similar results using eight mice in each experiment, n=24.

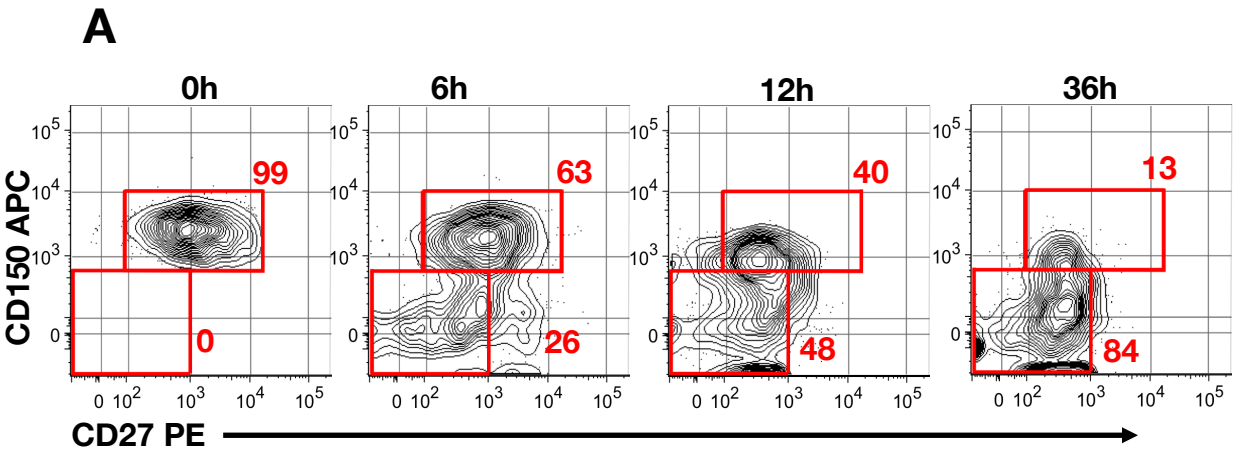

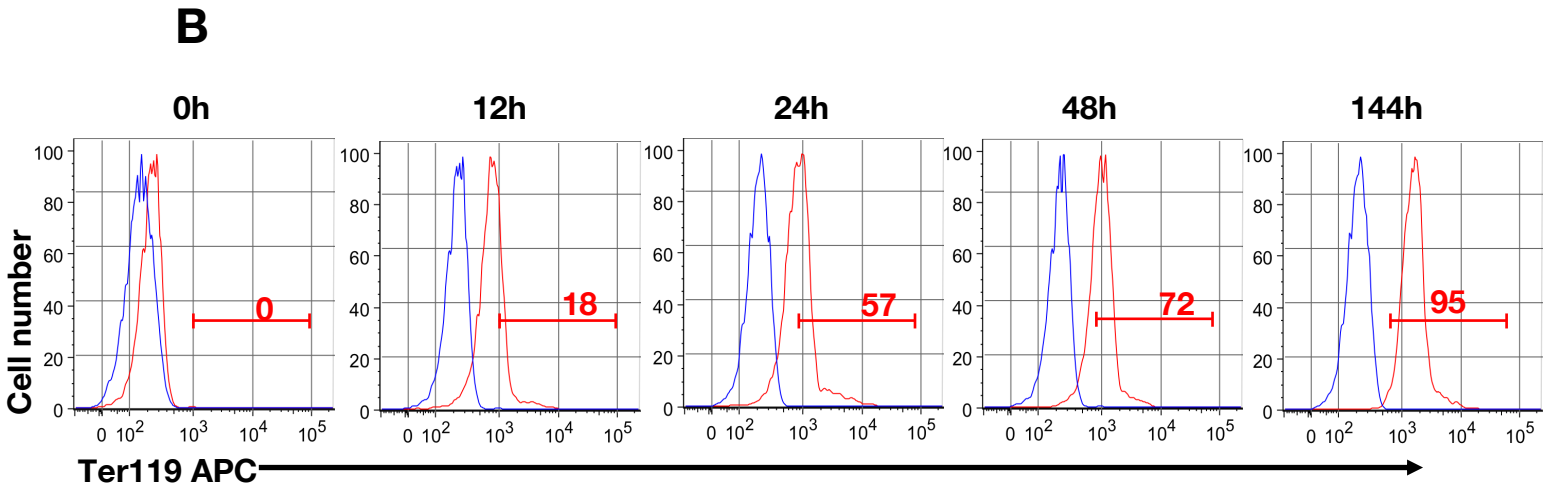

Figure 3.4 Lineage commitment fate of CD150⁺ CD27^{int} and CD150⁻ CD27⁻ HPC subsets in vitro

(A) CD150⁺ CD27^{int} HPC subset were purified by FACS from steady state LIN⁻ BM cells and stained for surface expression of CD150 and CD27 before and at several time points after culture under erythroid conditions. CD150⁺ CD27^{int} HPC exhibit erythroid potential and differentiate to CD150⁻ CD27⁻HPC *in vitro*. Data represents three independent experiments, using eight female C57BL/6 mice in each experiment, n=24. **(B)** CD150⁻ CD27⁻ HPC subset were purified by FACS from steady state LIN⁻ BM cells and stained for surface expression of Ter119 before (Post sort, blue line shows unstained control) and at several time points after culture under erythroid conditions. CD150⁺ CD27^{int} HPC is a direct precursor of CD150⁻ CD27⁻ HPC and both populations exhibit erythroid potential with the latter differentiating to Ter119⁺ erythroblasts *in vitro*. **(A and B)** Data represents three independent experiments, using eight female C57BL/6 mice in each experiment, n=24.

Table 3.1 CD150⁺ CD27^{int} HPC is a direct precursor of CD150⁻CD27⁻HPC

Time (hours)	CD150⁺ CD27^{int} HPC (mean ± SD)	CD150⁻ CD27⁻HPC (mean ± SD)
0	98.3 ± 0.5	0
12	66.0 ± 3.6	23 ± 3.1
24	43.3 ± 3.5	42 ± 7.2
36	15.3 ± 2.5	76.6 ± 7

Note: Values represent the frequency of $CD150^+$ $CD27^{int}$ and $CD150^-CD27^-$ HPC subsets at several time-points in culture under erythroid conditions.

Table 3.2 $CD150^-CD27^-$ HPC differentiate to $Ter119^+$ erythroblasts *in vitro*

Time (hours)	$Ter119^+$ Cells (mean ± SD)
0	0
12	16.3 ± 1.5
24	52.6 ± 4.5
48	68.0 ± 3.6
144	90.6 ± 3.8

Note: Values represent the frequency of $Ter119^+$ cells arising from the differentiation of $CD150^-CD27^-$HPC under erythroid conditions.

3.4 Defining erythroid precursors in the adult BM in steady state

Previous studies identifying erythroid precursors involved staining the whole BM using two markers CD71 and Ter-119 without eliminating other BM subsets which are prone to possible variation in their numbers in the BM as part of the circadian rhythm of the neuro-endocrine system. This could impinge on the calculated frequencies and absolute numbers of erythroid precursors under homeostatic condition and in infection-induced state. I refined the identification scheme to be less dependent on possible variations of other BM subsets.

To resolve erythroid precursors in steady state, pooled BM cells from two or three female C57BL/6 mice were first physically depleted of $CD3\varepsilon^+$, $CD11b^+$, $CD19^+$ and $Gr1^+$ cells by magnetic activated cell sorting (MACS) using biotinylated monoclonal

antibodies against these surface markers, then labelled with fluorochrome conjugated anti-CD71, anti-Ter119 and streptavidin. 7AAD was used to distinguish live from dead cells. The gating strategy for identifying erythroid precursors involved electronically excluding residual CD3ε$^+$, CD11b$^+$, CD19$^+$ and Gr1$^+$ BM cells, dead cells and doublets. The cells were first resolved based on surface expression of CD71 and Ter119 with the proerythroblasts identified as CD71$^+$ Ter119^{int} cells. The Ter119$^+$ cells were then resolved into basophilic, polychromatic and orthochromatic erythroblasts based on surface expression of CD71 and cell size in accordance with the gating strategy employed by Chen and colleagues (33). I observed a gradual decrease in CD71 expression and cell size from the basophilic to the orthochromatic erythroblast (Figure 3.5A). Using this combination of markers and gating strategy, I observed that the steady state physiological progression of terminal erythroblast maturation follows a 1:2:4:8 pattern in frequency (Figure 3.5B).

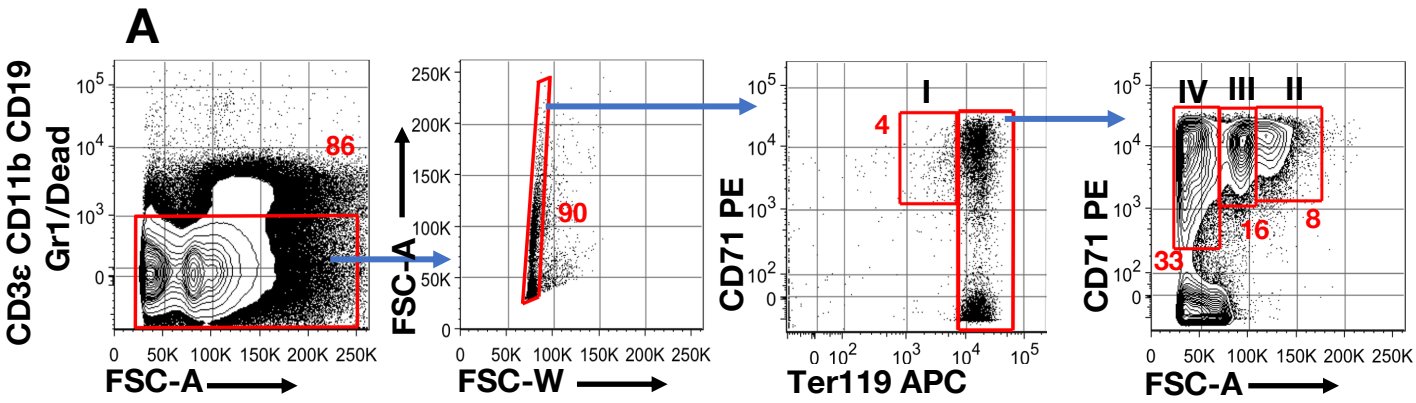

I: Proerythroblast (CD71$^+$Ter119^{int})

II: Basophilic erythroblast (CD71$^+$Ter119$^+$FSC-A^{hi})

III: Polychromatic erythroblast (CD71$^+$Ter119$^+$FSC-A^{int})

IV: Orthochromatic erythroblast (CD71$^+$Ter119$^+$FSC-A^{lo})

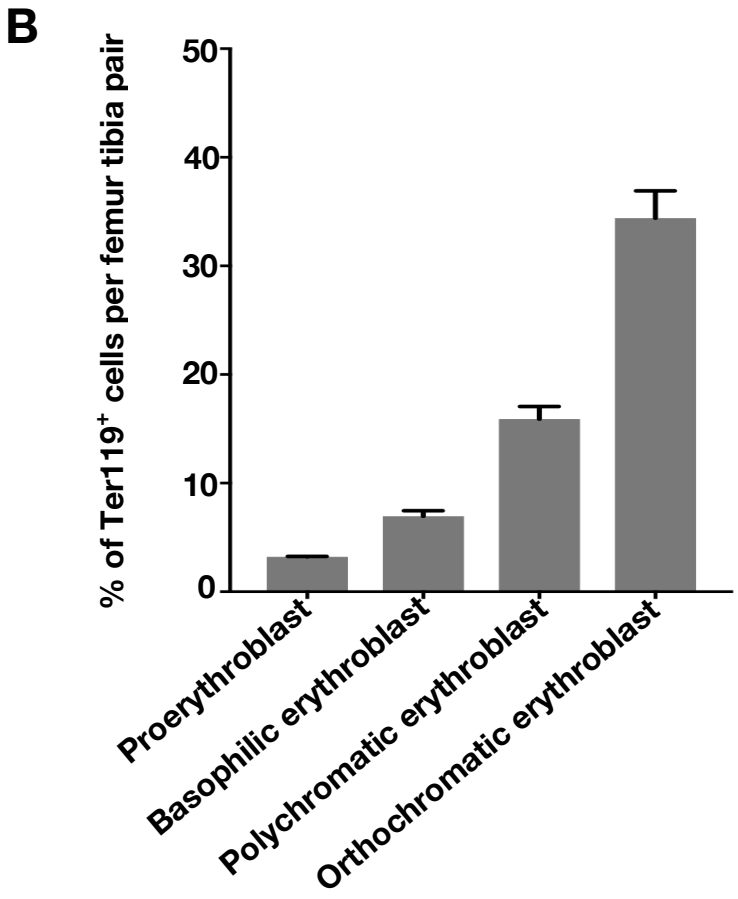

Figure 3.5 Characterisation of BM erythroid precursors in steady state

BM cells were depleted of T cells, monocytes, B cells and granulocytes by MACS using biotinylated monoclonal antibodies against CD3ε, CD11b, CD19 and Gr1, then stained with Streptavidin-PerCP-Cy5.5, CD71-PE and Ter119-APC. 7AAD was used to exclude dead cells. **(A)** Gating strategy for the identification of erythroid precursors. I, II, III and IV represent the proerythroblasts, basophilic erythroblasts, polychromatic erythroblasts and orthochromatic erythroblasts respectively. (**B**) Bar chart showing the mean frequency of erythroid precursors as a percentage of all Ter119$^+$ cells. Among all Ter-119$^+$ BM cells, proerythroblasts, basophilic erythroblasts, polychromatic erythroblasts and orthochromatic erythroblasts had a frequency of 3.5 ± 0.1%, 7.1 ± 0.5%, 15.9 ± 1.2% and 34.4 ± 2.5%, a ratio of 1:2:4:8 demonstrating the expected doubling of cell number with each successive mitosis.

Data represents six individual experiments using two to three mice per experiment. Bars represent mean ± SEM , n=16 mice.

3.5 Quantitation of haematopoietic progenitor cells and erythroid precursors in steady state.

To determine the absolute number of HPC subsets and erythroid precursors, I opted for a different approach. Rather than physically depleting LIN^+ cells I electronically excluded all LIN^+ cells as described in the Materials and Methods.

Some of the merits of electronic exclusion over physical depletion of LIN^+ cells are reproducibility, reliability and ease of processing under pathological conditions. Also, at the start of sample acquisition, all the cell types in the BM are present at the normal frequency in steady state, calculated gate frequencies are a fraction of the entire BM and can be used to determine the absolute number of cells per femur/tibia pair. Furthermore, erythroid precursors have ferrous iron (Fe^{2+}) in the haem complex which might result in these cells being trapped in the magnetic column and hamper recovery.

To determine the absolute number of $CD150^-CD27^-$, $CD150^-CD27^+$ and $CD150^+CD27^{int}$ HPC subsets, first I prepared single-cell suspensions of BM obtained from femur and tibia pair of each mouse and determined the cellularity. Next, I labelled the BM cells with FITC conjugated monoclonal antibodies against lineage markers, CD117, Sca-1, CD150 and CD27.

After excluding dead cells, doublets and LIN^+ cells, the LIN^- cells had a frequency of $1.2 \pm 0.3\%$ of total BM cells (Figure 3.6A) and a mean absolute number per femur/tibia pair of $5.1 \times 10^5 \pm 2.4 \times 10^4$ (Figure 3.6B) The LIN^- cells were further resolved on the basis of CD117 and Sca-1 to identify the HPC pool. Within the HPC pool, I observed in steady state that the $CD150^-CD27^+$ HPC subset was the most abundant, while the $CD150^+CD27^{int}$ HPCs were the least abundant (Figure 3.6B)

To determine the absolute number of erythroid precursors, I prepared single-cell suspensions of BM obtained from femur and tibia pair of each mouse, then determined the cellularity. After excluding T cells, monocytes, B cells and granulocytes, live single cells were resolved based on surface expression of CD71 and Ter119 as previously described in Figure 3.5A. Using the calculated frequencies

and BM cellularity, the absolute number of each erythroid precursor per femur/tibia pair was determined. In steady state, the mean BM cellularity was $4.6 \times 10^7 \pm 2.4 \times 10^6$, while the mean absolute number of proerythroblasts, basophilic erythroblasts, polychromatic erythroblasts and orthochromatic erythroblasts per femur/tibia pair was $7.2 \times 10^5 \pm 1.8 \times 10^5$, $1.7 \times 10^6 \pm 2.5 \times 10^5$, $3.9 \times 10^6 \pm 2.1 \times 10^5$ and $8.0 \times 10^6 \pm 6.1 \times 10^5$ respectively (Figure 3.6C).

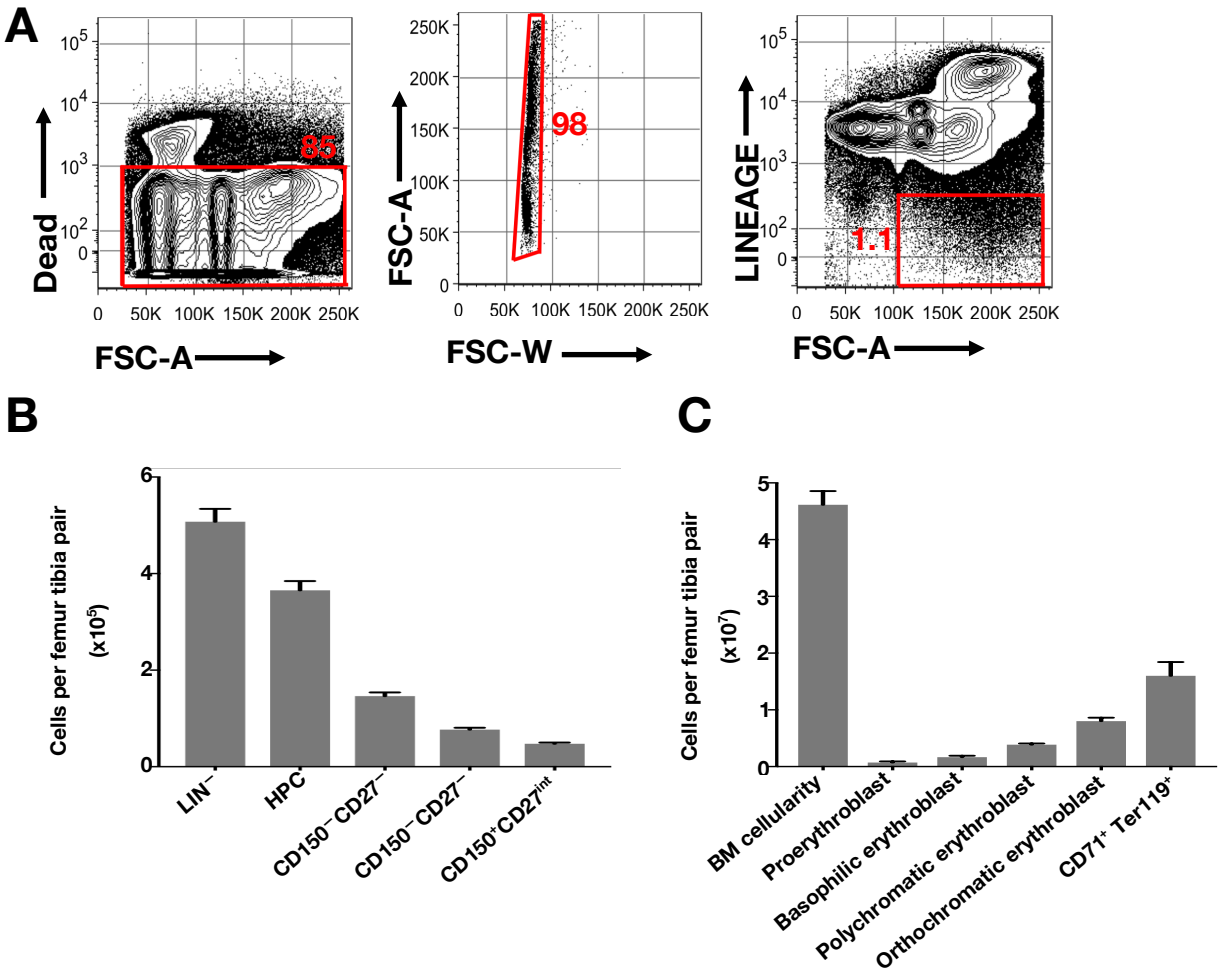

Figure 3.6 Quantitation of erythroid progenitors and precursors in murine BM in steady state

(A) Representative FACS plots illustrating the frequency of LIN^- cells per femur/tibia pair, in which LIN^+ cells have been electronically excluded. Data represents six experiments using two to three female mice in each experiment, n =16. **(B)** Absolute number per femur tibia pair of LIN^- cells, HPC, $CD150^-CD27^-$, $CD150^+CD27^{int}$ and $CD150^-CD27^+$HPC subsets. **(C)** Absolute number per femur tibia pair of all BM cells, proerythroblasts, basophilic erythroblasts, polychromatic erythroblasts, orthochromatic erythroblasts and all $CD71^+$ $Ter119^+$ cells. **(B and C)** Results are representative of six

independent experiments using two to three female mice in each experiment. Values represent mean ± SEM, n=16 mice.

3.6 Discussion

The BM under homeostatic conditions is the only site of erythropoiesis in mice and humans. Hence, the accurate enumeration of erythroid populations with a high degree of accuracy is a pre-requisite for the study of disordered erythropoiesis. Furthermore, it is the basis of the prospective isolation of developmental-ordered subpopulations for further analysis.

For almost two decades, the surface markers CD16/32 and CD34 have been used to identify the three main subpopulations within the HPC pool; MEP, CMP and GMP. This marker combination only poorly resolves these HPC subsets and result in low purity of FACS sorted cells. Data from our lab using this marker combination, showed considerable contamination of FACS purified MEPs by CMPs (68). Furthermore, the use of CD16/32 and CD34 does not permit the identification of a recently described population within the HPC pool the Pre-MEP. There is therefore a need for novel marker combinations that can identify these HPC subsets at a greater resolution and high purity.

I sought surface markers that were stable during infection and based on published works (19,68) , I came up with two surface markers namely CD150 and CD27. By substituting CD16/32 and CD34 for CD150 and CD27, I was able to show heterogeneity within the HPC pool, similar to findings by Pronk and colleagues (19). Furthermore, I was able to identify a novel population within the HPC pool which is $CD150^{+}CD27^{int}$. Phenotypic profiling revealed that both the $CD150^{+}CD27^{int}$ and $CD150^{-}CD27^{-}$ lacked surface expression of CD135 whereas majority of the $CD150^{-}CD27^{+}$ cells expressed CD135 on their surface. CD135 promotes the survival and proliferation of myeloid progenitors (127,128) and its expression on the $CD27^{+}$cells, further confirms that CD27 is a marker for myeloid commitment in the HPC pool. The absence of CD135 surface expression on $CD150^{+}$ $CD27^{int}$ HPC subset clearly argues that this population is biased towards an erythroid lineage fate and might contain the pre-MEP. After *in vitro* functional assays, I demonstrated that the $CD150^{-}CD27^{-}$ HPC

subset is the MEP analogue while the $CD150^{+}CD27^{int}$ HPC subset is the Pre-MEP analogue. The $CD150^{+}CD27^{int}$ HPC subset committed to an erythroid fate under erythroid conditions, nevertheless, it remains to be seen if this recently described population exhibits some degree of lineage plasticity and is able to commit to a myeloid fate under myeloid conditions.

The use of CD71, Ter119 and cell size to identify erythroid precursors in BM was able to recapitulate the physiological progression of normal murine terminal erythroid differentiation at a ratio of 1:2:4:8. Any deviation from this ratio might be indicative of disordered erythropoiesis and could provide important leads for mechanistic studies defining stage-specific defects in erythroid maturation in inherited and acquired red cell disorders. In previous studies, the use of the surface markers CD71 and Ter119 alone to identify erythroid precursors in the BM had failed to achieve the expected ratio of 1:2:4:8 and this might have been due to the different gating strategies employed in the identification of these cells, as well as the failure to incorporate cell size in distinguishing the various stages of erythroblast maturation.

Similar to a previous study by Chen and colleagues (33), I observed a progressive decrease in cell size and surface expression of transferrin receptor as the erythroid precursors differentiated from the basophilic erythroblast to orthochromatic erythroblasts Furthermore it has been reported that the orthochromatic erythroblasts are the same size as mature erythrocytes (33,129) and this was my observation when I identified these populations. While the mature erythrocytes express Ter119 but do not express CD71, the orthochromatic erythroblasts express both Ter119 and CD71. In addition, immature reticulocytes express CD71 (130,131) and cluster in the same gate as the orthochromatic erythroblasts (33). An inherent problem in using CD71 and Ter119 to identify erythroid precursors, is that this marker combination does not permit the orthochromatic erythroblasts to be distinguished from immature reticulocytes.

in contrast to the mapping of the myeloid population in detail, the early erythroid subsets have been quite neglected. I have demonstrated an unpublished method for the identification and isolation of primitive erythroid progenitors at high purity. In this study, I defined erythroid progenitors within the HPC pool namely, the MEP as LIN^{-}

$CD117^{hi}$ Sca-$1^{-}CD150^{-}CD27^{-}CD135^{-}$ and the Pre-MEP as LIN^{-} $CD117^{hi}$ Sca-1^{-} $CD150^{+}CD27^{int}CD135^{-}$. Although the labelling of HPC with anti-CD150 and anti-CD27 fluorochrome conjugated monoclonal antibodies is sufficient to resolve the distinct erythroid progenitors within the HPC pool, it does not resolve the myeloid progenitors into distinct CMP and GMP with both progenitor populations clustering in the same gate, that is the $CD150^{-}CD27^{+}$ gate. Hence, I defined myeloid progenitors (CMP and GMP) as LIN^{-} $CD117^{hi}$ Sca-$1^{-}CD150^{-}CD27^{+}$. This limitation should not impair studies of disordered erythropoiesis, nevertheless, in studies of myelopoiesis, anti-CD16/32 fluorochrome conjugated monoclonal antibody could be incorporated to distinguish CMP which are $CD16/32^{lo}$ from GMP which are $CD16/32^{hi}$.

The use of CD150/CD27 marker combination to resolve HPC subsets is a significant contribution to the field and provides better resolution of erythroid progenitors (MEP and Pre-MEP), higher purity of FACS sorted cells and clearly segregates myeloid from erythroid progenitors. A notable contribution of this study is that the ability to isolate primitive erythroid progenitors in large quantity and high purity should enable a detailed molecular characterisation of these populations and provide useful insights into the mechanisms of erythropoiesis. The purified erythroid cells might also be useful for screening drugs that would specifically target distinct erythroid stages which could lead to novel therapeutic approaches for patients with disordered erythropoiesis. In future studies on the consequence of malaria on erythroid development in wild type mice and in mice lacking IFN-γ signalling specifically in haematopoietic cells, this marker combination will be used to identify the MEP, Pre-MEP and CMP/GMP. I have referred to the MEP, Pre-MEP and CMP/GMP population simply as CD27 neg. CD27 int. and CD27 pos. HPC respectively in subsequent chapters.

.

CHAPTER 4

IMPACT OF MALARIA ON ERYTHROID DEVELOPMENT

4.1 Introduction

During malaria, the exact stage of erythroid development in the BM, at which suppression of erythropoiesis sets in remains unknown. Furthermore, there is at present, no study on malaria dyserythropoiesis that has investigated cells with erythroid potential but lacking myeloid and lymphoid potential, that are more primitive than the BFU-e. Hence, malaria dyserythropoiesis could be due to defective potential for erythroid development in HSCs, MPPs or erythroid precursors alone or in combination.

The aetiology of SMA is multifactorial but two main mechanisms stand out, the destruction of parasitised and non-parasitised erythrocytes as a result of parasite replication and splenic clearance respectively, and the suppression of erythropoiesis in the BM. These mechanisms have been implicated in both human and mouse malaria models (98). Several studies have reported that this suppression of BM erythropoiesis during malaria correlates with the degree of parasitaemia(132). I aimed to determine how the erythroid progenitors and precursors defined in the preceding chapter are impacted by experimental malaria and whether the suppression of erythroid development in the BM is dependent on the degree of parasitaemia.

To determine if BM suppression during malaria correlates with the degree of parasitaemia, I used three different models of infection that differ in virulence, parasite burden at peak parasitaemia and the immune response elicited, namely the serial blood passage (SBP), the mosquito transmission (MT) and the sporozoite inoculation (SI) models. I established experimental malaria in mice using the rodent malaria parasite *Plasmodium chabaudi chabaudi* AS (Pcc AS). *Pcc* AS establishes synchronous, chronic and recrudescing blood-stage infections in rodents, and exhibits many characteristics associated with the pathogenesis of human malaria, such as rosetting, sequestration and antigenic variation (97). Some of the features of *Pcc* AS malaria such as severe anaemia, splenomegaly and BM suppression, make it a very useful model for studying abnormal erythroid development. To dissect the exact stage of erythroid development that BM suppression sets in, I investigated populations with a capacity for erythroid lineage commitment that are more primitive

than the BFU-e namely the MEP and Pre-MEP. The investigation of the impact of malaria on the most primitive erythroid progenitors is the first of its kind as the MEP and pre-MEP were only able to be identified by flow cytometry in the recent years.
In addition, I investigated the impact of malaria on the latter stages of erythropoiesis, that is, the proerythroblast to the orthochromatic erythroblast stages. Rather than analysing this latter stage as a whole ($CD71^+$ $Ter119^+$ cells), I have analysed each distinct population at this stage. I also expanded my investigation to include an additional site of erythropoiesis, the spleen.

Extramedullary haematopoiesis in the spleen during malaria has been reported in several studies (68), the architecture of the spleen (surrounded by a capsule made up of elastic fibres which can stretch up to 1.5 times their length) as opposed to the BM, permits its expansion during infection, providing adequate room for the influx and proliferation of progenitors (133). I investigated whether the reported increase in the number of erythroid progenitors in the spleen during malaria (134) results in an increased splenic erythroid output.

4.2 Impact of acute malaria infection on BM and splenic cellularity

To set up experimental malaria, female C57BL/6 mice were administered an intraperitoneal injection of 10^5 parasitised erythrocytes. These parasitised erythrocytes were obtained from donor C57BL/6 mice that were infected with serially blood passaged *Pcc* AS, exposed to bites of *Pcc* AS infected female *Anopheles stephensi* or injected with *Pcc* AS sporozoites, for the serial blood passage, mosquito transmission and sporozoite inoculation models of infection respectively. These infection models have been discussed in detail in the Materials and Methods. Naïve litter-mates were used as controls.

Peripheral parasitaemia was monitored by thin blood smear throughout acute infection. In the SBP model, there was a rapid increase in parasite density, reaching >20% at day 7 post-infection, while parasite growth rate was much slower

in the MT and SI models, with parasitaemia that did not exceed 1% at the time-points sampled (Figure 4.1A).

At day 5 and 7 post-infection, BM from naïve and infected *Pcc* AS mice were obtained and the cellularity was determined (Figure 4.1B). Changes in the BM cellularity, which considers the absolute number all the cells in the BM, as well as changes in the absolute number of BM LIN^- cells resulting in a hyper-proliferative or hypo-proliferative state are indicative of potential pathology. At day 5 post-infection there was no difference in BM cellularity between naïve and infected mice while at day 7 post-infection, I observed a significant contraction in the BM cellularity which coincided with the peak parasitaemia at the time points sampled. This contraction in BM cellularity reflected in the number of LIN^- BM cells. At day 5 post-infection, a significant reduction in number of LIN^- BM cells had already set in, with an even greater reduction at day 7 post-infection (Figure 4.1C). Spleens were harvested from naïve and infected mice, and splenic cellularity was determined. In striking contrast to my observation in the BM, there was a significant increase in splenic cellularity at day 7 post-infection (Figure 4.1D). The spleens from infected mice were also larger (Figure 4.1E) and weighed significantly more than spleens from naïve mice (Figure 4.1F).

A

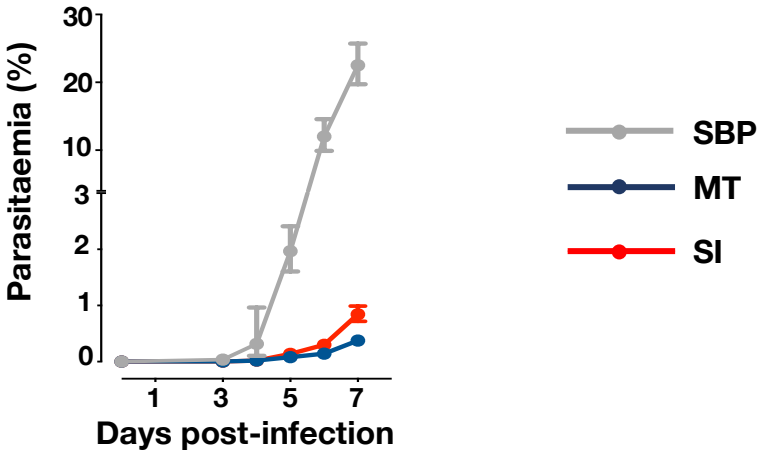

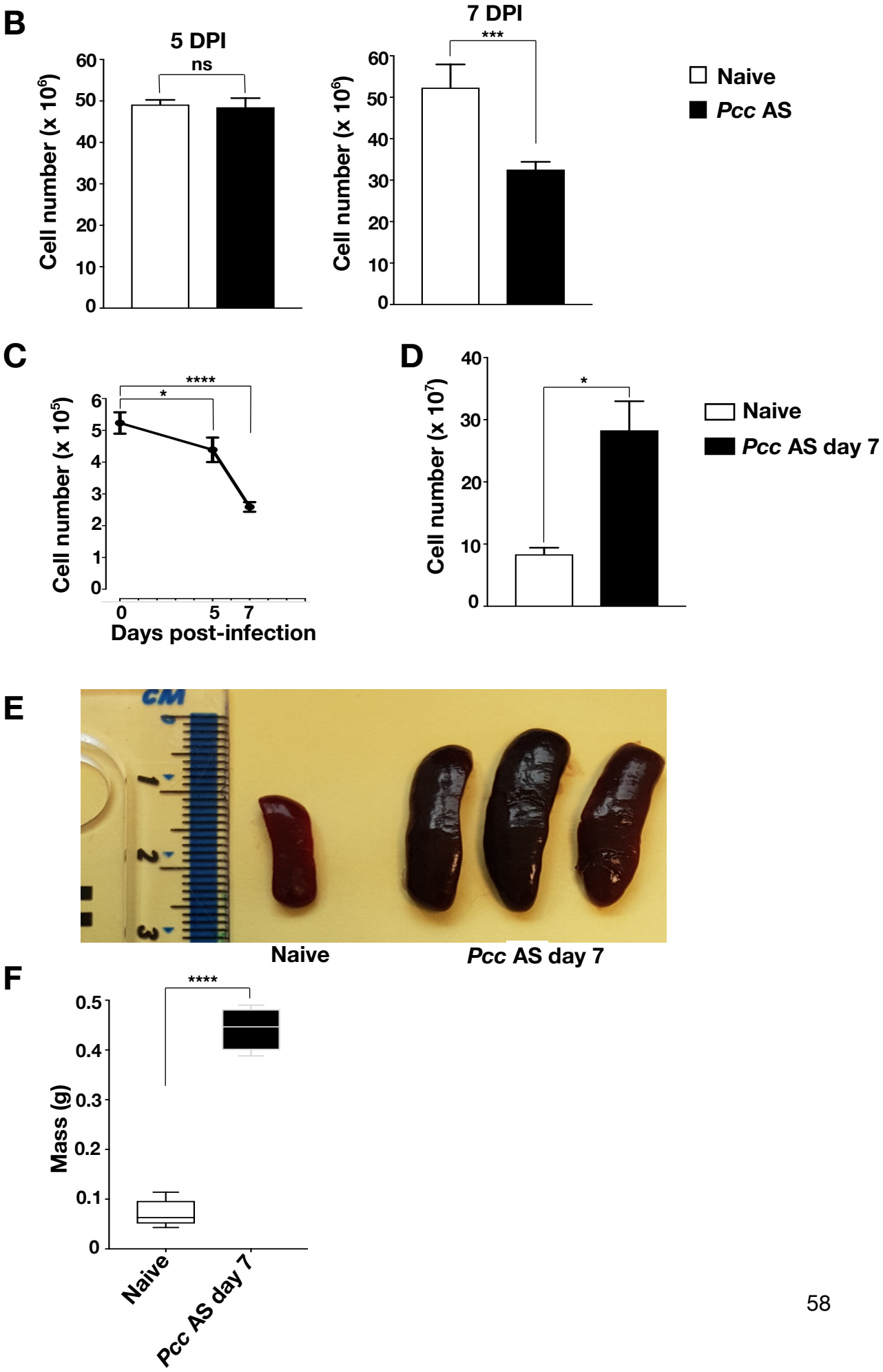
B
5 DPI
ns
7 DPI
***
Cell number (x 10^6)
Naive
Pcc AS
C
****
*
Cell number (x 10^5)
Days post-infection
D
*
Cell number (x 10^7)
Naive
Pcc AS day 7
E
CM
Naive
Pcc AS day 7
F
****
Mass (g)
Naive
Pcc AS day 7

Figure 4.1 Contraction of BM cellularity and increase in splenic cellularity during acute malaria infection

Female wildtype C57BL/6 mice were infected with 10^5 *Pcc* AS parasitised erythrocytes and naïve littermates were used as controls **(A)** Geometric mean parasitaemia in three malaria models of infection (SBP, MT and SI), the error bars indicate 95% confidence intervals. **B**-**F** show results for SBP model of infection. **(B)** Absolute number per femur/tibia pair of BM cells in naïve and infected mice at day 5 and 7 post-infection. Of note is the significant reduction in BM cellularity in infected mice at day 7 post-infection. **(C)** Contraction of BM LIN^- cells during acute *Pcc* AS infection. **(D)** Absolute number of cells per spleen in naïve and infected mice. **(E)** Image showing the spleens from naive and infected mice at day 7 post-infection. **(F)** Box and whisker plot showing mass of spleens from naive and infected mice at day 7 post-infection.

(A – F) Data shown are from two independent experiments. **(B, C, D, F)** Values represent mean ± SEM, n = 10 mice for SBP and SI models and n = 6 mice for MT model and naïve controls. Significance was calculated using the Student's t-test. Asterisks represent statistically significant differences (ns: not significant; *: $P<0.05$; **: $P<0.01$; ***: $P<0.001$; **** :$P<0.0001$).

4.3 Changes in BM haematopoietic progenitor cell pool in BM and spleens of mice with *P. c. chabaudi* AS malaria

HSCs and multipotent progenitors are characterised in steady state by high expression of c-Kit and Sca-1. In contrast, HPCs are negative for Sca-1 but still retain high levels of c-Kit at the surface (68). During malaria and in systemic infections, there is a release of proinflammatory cytokines, in particular IFN-γ which directly increases *Ly6a* transcription and causes upregulation of Sca-1 on HPCs resulting in an amalgamation of the HPC pool and the LSK pool (68). The amalgamation of the LSK and HPC pool has been well documented in different experimental conditions.(75,102,135,136). Using the SBP, MT and SI models of infection, I investigated if these changes could be observed in the HPC pool which constitutes the most abundant cell pool within the LIN^- fraction of the BM and is made up of the MEP, Pre-MEP, CMP and GMP.

At day 5 and day 7 post-infection, BM from naïve and *Pcc* AS infected mice were obtained and the LIN^+ cells were excluded using lineage markers as described in Chapter 3 and also in the Materials and Method. The resulting LIN^- cells were labelled

with fluorochrome conjugated monoclonal antibodies against CD117 and Sca-1 to identify the HPC and LSK compartments.

In agreement with published work by Belyaev and colleagues (68), At day 7 post-infection, the HPC compartment showed an upregulation of Sca-1 expression on virtually all cells in the SBP, MT and SI models of infection **(Figure 4.2 A-C)**. This upregulation of Sca-1 had already set in at day 5 in both the SBP and SI models. The upregulation of Sca-1 has been shown to be induced by proinflammatory cytokines namely IFN-γ (137), and my findings suggest the presence of systemic IFN-γ acting in progenitor niches in the BM.

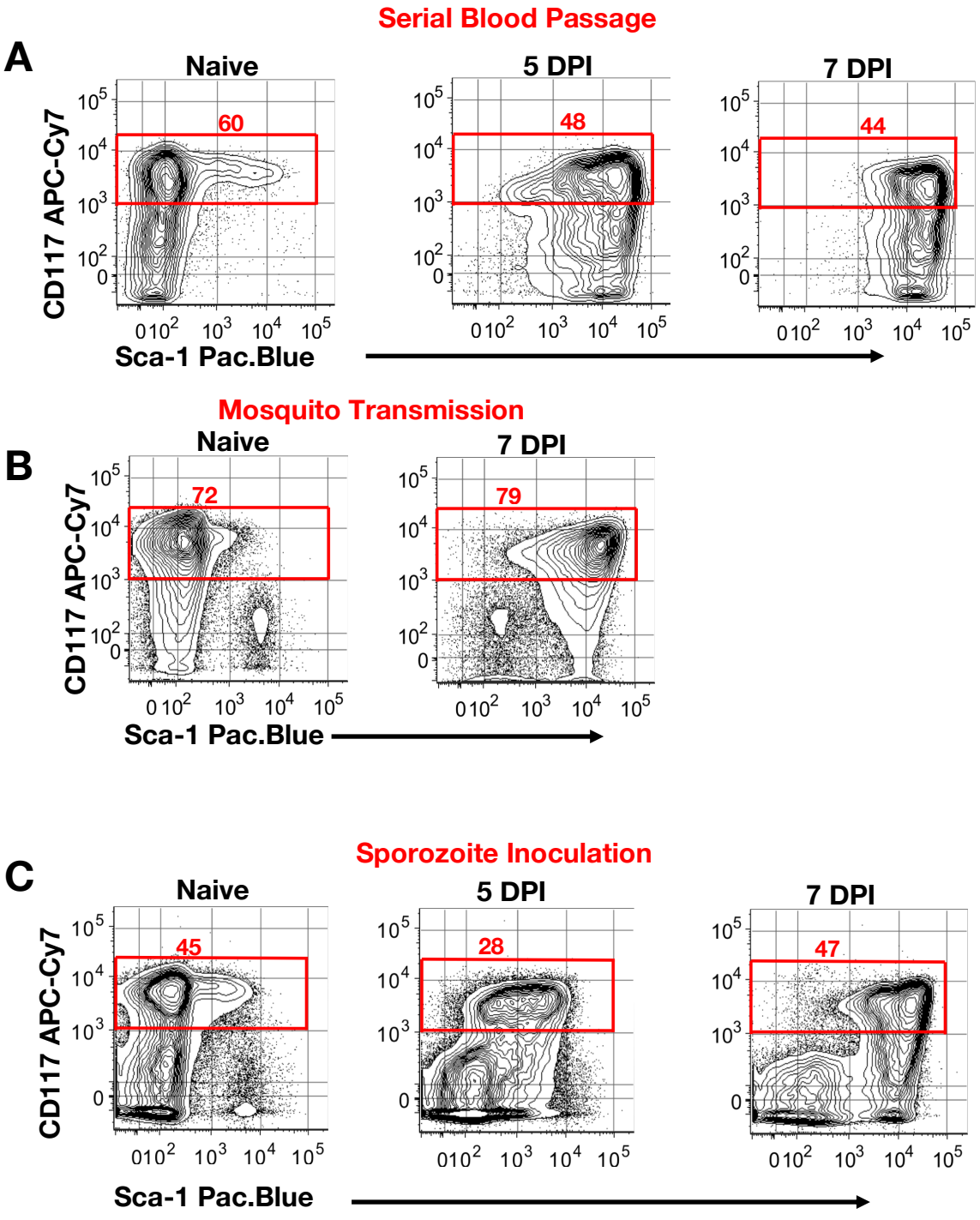

Figure 4.2 Infection induced upregulation of Sca-1 on HPCs

LIN$^-$ cells from naïve controls and *Pcc* AS infected mice at day 5 and 7 post-infection were stained with CD117 and Sca-1. Sca-1 is upregulated on BM HPCs in **(A)** SBP **(B)** MT **(C)** SI models of infection. Data represents results from two independent experiments, n=10 mice per time point (A) or one experiment, n=5 mice per time point (B and C).

The infection induced upregulation of Sca-1 on HPCs results in the amalgamation of the HPC and LSK pools creating an operational problem of how to identify the Pre-MEP, MEP, CMP and GMP during malaria, which in steady state lack surface expression of Sca-1. To address this, the HPC gate was extended to include both CD117^{hi} Sca1$^-$ and CD117^{hi} Sca-1$^+$ cells (Figure 4.3), these cells were further resolved using CD150 and CD27 to identify the Pre-MEP, MEP, CMP and GMP analogues as shown in Figure 4.3. The functional names MEP, Pre-MEP, CMP and GMP were ascribed on the basis that in steady state these populations are Sca-1$^-$, hence, during malaria I have referred to these populations as analogues.

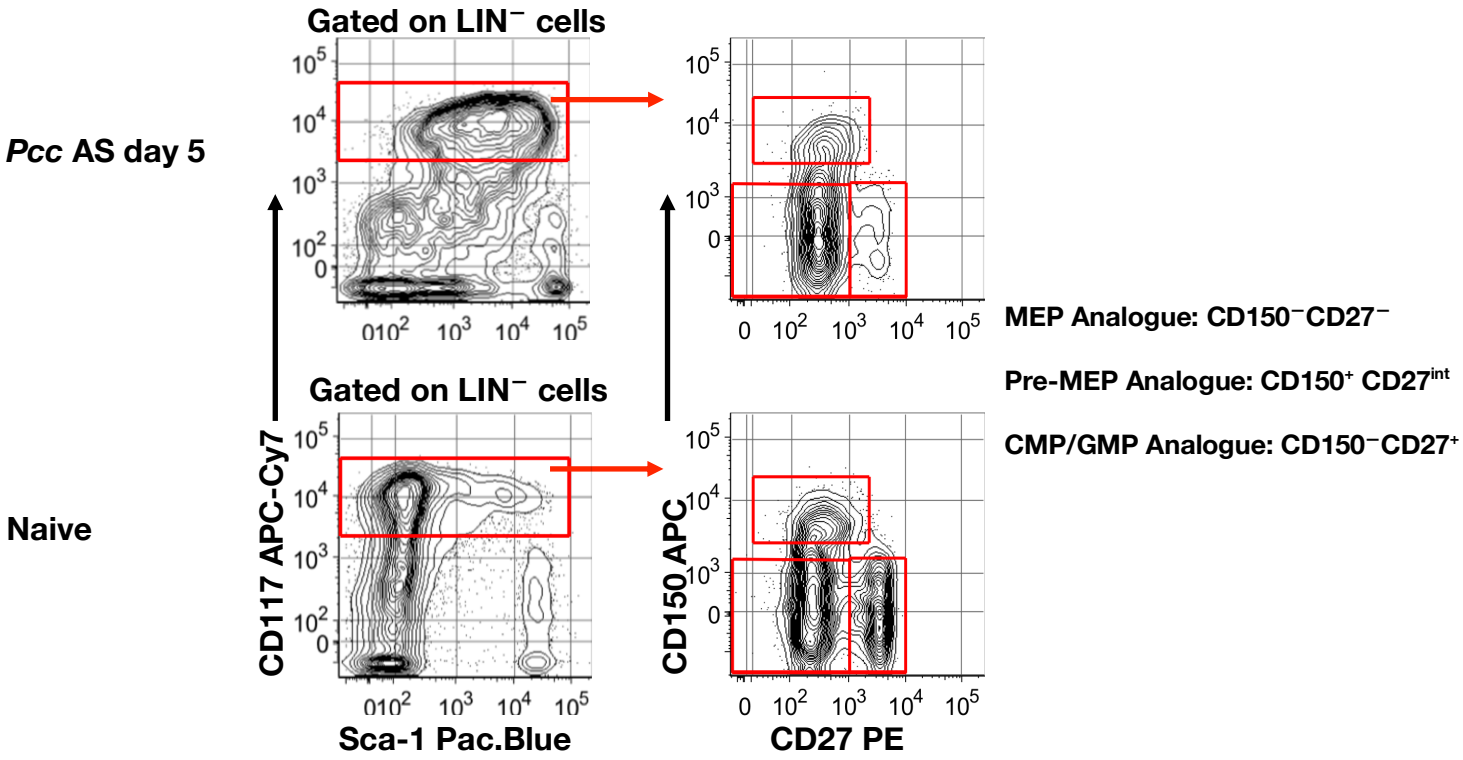

Figure 4.3. Identification of erythroid and myeloid progenitors during malaria

Gating strategy for identifying erythroid and myeloid progenitors during malaria. LIN$^-$ BM cells from naïve controls and *Pcc* AS infected mice at day 5 post-infection were stained with fluorochrome conjugated monoclonal antibodies against CD117, Sca-1, CD150 and CD27. CD117^{hi} LIN$^-$ cells are resolved into MEP (CD150$^-$CD27$^-$), Pre-MEP (CD150$^+$CD27^{int}) and CMP/GMP (CD150$^-$CD27$^+$) analogues.

To determine the impact of malaria on erythroid progenitors, LIN$^-$ BM cells from naïve and *Pcc* AS infected mice at day 5 and day 7 post-infection were stained with monoclonal antibodies against CD117, Sca-1, CD150 and CD27. In the SBP model, I observed at days 5 and 7 post-infection, a significant increase in the frequency and absolute number of MEP analogue, a significant decrease in the number of CMP/GMP analogue but no significant difference in the Pre-MEP analogue (Figure 4.4A-D) Previous work in our lab demonstrated that this contraction in BM myelopoiesis during malaria is as a result of the mobilisation of the myeloid progenitors to the spleen (68). Similar observations were made in the MT and SI model (Figure 4.4E-H), but unique to the MT model, was a significant decrease in the Pre-MEP analogue at day 7 post-infection which might relate to differences in elicited immune response and kinetics of the cytokine milieu in these models (124).

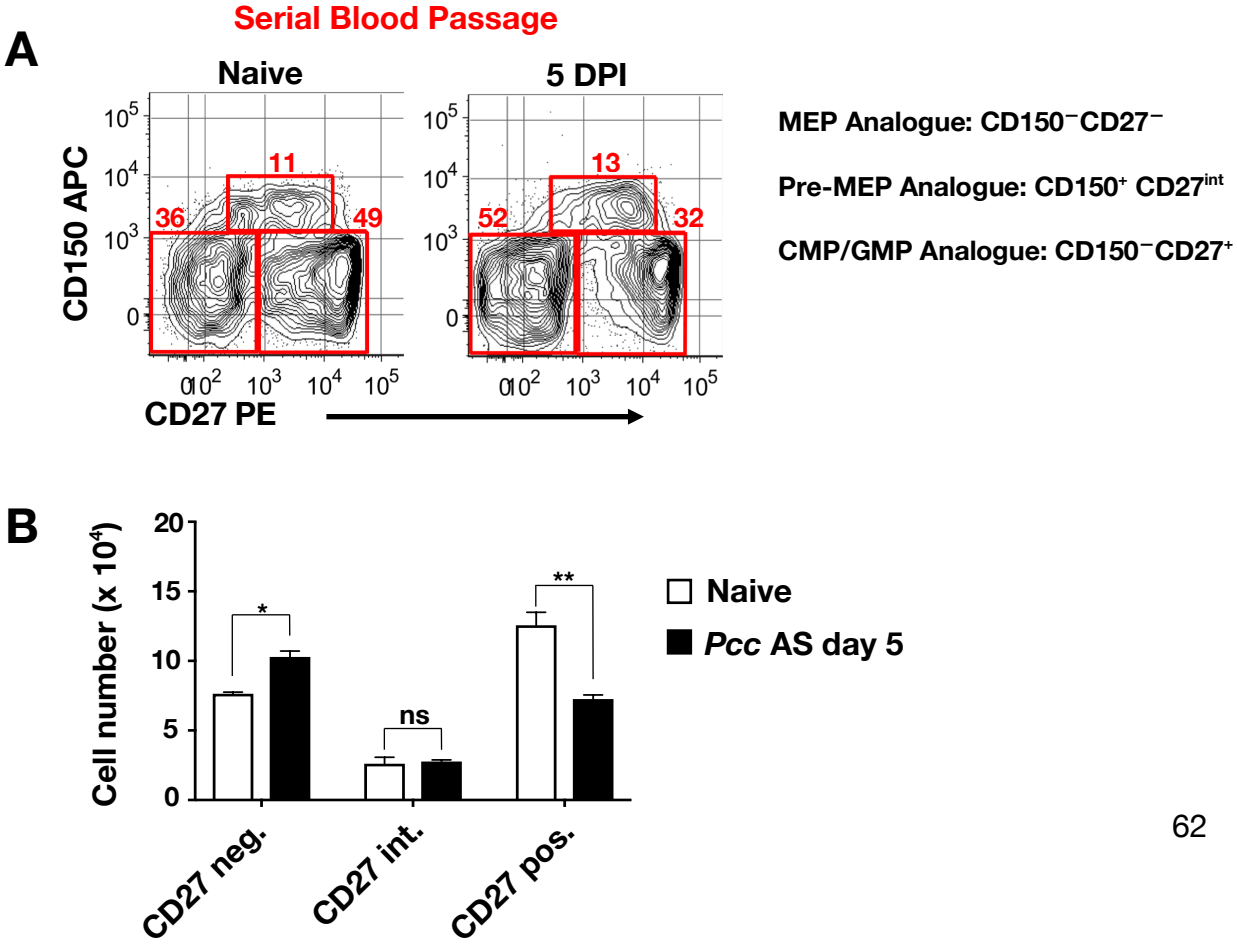

C

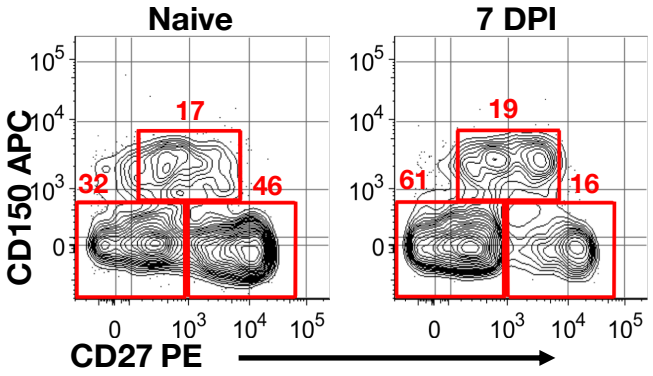

MEP Analogue: CD150^{-}CD27^{-}

Pre-MEP Analogue: CD150^{+} CD27^{int}

CMP/GMP Analogue: CD150^{-}CD27^{+}

D

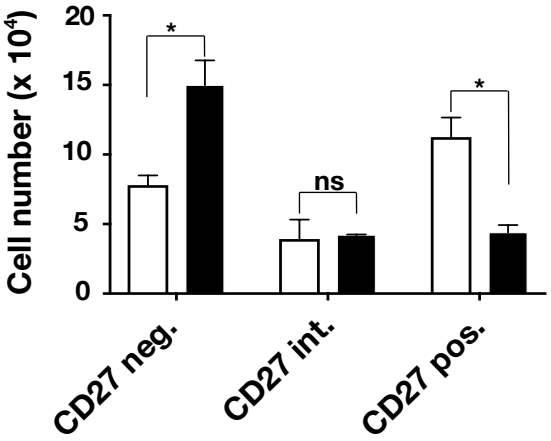

E

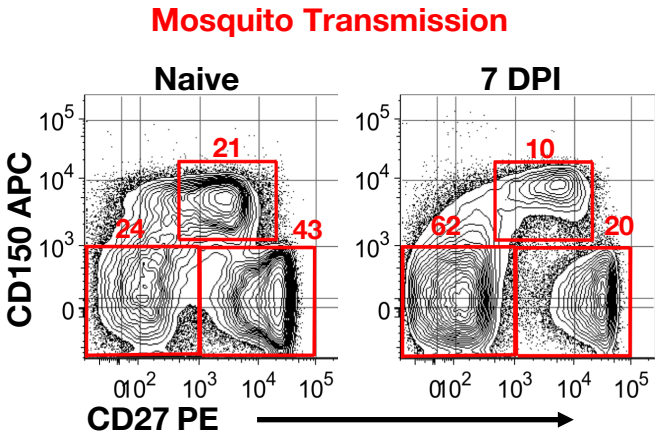

MEP Analogue: CD150^{-}CD27^{-}

Pre-MEP Analogue: CD150^{+} CD27^{int}

CMP/GMP Analogue: CD150^{-}CD27^{+}

F

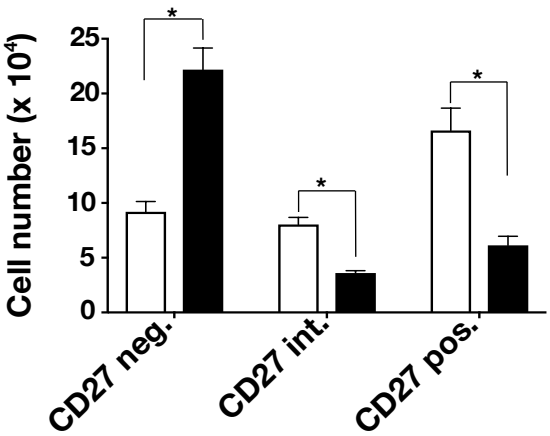

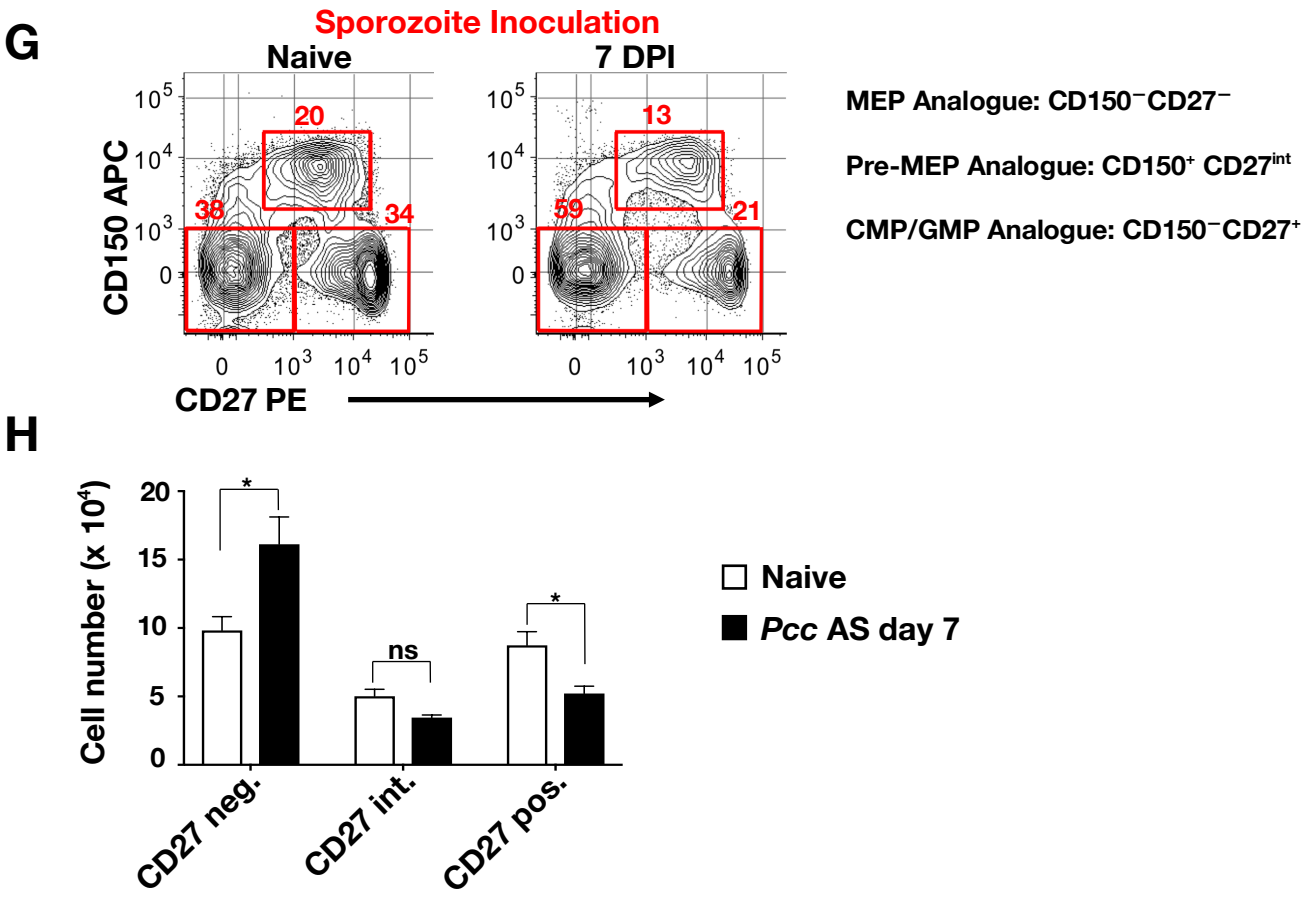

Figure 4.4 Infection induced expansion of erythroid progenitors and contraction of myeloid progenitors in three malaria models

Representative FACS Plot illustrating the frequency of MEP, Pre-MEP and CMP/GMP analogues in the BM of naive and *Pcc* AS infected mice in **(A)** SBP model at day 5 post infection, and at day 7 post-infection in **(C)** SBP model **(E)** MT model and **(G)** SI model. Absolute number per femur/tibia pair of MEP (CD27 neg), Pre-MEP (CD27int) and CMP/GMP (CD27 pos) analogues in naive and *Pcc* AS infected mice at **(B)** day 5 post infection in SBP model, and at day 7 post-infection in **(D)** SBP model **(F)** MT model and **(H)** SI model. **(A-D**) Data represents results from two independent experiments, values represent mean ± SEM, n=10 *Pcc* AS infected mice per time point and n= 6 naïve mice per time point. (E-F) Data represents results from one experiment, values represent mean ± SD, n=5 *Pcc* AS infected mice per time point and n= 3 naïve mice per time point. Significance was calculated using the Student's t-test. Asterisks represent statistically significant differences (ns: not significant; *: $P<0.05$; **: $P<0.01$).

It has been demonstrated by Belyaev *et al.* (68) that during acute malaria infection with *P. chabaudi*, the myeloid progenitors which are in the same developmental subset as the most primitive erythroid progenitors as defined by expression of CD117

and Sca-1, are mobilised to the spleen which results in an increase in the number of myeloid progenitors in the spleen. I investigated if the same might be true for the erythroid progenitors.

C57BL/6 mice were infected with 10^5 *Pcc* AS parasitised erythrocytes using the SBP model of infection. At day 7 post-infection, spleens were obtained from infected mice and naïve controls, and LIN^+ cells were electronically excluded as described in Chapter 3 and Materials and Methods. Similar to the BM, LIN^- splenocytes were resolved using monoclonal antibodies against CD150, Sca-1, CD150 and CD27 to identify the MEP, Pre-MEP and CMP/GMP analogues in the spleen.

At day 7 post-infection, I observed an increase in the frequency of the MEP analogue, but a contraction in the frequency of Pre-MEP and CMP/GMP analogues (Figure 4.5A). Despite the contraction in frequency, the considerable increase in splenic cellularity during *Pcc* AS malaria, resulted in a significant increase in the absolute number per spleen of all erythroid and myeloid progenitors. (Figure 4.5B). I observed an 18-fold increase in the absolute number of the MEP analogue which was surprising as one would expect such an increase to contribute in ameliorating SMA.

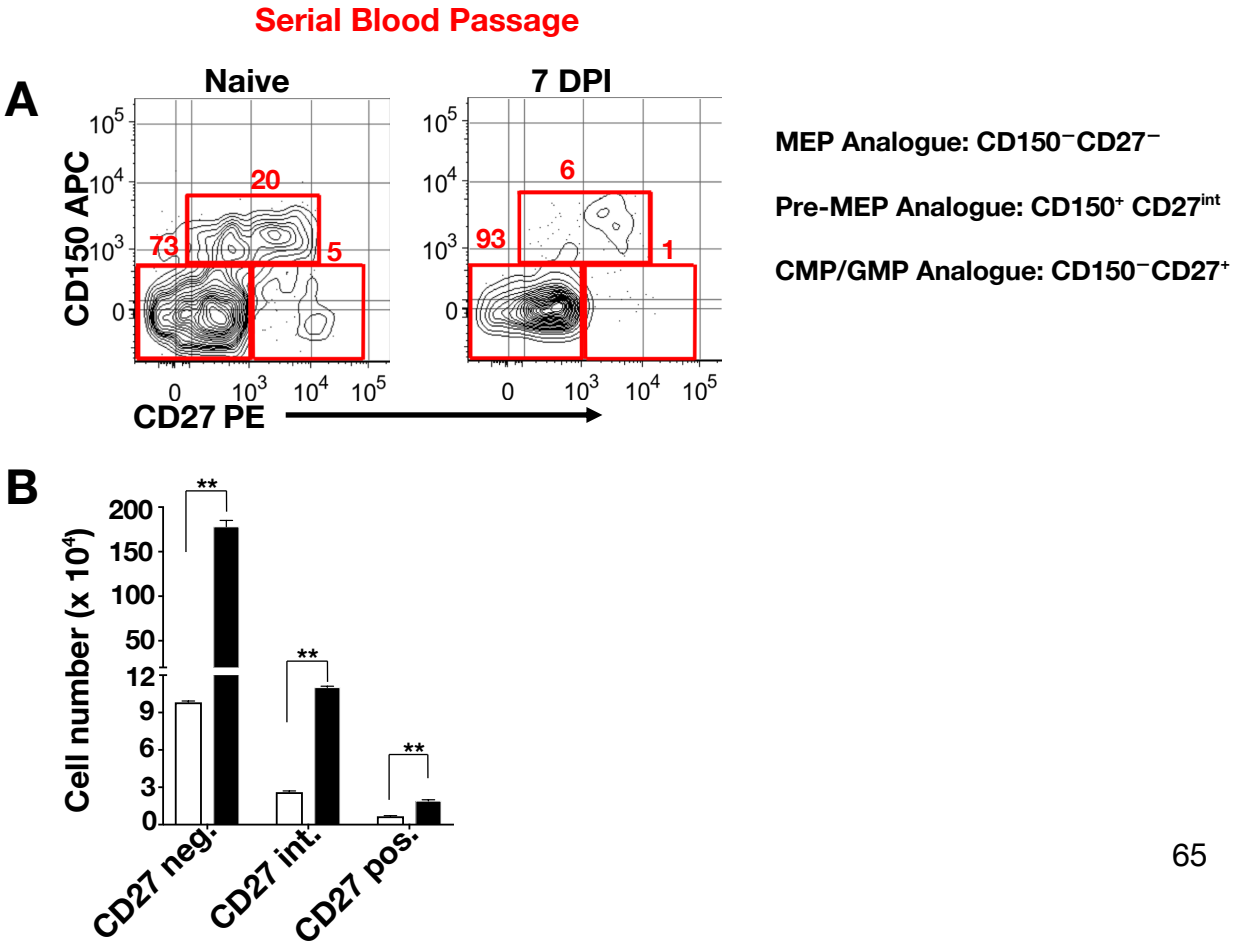

Figure 4.5 Infection induced increase in number of MEP analogue in spleen of mice with P. c. chabaudi AS malaria

(A) FACS plots illustrating the frequency of MEP, Pre-MEP and CMP/GMP analogues in the spleen of naive and *Pcc* AS infected mice at day 7 post-infection using the SBP model of infection. **(B)** Absolute number of MEP (CD27 neg), Pre-MEP (CD27int) and CMP/GMP (CD27 pos) analogues per spleen of naive and *Pcc* AS infected mice at day 7 post-infection using the SBP model. (A and B) Data represents results from two independent experiments, values represent mean ± SEM, n=10 *Pcc* AS infected mice per time point and n= 6 naïve mice per time point. Asterisks represent statistically significant differences (ns: not significant; **: $P<0.01$).

4.4 Changes in erythroid precursors in BM and spleen of mice with *P. chabaudi* malaria

The suppression of erythropoiesis during malaria, in humans and in mouse models has been well documented. Low reticulocytosis, indicative of reduced RBC output is an important feature of SMA. This low reticulocytosis during malaria is associated with suppressed proliferation, differentiation and maturation of erythroid precursors (138). To further dissect the impact of malaria on erythroid development, I determined if the observed increase in the MEP analogue in spleen and BM during malaria would reflect in the number of downstream erythroid precursors in both sites.

C57BL/6 mice were infected with 10^5 *Pcc* AS parasitised erythrocytes using the SBP, MT and SI models of infection. At day 5 (SBP only) and day 7 post-infection, BM from femur and tibia pair of naïve and infected mice was obtained and the frequency and absolute number of erythroid precursors per femur/tibia pair was determined as described in Chapter 3.

To the best of my knowledge, changes in the expression of surface markers used to identify erythroid precursors has not been reported during infection, hence, during experimental malaria, these cells were identified using surface markers and gating strategy as in steady state. At day 7 post-infection, I observed a significant contraction of each erythroid precursor stage regardless of the model of infection (Figure 4.6A-F). The frequency of the orthochromatic erythroblasts in infected mice was similar to naïve controls in all three models of infection, but the substantial

contraction in BM cellularity during infection accounted for the significant decrease in this population. The observed increase in the BM MEP analogue during malaria failed to reflect in downstream erythroid precursors suggesting impaired differentiation and/or the mobilisation of this population to the spleen which might account for the 18-fold increase of this population in the spleen.

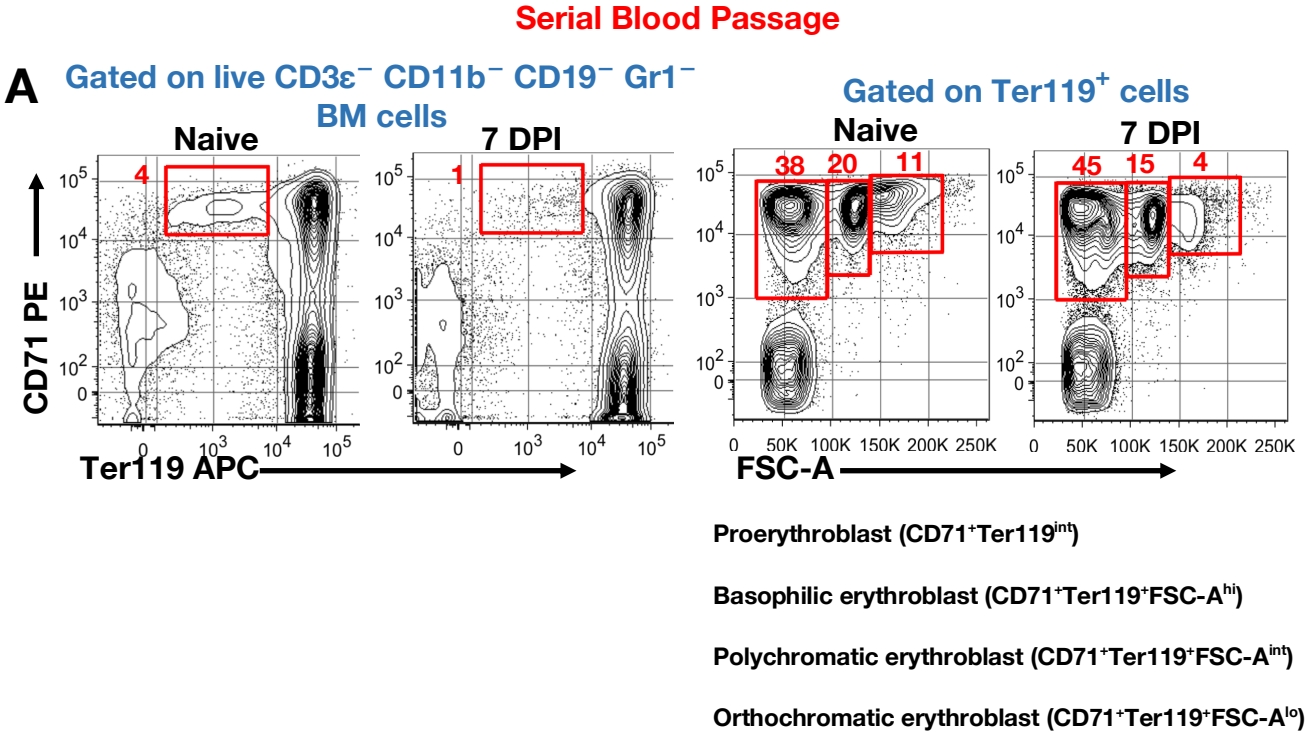

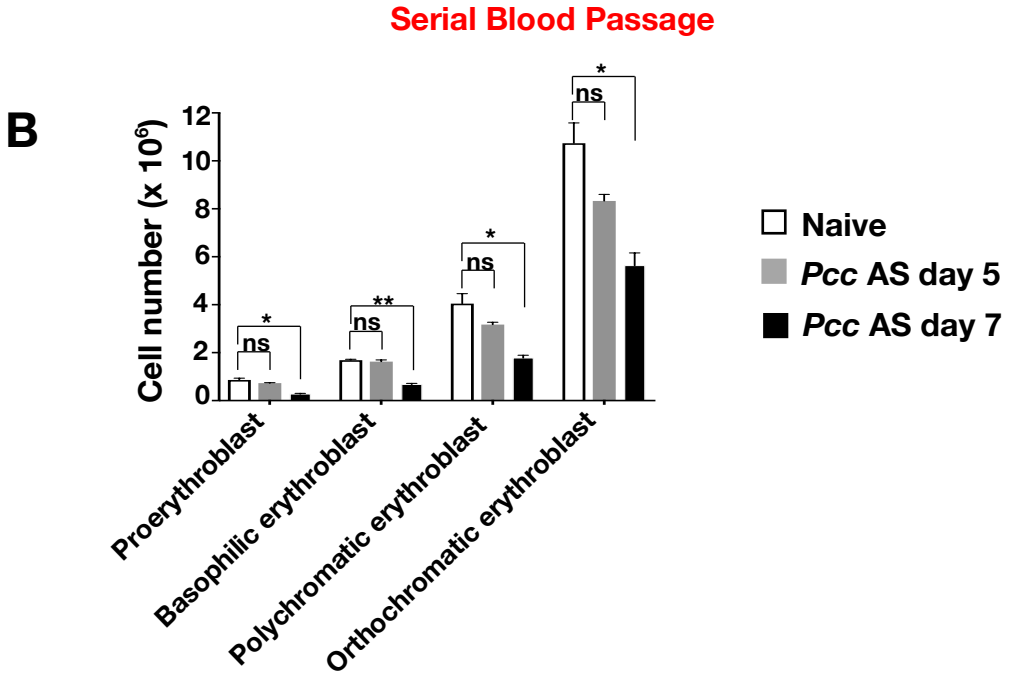

Mosquito Transmission

C

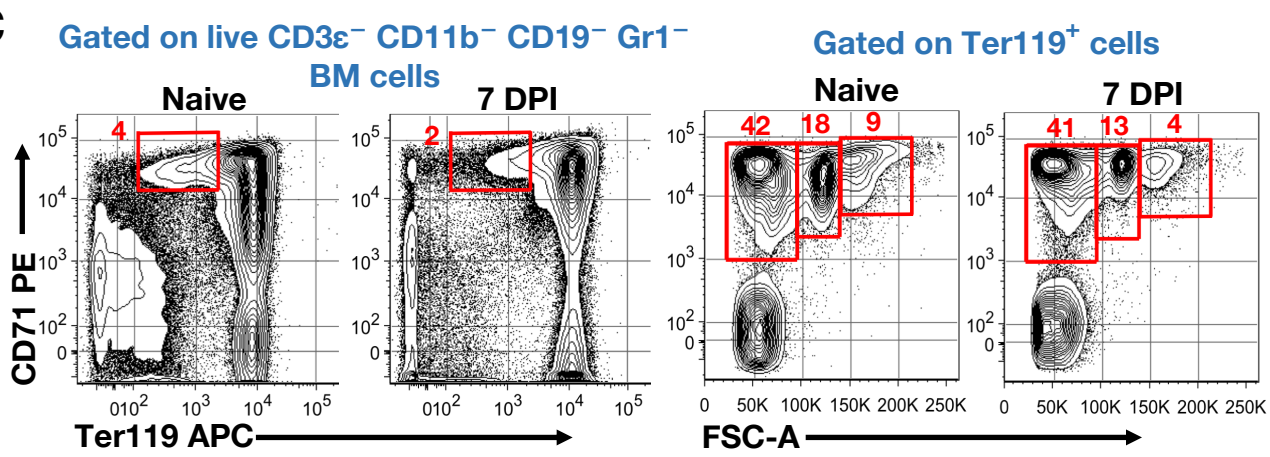

Proerythroblast (CD71⁺Ter119^{int})

Basophilic erythroblast (CD71⁺Ter119⁺FSC-A^{hi})

Polychromatic erythroblast (CD71⁺Ter119⁺FSC-A^{int})

Orthochromatic erythroblast (CD71⁺Ter119⁺FSC-A^{lo})

Mosquito Transmission

D

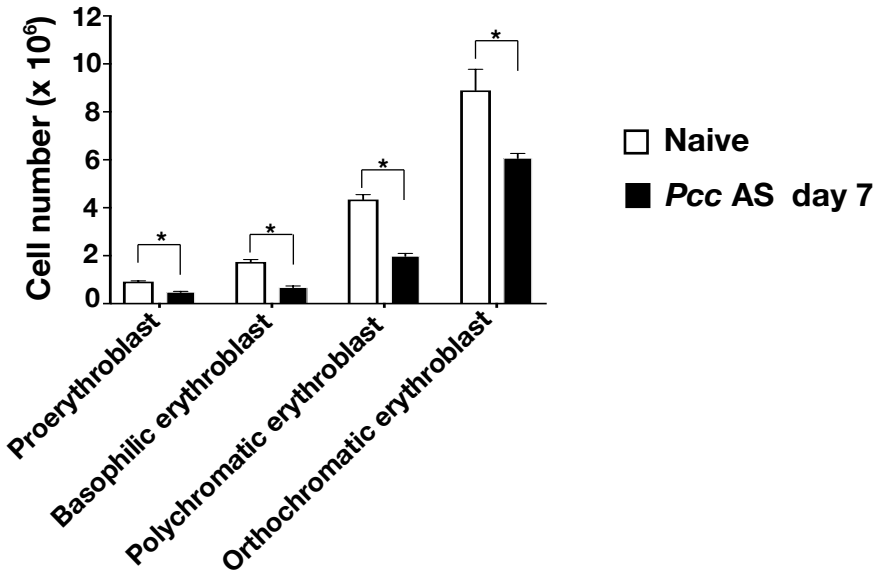

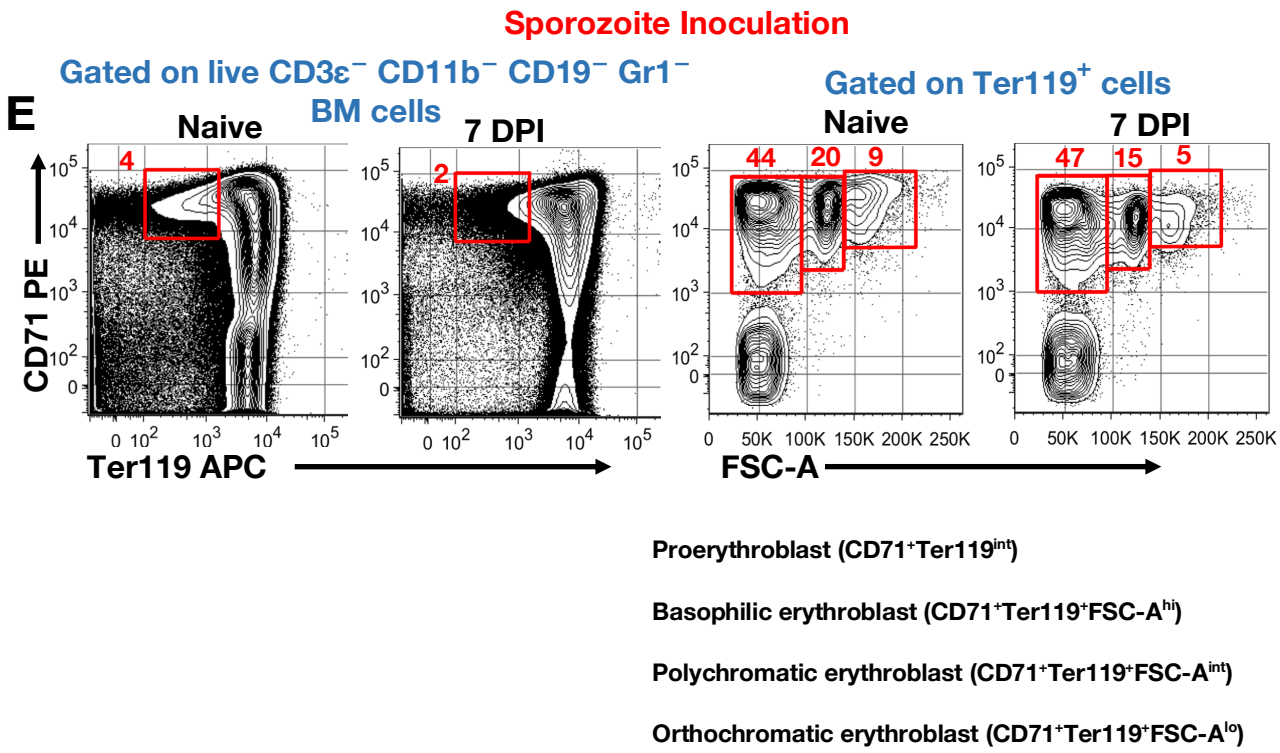

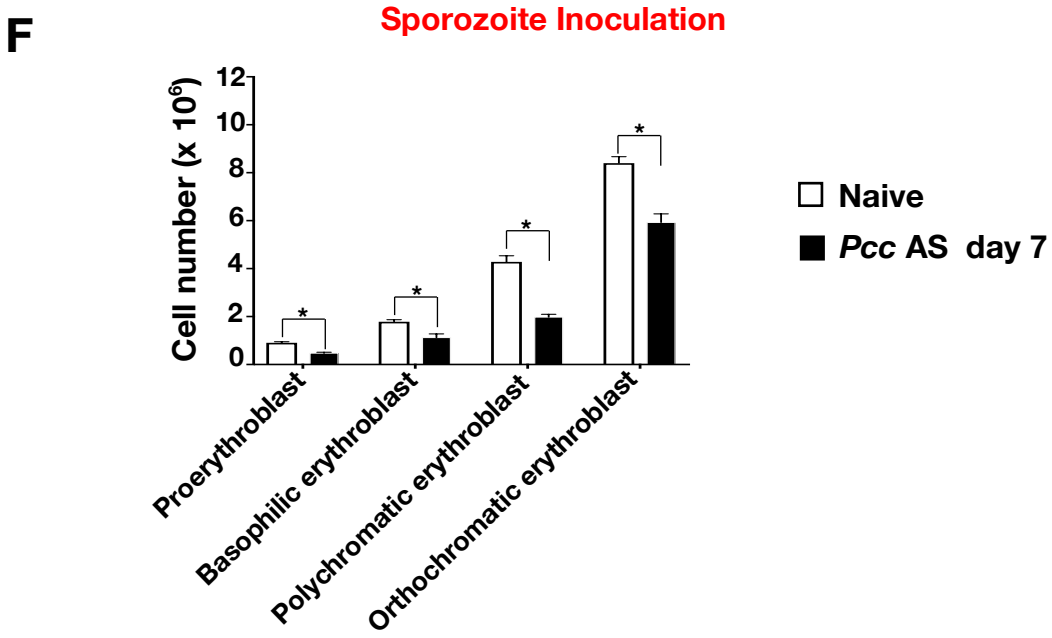

Figure 4.6 Contraction of erythroid precursors in BM of mice infected with P. c. chabaudi AS.

BM cells from naïve controls and *Pcc* AS infected mice were stained with fluorochrome conjugated antibodies against CD3ε, CD11b, CD19, Gr1, CD71, Ter119 and live-dead discriminator 7AAD. Cells expressing CD3ε, CD11b, CD19 and Gr1 as well as dead cells and doublets were excluded from analysis. FACS plots illustrating the frequency of erythroid precursors in the BM of naive and *Pcc* AS infected mice at day 7 post-infection using the SBP **(A)**, MT **(C)** and SI **(E)** models of infection. Absolute

number of erythroid precursors per femur/tibia pair in naive and *Pcc* AS infected mice at day 5 and 7 post-infection using the SBP **(B)**, and at day 7 post-infection using the MT **(D**) and SI **(F)** models of infection. **(A,B)** Data represents results from two independent experiments, values represent mean ± SEM, n=10 *Pcc* AS infected mice per time point and n= 6 naïve mice per time point. Significance was calculated using one-way ANOVA and Tukey multiple comparisons test. **(C-F)** Data from one experiment, values represent mean ± SD, n=5 *Pcc* AS infected mice per time point and n= 3 naïve mice per time point. Significance was calculated using the Student's t-test. Asterisks represent statistically significant differences (ns: not significant; *: $P<0.05$; **: $P<0.01$).

Next, I determined if the infection induced increase in the MEP analogue in the spleen would reflect in the number of erythroid precursors in this organ. C57BL/6 mice were infected with *Pcc* AS using the SBP model of infection. At day 7 post-infection, spleens from naïve controls and infected mice were obtained and the frequency and absolute number of erythroid precursors per spleen was determined in a similar manner as in the BM, which has been described in Chapter 3**.** No change in the frequency of proerythroblasts was observed, but a decrease in frequency of basophilic, polychromatic and orthochromatic erythroblasts was evident in spleens of infected mice (Figure 4.7A). Due to the significant increase in spleen cellularity during infection, the decreased frequency of erythroid precursors in infected mice did not translate to a decrease in their absolute numbers per spleen. Instead, there was a significant increase in the absolute number of proerythroblasts but no significant difference in all downstream erythroid precursors (Figure 4.7B). The expansion of erythroid progenitors in the BM and spleen which failed to reflect in the number of erythroid precursors, clearly indicates a block in erythroid development at both sites.

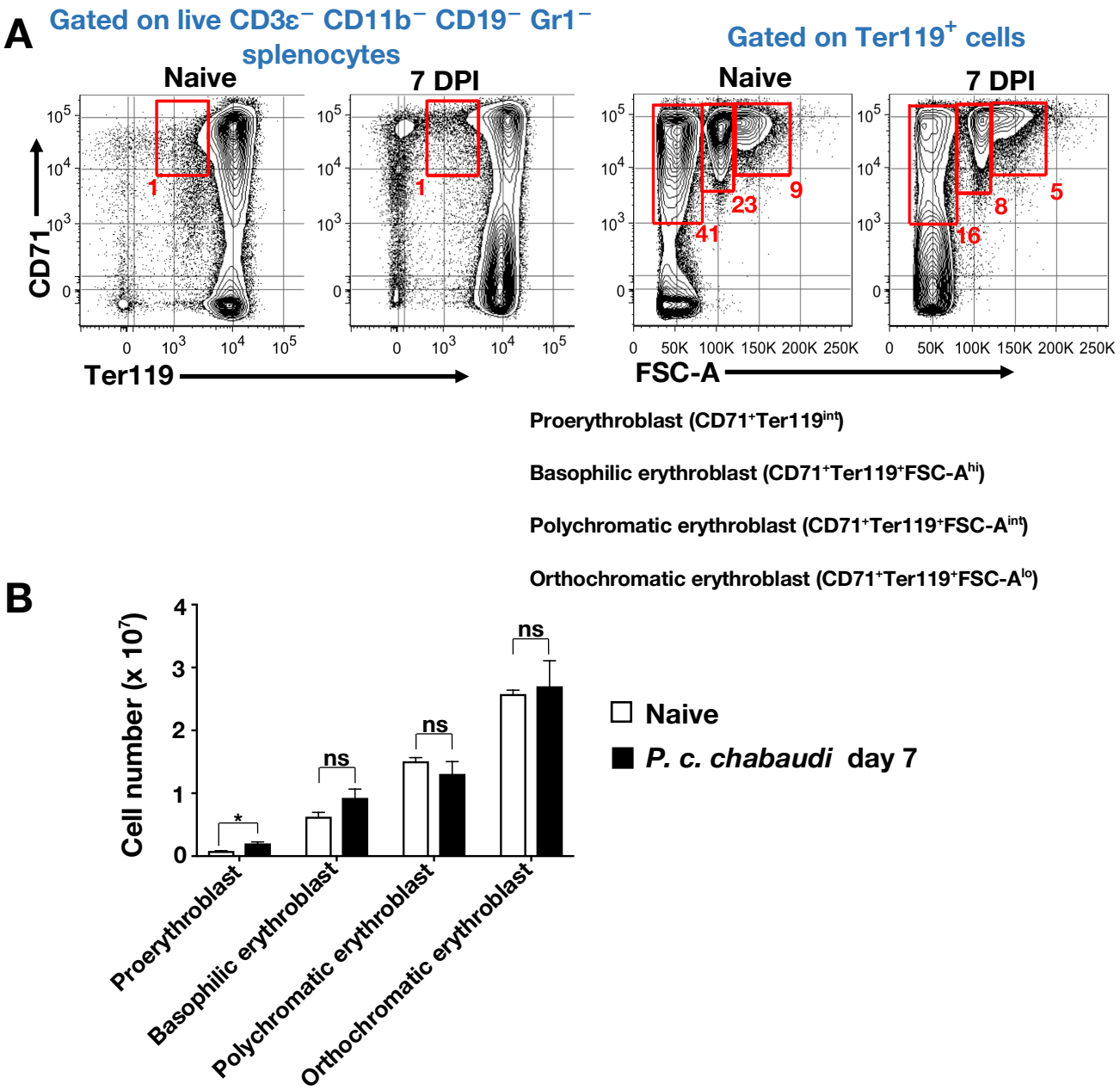

Figure 4.7 Absence of increased extramedullary erythropoiesis during P. chabaudi malaria

C57BL/6 mice were infected with 10^5 *Pcc* AS parasitised erythrocytes using the SBP model of infection. Uninfected littermates were used as controls **(A)** FACS plots illustrating the frequency of erythroid precursors in the spleen of naive and infected mice at day 7 post-infection using the SBP model of infection. **(B)** Bar chart showing the absolute number of erythroid precursors per spleen of naive and *Pcc* AS infected mice at day 7 post-infection using the SBP model. Data represents results from two independent experiments, values represent mean ± SEM, n=10 *Pcc* AS infected mice per time point and n= 6 naïve mice per time point. Significance was calculated using the Student's t-test. Asterisks represent statistically significant differences (ns: not significant; *: P<0.05).

4.5 Serum levels of proinflammatory cytokines potentially mediating dyserythropoiesis

Following the observation that the block in erythropoiesis during malaria was not restricted to the BM but also manifested in the spleen, I focussed on host derived factors that could be acting at these two sites to simultaneously block erythropoiesis. Two key proinflammatory cytokines namely, IFN-γ and TNF-α have been implicated as soluble mediators of dyserythropoiesis during malaria. Due to the challenges in measuring accurately the exact acting concentration of the secreted proteins in the BM and spleen, I determined the serum concentration of these cytokines before and at several time points after infection with *Pcc* AS by enzyme linked immunosorbent assay (ELISA) as described in the Materials and Methods. Prior to infection, IFN-γ was undetectable in serum but following infection, there was a transient spike in IFN-γ concentration, peaking at day 5 (Figure 4.8A). In contrast, there was basal levels of TNF-α prior to infection, which increased and peaked at day-7 post-infection at the time points sampled (Figure 4.8B). These observations suggest that IFN-γ and/or TNF-α could be mediating early dyserythropoiesis independently or synergistically.

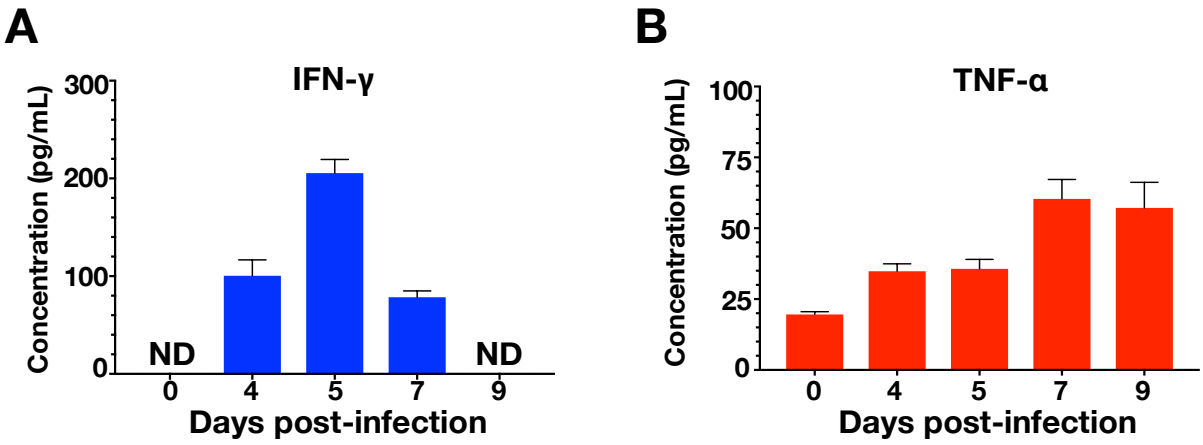

Figure 4.8 Kinetics of IFN-γ and TNF-α during P. c. chabaudi* AS *malaria

C57BL/6 mice were infected with 10^5 *Pcc* AS parasitised erythrocytes using the SBP model of infection. Serum concentration of **(A)** IFN-γ and **(B)** TNF-α during the course of acute malaria. Data represents results from two independent experiments, values represent mean ± SEM, n=10 mice per time point

4.6 Discussion

SMA is a common life-threatening complication of *P. falciparum* malaria in young children under the age of five years. This severe form of anaemia ensues when the accelerated destruction/removal of parasitised and non-parasitised erythrocytes is not compensated for by an already suppressed BM. It is known that BM suppression is generally present in all cases of *P. falciparum* malaria (139), nevertheless, there are conflicting reports on the role of parasite density in bone marrow suppression. Some studies have linked the increased destruction of erythrocytes associated with high parasite density to bone marrow inhibition (139,140), Pathak *et al.* reported that BM inhibition correlates with the degree of parasitaemia and can be reversed following clearance of peripheral parasitaemia (141), while other researchers have reported that bone marrow inhibition manifests after treatment and following parasite clearance (142–144).

In this chapter, I demonstrated that the suppression of erythropoiesis in the BM and spleen does not correlate with peripheral parasitaemia but might be driven by host derived mediators such as IFN-γ and TNF-α. *P. chabaudi* infected erythrocytes are known to sequester in organs during blood stage infection (97), thus, despite the low peripheral parasitaemia in the MT and SI models of infection, the parasite density in tissue was not accounted for in all models of infection. This information is vital to draw conclusions on the role of parasite density in BM suppression. The contraction in BM cellularity during acute malaria could be explained by the mobilisation of myeloid progenitors from the BM to the spleen and the block in erythroid differentiation. The contraction of LIN^- BM cells during acute malaria with *Pcc* AS is in line with previous published work by our lab in which the most pronounced contraction of LIN^- BM cells was observed at day 7 post-infection (68). This contraction of LIN^-cells was shown to be dependent on IFN-γ signalling via the stroma compartment (68).

The spleen is a site of extramedullary haematopoiesis during stress and is the main organ that generates the immune response to malaria parasite and controls the removal of parasitised RBCs (145,146). One of the hallmarks of infection with malaria

parasite is splenomegaly, so much so that the spleen size has been used as a tool to determine the intensity of malaria transmission in endemic areas (147). It has been known for about three decades that during malaria in mouse models there is a contraction in the number of BM BFU-e but an increase in splenic BFU-e and CFU-e (134), providing evidence of extramedullary erythropoiesis during malaria. Consistent with the significant expansion of the MEP analogue in the BM, I observed an even greater expansion of the splenic MEP analogue. Further study is required to determine if this was as a result of proliferation of native splenic erythroid progenitors or the mobilisation of BM erythroid progenitors to the spleen in a similar manner as the myeloid progenitors. The mobilisation of myeloid progenitors to the spleen during acute malaria with *Pcc* AS to generate the immune cells necessary to control parasite replication has been reported previously by our lab (68) and together with the expansion of the MEP analogue contributes to the increased spleen size and cellularity observed.

During *Pcc* AS malaria, the exact stage at which suppression of erythropoiesis sets in is yet to be reported and my results suggest that this suppression could be occurring at multiple stages. The contraction of the Pre-MEP in the MT model of infection which one could argue better mimics human infection, suggests that suppression of erythropoiesis during malaria might set in at stages upstream of the Pre-MEP such as the MPP2 and HSCs. Furthermore, it remains unknown if the MEP would exhibit a higher proliferative capacity in the absence of mediators of dyserythropoiesis such as IFN-γ and TNF-α.

In humans, it is well established that a decreased number of erythroblasts and circulating reticulocytes occur in *P. vivax* and *P. falciparum* malaria (95,132,148). In murine models, experimental *P. berghei* infection, resulted in a dramatic decrease in the number of erythroblasts as early as 24 hours post-infection (149). The suppression of erythropoiesis during malaria could be due to a complex mechanism that involves both the increased destruction of erythroblasts and a decreased rate of proliferation of these cells in the BM.

A draw-back of some of these studies is that the gating strategy for identifying the erythroblasts are not shown while in studies where they are shown, earlier gating

strategies were used. A recent study of the suppression of erythropoiesis in murine models reported an increase in the frequency of splenic erythroblasts in mice infected with either *P. chabaudi* or *P. berghei* in comparison to naive controls. However, this study used either CD71 or Ter119 to identify erythroblasts but not in combination, as such, the $Ter119^{+}$ splenocytes were not entirely erythroblasts but included reticulocytes and RBCs while the $CD71^{+}$ cells could have been any proliferating cell in the spleen (150).

Using a gating strategy that permits the identification of all four erythroblast populations, namely the proerythroblast, basophilic erythroblast, polychromatic erythroblast and orthochromatic erythroblast, I observed that the 1:2:4:8 ratio of erythroblast maturation observed in steady state was perturbed during malaria. Furthermore, I observed in the BM, a similar degree of contraction in the number of erythroid precursors in all three models of infection. In comparison to the BM, the suppression of erythroid development was much greater in the spleen. During the immune response to malaria, the spleen is the main anatomical site in which immune cells are brought into close proximity and interact with foreign malarial antigens, as such, it is expected that the highest concentration of proinflammatory cytokines such as IFN-γ secreted by immune cells particularly the $CD4^{+}$ T-cells would be in the spleen. This would account for the considerable suppression of erythropoiesis at this site. These observations clearly argue in favour of pro-inflammatory cytokines in mediating suppression of erythropoiesis during malaria.

Based on the kinetics of IFN-γ and TNF-α in serum during malaria, I was unable to deduce which of these pro-inflammatory cytokines might be mediating dyserythropoiesis. Cytokines are potent even at extremely low concentrations and despite IFN-γ peaking earlier than TNF-α in the SBP model of infection, the concentration of TNF-α even at day 4 post-infection could have been responsible for this inhibition of BM erythropoiesis. To dissect this further I established experimental malaria in genetic knock out mice incapable of IFN-γ signalling specifically in haematopoietic cells. This is discussed in the next chapter. The SBP model of infection alone was used in further studies.

4.7 Conclusion

I set out to investigate the impact of malaria on erythropoiesis and made some key findings. One of these findings is similar to what has been observed in some human studies that BM suppression can occur even in the absence of microscopically detectable or very low parasitaemia. This suggests that the suppression of erythroid development is independent of peripheral parasite density but is most likely due to a dysregulated immune response. To further investigate the role of IFN-γ, I have utilised a novel mouse strain lacking IFN-γ signalling in only haematopoietic cells (discussed in chapter 5).

Based on this data and work that has been published by our laboratory on the impact of malaria on the BFU-e and CFU-e (67), all stages downstream of the MEP analogue are clearly impacted by malaria. Despite the expansion of the MEP analogue which suggests some degree of erythroid response to malaria, one cannot exclude the possibility that in malaria this population has a higher proliferation index and/or remains longer in this development stage. However, my results identify this population, upstream of the mature erythrocyte, as stable in all three mouse models of malaria.

Contraction of the pre-MEP was only evident in the MT model, which is most likely due to the peculiarities of the models in that, they differ in key elements such as parasitaemia, virulence, pro-inflammatory cytokine induction and immune response elicited.

In summary, at early time points in malaria, there is an infection-induced suppression of erythroid development in the BM and spleen which is independent of the degree of peripheral parasitaemia and suggests the role of pro-inflammatory cytokines in mediating this process.

CHAPTER 5

IMPACT OF MALARIA ON ERYTHROID DEVELOPMENT IN THE ABSENCE OF IFN-γ SIGNALLING IN HAEMATOPOIETIC CELLS

5.1 Introduction

The lack of correlation between peripheral parasitaemia and anaemia in severe malarial anaemia suggests that factors besides schizont rupture and erythrophagocytosis contribute to anaemia. It is well documented that proinflammatory cytokines such as TNF-α, IFN-γ and IL-6 have an adverse effect on erythroid development, leading to anaemia in multiple diseases including chronic infections, chronic inflammatory diseases, myelodysplastic syndromes and malignancy (113,115,151–157). In malaria, it has been proposed that these proinflammatory cytokines play a central role in mediating mechanisms that lead to anaemia (105,158,159).

My observation in the preceding chapter that the suppression of erythropoiesis in the BM during experimental malaria can be observed in models which are characterised by high as well as low peak parasitaemia, strongly suggests that the blood stage parasite antigens and/or by-products of parasite-driven haemoglobin catabolism, such as hemozoin, are sufficient to elicit a robust proinflammatory cytokine response, capable of suppressing erythroid development in the BM.

In a murine model of anaemia of chronic disease, the anaemia in these mice was fully dependent on IFN-γ mediated upregulation of the transcription factor Pu.1, a known antagonist of the erythroid transcription factor GATA-1 (113). In this model, IFN-γ was responsible for the reduced life span of red blood cells and the inhibition of BM erythroid output. There was no evidence for increased apoptosis of erythroblast populations in this study.

In studies *in vitro*, the induction of apoptosis in erythroid cells has been the central mechanism by which IFN-γ indirectly mediates the suppression of erythropoiesis, but in *in-vivo* settings and particularly during malaria, the specific pathways linking IFN-γ to dyserythropoiesis are poorly defined. Furthermore, It remains unknown if the suppression of erythropoiesis by IFN-γ is a consequence of a direct signalling in haematopoietic cells especially in cells of the erythroid lineage or whether it is a consequence of IFN-γ signalling in non-haematopoietic compartments such as the mesenchymal-derived subsets of niche-forming cells.

The purpose of this study was to determine *in vivo*, if the ablation of IFN-γ signalling in the haematopoietic compartment alone was sufficient to abate BM suppression during malaria, resulting in increased BM and splenic erythroid output. To address this question, I have taken advantage of the *Cre/loxP* recombination system (160). I used tissue-specific conditional knockout mice in which the *Ifngr2* gene, which encodes the IFN-γ receptor β chain was specifically deleted on all haematopoietic cells.

The α chain of IFN-γ receptor is the ligand binding component while the β chain is responsible for downstream signalling (161). By deleting Ifngr2 strictly on only the haematopoietic cells in the *Vav1::iCre/Ifngr2*$^{fl/fl}$ mice, I expected that all haematopoietic cells in this strain of mice would be incapable of IFN-γ signalling while the *Ifngr2*$^{fl/fl}$ and *Vav1::iCre* mice serving as controls would have intact IFN-γ signalling.

5.2 Ablation of IFN-γ signalling in haematopoietic cells does not alter the number of erythroid and myeloid progenitors in steady state

Prior to establishing experimental malaria, I determined if mice that had undergone ontogeny in the absence of IFN-γ signalling in haematopoietic cells would result in changes in their number of HPC sub-populations in comparison to mice with intact IFN-γ signalling. Live LIN$^-$ cells from naïve *Vav1::iCre/Ifngr2*$^{fl/fl}$, *Vav1::iCre* and *Ifngr2*$^{fl/fl}$ mice were labelled with fluorochrome conjugated monoclonal antibodies against CD117, Sca-1, CD150 and CD27 as described in preceding chapter, and the absolute number of MEP, Pre-MEP and CMP/GMP was determined. I observed no significant difference in the absolute number of these progenitor populations in IFN-γ deficient mice and controls in steady state (Figure 5.1).

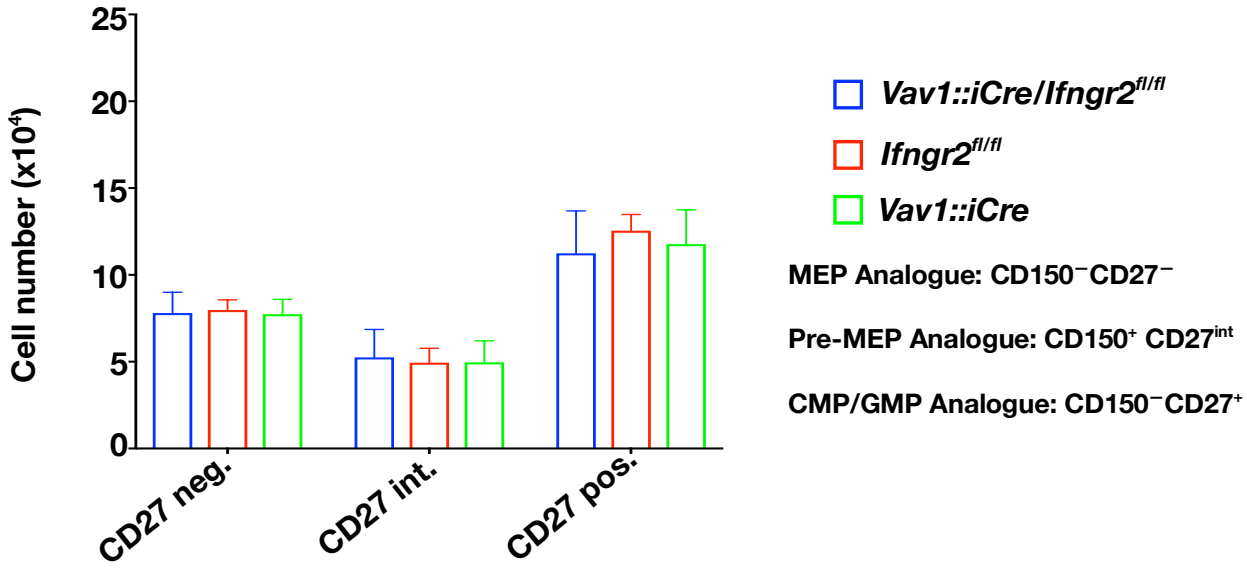

Figure 5.1 Vav1::iCre/Ifngr2$^{fl/fl}$, Ifngr2$^{fl/fl}$ and Vav1::iCre mice exhibit no difference in absolute number of HPC subsets in steady state

Absolute number per femur/tibia pair of MEP, Pre-MEP and CMP/GMP in *Vav1::iCre/Ifngr2$^{fl/fl}$, Ifngr2$^{fl/fl}$ and Vav1::iCre* mice in steady state. Results are representative of two independent experiments. Values represent mean ± SEM, n = 10 mice per group. Significance was calculated using one-way ANOVA.

5.3 Upregulation of Sca-1 on HPCs during malaria is directly dependent on IFN-γ signalling in haematopoietic cells

Next, I established experimental malaria in IFN-γ signalling deficient and control mice. *Vav1::iCre/Ifngr2$^{fl/fl}$, Ifngr2$^{fl/fl}$ and Vav1::iCre* mice were infected intraperitoneally with 10^5 *Pcc AS* parasitised erythrocytes using the SBP model of infection and the upregulation of Sca-1 on cells within the HPC pool was evaluated. Our laboratory previously demonstrated both *in vitro* and *in vivo* that upregulation of Sca-1 on HPCs is dependent on IFN-γ signalling in these cells (68). This experiment served two purposes in this current study: It served as a functional read-out to confirm the genotype of mice used in this study and to ascertain whether the deletion of the β chain of IFN-γ receptor alone was sufficient to abrogate the upregulation of Sca-1

during malaria, thereby confirming the absence of down stream signalling despite the receptor being able to bind to its ligand via the α chain.

At days 5 and 7 post-infection, I observed no change in surface expression of Sca-1 on HPC subpopulations in *Vav1::iCre/Ifngr2*$^{fl/fl}$ mice, whereas in control mice, upregulation of Sca-1 on HPC subsets had set in at day 5 post-infection (Figure 5.2A), with much greater upregulation at day 7 post-infection (Figure 5.2B). These observations are in agreement with previous work in our lab in which mice that lacked the α chain of the IFN-γ receptor on all cells (*Ifngr1-null*) failed to upregulate Sca-1 during malaria, whereas mice with the intact receptor upregulated Sca-1 on their surface(68). These observations were expected considering that that *Ly6a* which encodes Sca-1 is a direct target gene of IFN-γ signalling (162).

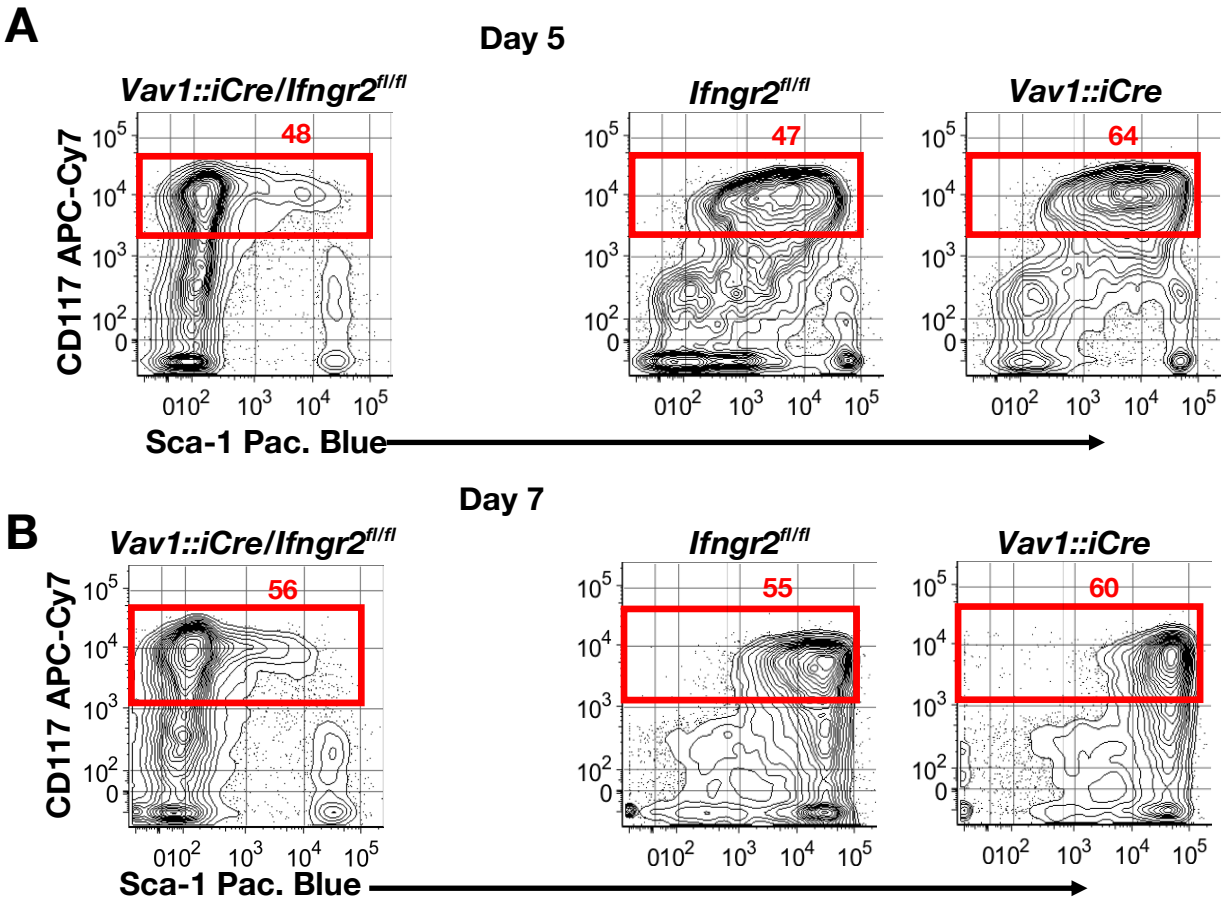

Figure 5.2 Vav1::iCre/Ifngr2$^{fl/fl}$ mice do not upregulate Sca-1 during malaria.

Representative FACS plots illustrating the upregulation of Sca-1 on HPCs at **(A)** day 5 **(B)** day 7 post-infection in *Ifngr2*$^{fl/fl}$ and *Vav1::iCre* mice, whereas HPCs in *Vav1::iCre/Ifngr2*$^{fl/fl}$ mice failed to

upregulate Sca-1 during experimental malaria. Data is representative of two independent experiments using three to five mice per group in each experiment.

5.4 IFN-γ signalling in haematopoietic cells is crucial for malaria parasite control

There have been several correlations between circulating levels of IFN-γ and protection against severe malaria in humans. IFN-γ has been implicated in mediating protective immunity against the pre-erythrocytic and erythrocytic stages of malaria parasites(163–165). In the Fulani tribe in Mali which are naturally resistant to *P. falciparum* malaria there was a much stronger inverse correlation between parasite density and circulating IFN-γ levels in comparison to surrounding tribes (166). In murine models of malaria (using *P. chabaudi* and *P. yoelii*), IFN-γ deficient mice had more elevated and prolonged parasitaemia than control mice (167).

To further dissect the contribution of IFN-γ signalling in haematopoietic cells in the control of parasite density, I monitored the course of parasitaemia in female *Vav1::iCre/Ifngr2*$^{fl/fl}$ and control mice during the acute phase of *Pcc* AS malaria by examination of thin blood smear. Following infection with 10^5 *Pcc AS* parasitised erythrocytes, peak parasitaemia was observed at day 7 post-infection in IFN-γ deficient and control mice (Figure 5.3A), and at this time point, parasitaemia was significantly higher in IFN-γ deficient mice compared to control mice (Figure 5.3B). My results suggest that intact IFN-γ signalling in haematopoietic cells contributes in curtailing peripheral parasitaemia density during acute malaria.

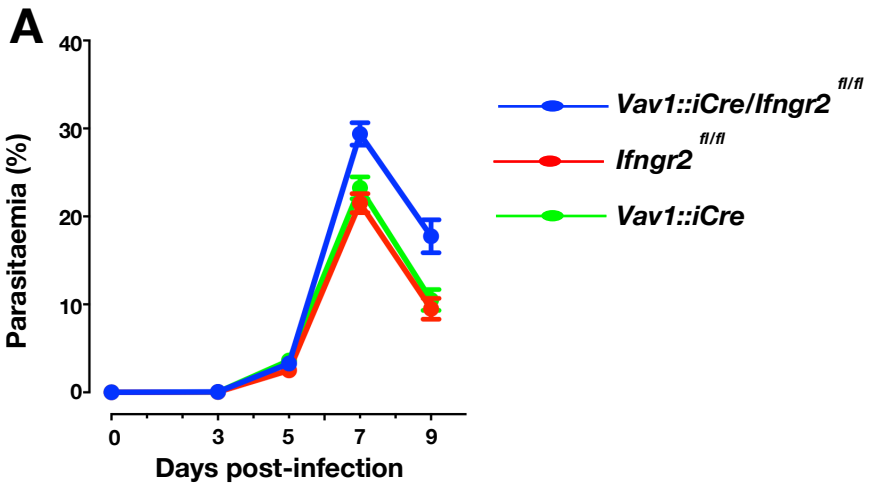

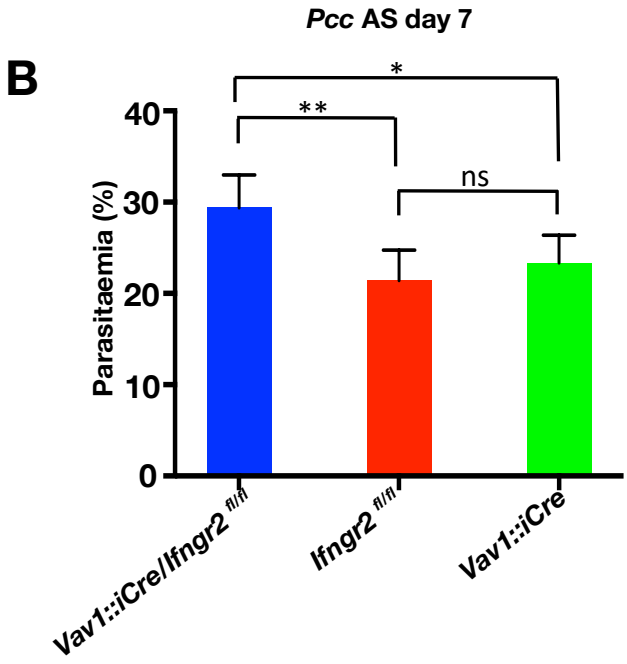

Figure 5.3 IFN-γ signalling in haematopoietic cells is crucial for malaria parasite control

Vav1::iCre/Ifngr2$^{fl/fl}$, *Ifngr2*$^{fl/fl}$ and *Vav1::iCre* mice were infected with 10^5 *Pcc* AS parasitised erythrocytes using the SBP model of infection. **(A)** Course of experimental malaria in *Vav1::iCre/Ifngr2*$^{fl/fl}$, *Ifngr2*$^{fl/fl}$ and *Vav1::iCre* mice. Parasitaemia was determined on the indicated days. **(B)** Parasitaemia at day 7 post-infection in *Vav1::iCre/Ifngr2*$^{fl/fl}$, *Ifngr2*$^{fl/fl}$ and *Vav1::iCre* mice. **(A,B)** Data represents results from two independent experiments, values represent mean ± SEM, n=10 *Pcc* AS infected *Vav1::iCre/Ifngr2*$^{fl/fl}$ and *Ifngr2*$^{fl/fl}$ mice and 6 *Pcc* AS infected *Vav1::iCre mice* per time point. Significance was calculated using one-way ANOVA and Tukey multiple comparisons test. Asterisks represent statistically significant differences (ns: not significant; *: P<0.05; **: P<0.01).

5.5 Contraction of Lineage negative bone marrow cells during acute malaria is dependent on IFN-γ signalling in haematopoietic cells.

During acute *Pcc* AS malaria in WT C57BL/6 mice, I observed a contraction in the absolute number per femur tibia pair of LIN$^-$ BM cells (Figure 4.1C). Our laboratory previously showed that this contraction is dependent on IFN-γ signalling coupled with the egress of myeloid progenitors out of the BM into the spleen (68). Using radiation

chimaeras, the effect of IFN-γ signalling on the loss of myeloid committed BM progenitors was attributed to an irradiation insensitive cellular component in that study.

Adopting a refined genetic approach in this study, *Vav1::iCre/Ifngr2*$^{fl/fl}$, *Ifngr2*$^{fl/fl}$ and *Vav1::iCre* mice were infected with 10^5 *Pcc* AS parasitised erythrocytes using the SBP model of infection. At day 5 and 7 post-infection BM was obtained and labelled with FITC conjugated monoclonal antibodies against lineage markers as described in preceding chapters. After excluding doublets, dead cells and FITC positive cells, the frequency and absolute number of residual LIN$^-$ cells was determined. At day 7 post-infection which corresponds to peak parasitaemia, the frequency (Figure 5.4A) and absolute number per femur/tibia pair (Figure 5.4B) of LIN$^-$ cells was significantly higher in IFN-γ signalling deficient mice in comparison to controls. The contraction of BM LIN$^-$ cells observed in WT C57BL/6 mice in preceding chapter as well as in *Ifngr2*$^{fl/fl}$ and *Vav1::iCre* mice was completely abolished in *Vav1::iCre/Ifngr2*$^{fl/fl}$ mice. Taken together, this data suggests that the contraction of LIN$^-$ BM cells during malaria is a direct consequence of IFN-γ signalling in haematopoietic cells.

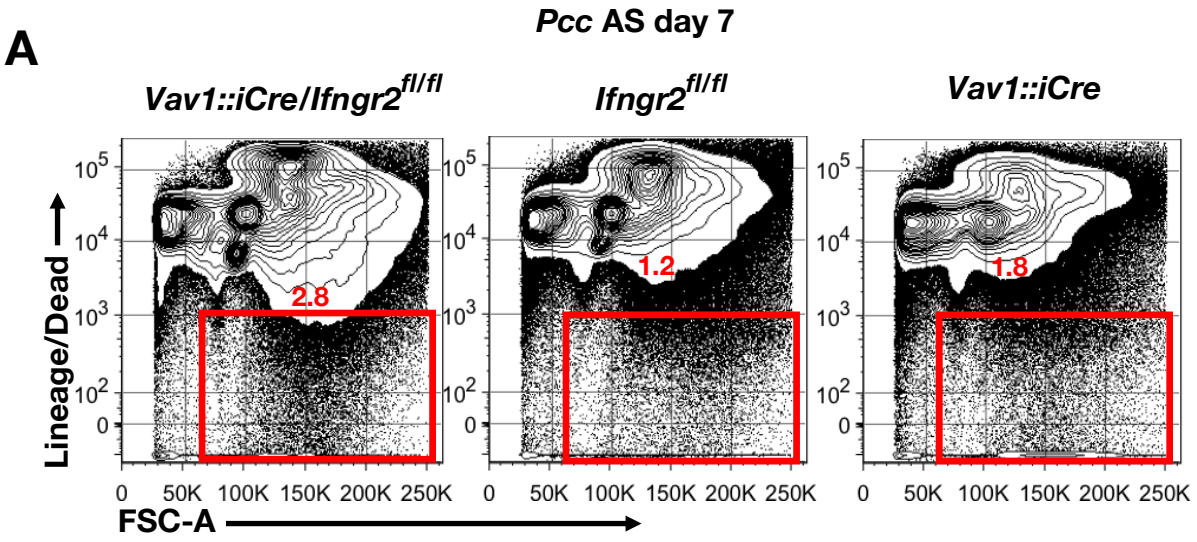

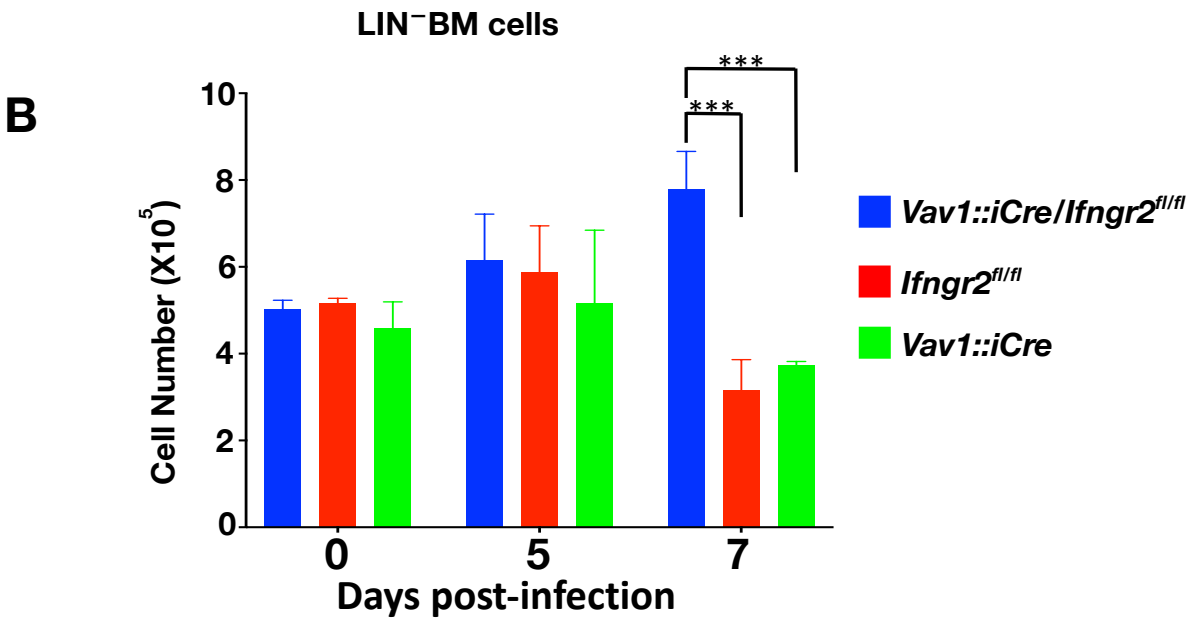

Figure 5.4 Loss of LIN⁻ BM cells during P. chabaudi malaria is dependent on IFN-γ signalling in haematopoietic cells

Frequency **(A)** and Absolute number per femur/tibia pair **(B)** of LIN⁻ BM cells in *Vav1::iCre/Ifngr2*$^{fl/fl}$, *Ifngr2*$^{fl/fl}$ and *Vav1::iCre* mice. The cells in the LIN⁻ gate are sparsely distributed in control mice in comparison to IFN-γ signalling deficient mice. Data represents results from two independent experiments, values represent mean ± SEM, n=10 *Pcc* AS infected *Vav1::iCre/Ifngr2*$^{fl/fl}$ and *Ifngr2*$^{fl/fl}$ mice and 6 *Pcc* AS infected *Vav1::iCre mice* per time point. Significance was calculated using one-way ANOVA and Tukey multiple comparisons test. Asterisks represent statistically significant differences (***: P<0.001).

5.6 IFN-γ signalling in haematopoietic cells is crucial for malaria dyserythropoiesis in bone marrow and spleen

To dissect the role of IFN-γ signalling on aberrant erythropoiesis during malaria, I infected female *Vav1::iCre/Ifngr2*$^{fl/fl}$, *Ifngr2*$^{fl/fl}$ and *Vav1::iCre* mice with 10^5 *Pcc* AS parasitised erythrocytes and at days 5 and 7 post-infection, I determined the frequency and absolute numbers of MEP, Pre-MEP and CMP/GMP analogues (in the BM alone), and erythroid precursors (in the BM and spleen). Naive age and gender-matched littermate *Vav1::iCre/Ifngr2*$^{fl/fl}$, *Ifngr2*$^{fl/fl}$ and *Vav1::iCre* mice were used as controls. Prior to infection and at several time points during infection, the serum concentration of IFN-γ and TNF-α was determined.

In the BM at day 5 post-infection, I observed a higher frequency of the CMP/GMP analogue and a lower frequency of the MEP analogue in IFN-γ deficient mice in comparison to controls (Figure 5.5A). Despite the higher frequency of the MEP analogue in the controls, the contour lines within the MEP analogue gate were more closely packed in IFN-γ signalling deficient mice than in controls indicating a higher concentration of events. Considering that the same number of events was acquired on the cytometer for IFN-γ signalling deficient and control mice, suggested that the frequency of the MEP analogue might not correlate with the absolute number in this instance.

There was an increase in the absolute number of the MEP analogue during infection regardless of genotype but no significant difference in the magnitude of this increase was observed between IFN-γ signalling deficient and control mice (Figure 5.5B). The contraction of the Pre-MEP analogue was evident in control mice, whereas in mice lacking IFN-γ signalling, this population remained stable during infection. Despite the infection induced contraction of the CMP/GMP analogue in all strains, the absolute number of this population remained significantly higher in *Vav1::iCre/Ifngr2*$^{fl/fl}$ mice in comparison to control mice. Contrary to previous work in our lab (68), this finding indicates that IFN-γ signalling in haematopoietic cells is crucial for the contraction of myeloid progenitors during malaria.

At day 7 post-infection, I observed an even greater reduction in the frequency of CMP/GMP analogue in control mice (Figure 5.5C). Similar to day 5, the frequency of the MEP analogue in IFN-γ signalling deficient mice was much lower than in control mice but the contour lines indicated a higher concentration of events in this group. Indeed, the absolute number of MEP analogue in *Vav1::iCre/Ifngr2*$^{fl/fl}$ mice was significantly higher than in *Ifngr2*$^{fl/fl}$ mice (Figure 5.5D). The absolute number of Pre-MEP analogue remained stable in IFN-γ signalling deficient mice and was significantly higher than in infected controls. There was a further reduction in the absolute number of CMP/GMP analogue in infected controls, while in IFN-γ signalling deficient mice the contraction of this population at day 7 post-infection was similar to day 5.

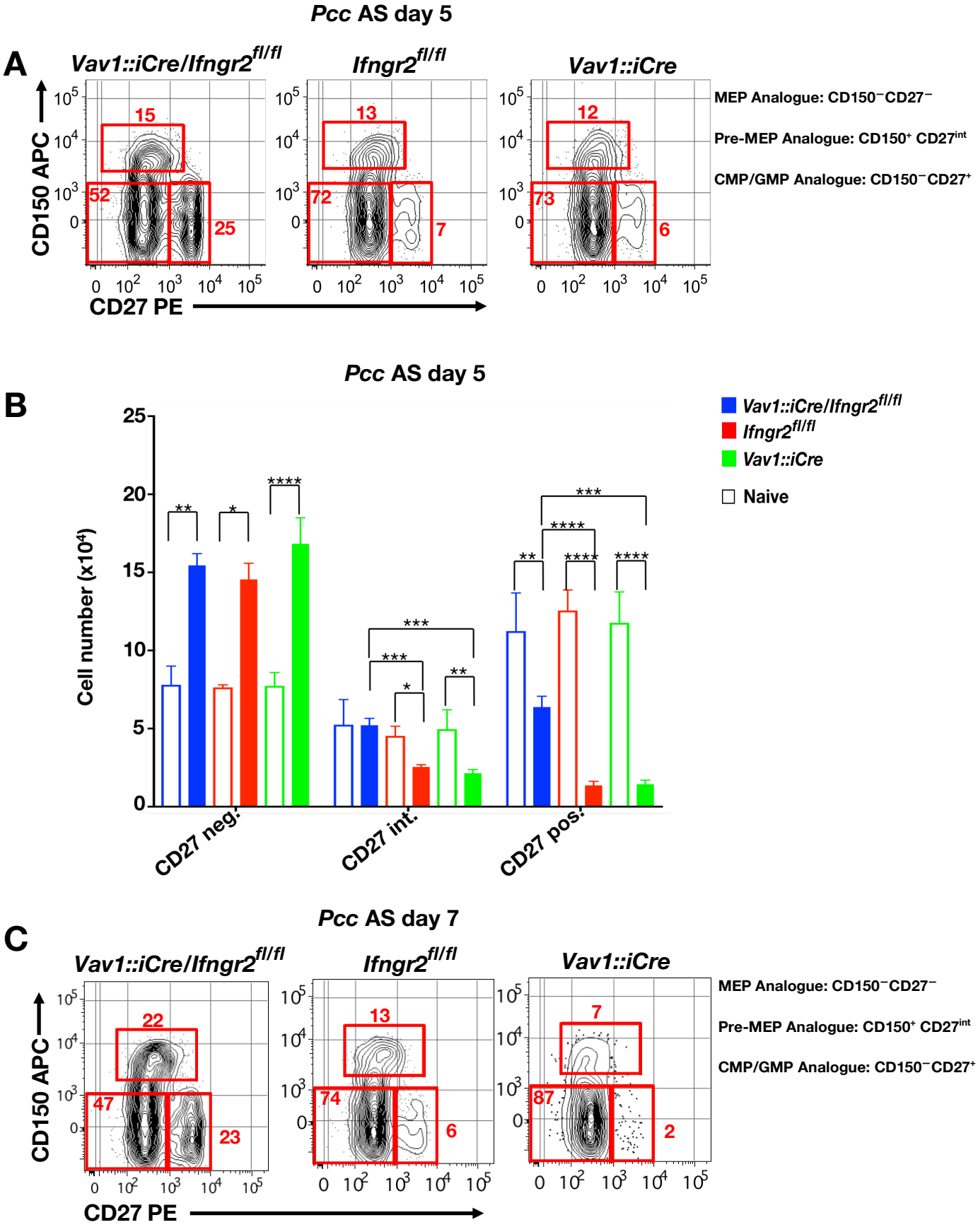
Pcc AS day 5
A
Vav1::iCre/Ifngr2fl/fl
Ifngr2fl/fl
Vav1::iCre
CD150 APC
CD27 PE
15
52
25
13
72
7
12
73
6
MEP Analogue: CD150−CD27−
Pre-MEP Analogue: CD150+ CD27int
CMP/GMP Analogue: CD150−CD27+
Pcc AS day 5
B
Cell number (x10⁴)
CD27 neg.
CD27 int.
CD27 pos.
Vav1::iCre/Ifngr2fl/fl
Ifngr2fl/fl
Vav1::iCre
Naive
Pcc AS day 7
C
Vav1::iCre/Ifngr2fl/fl
Ifngr2fl/fl
Vav1::iCre
CD150 APC
CD27 PE
22
47
23
13
74
6
7
87
2
MEP Analogue: CD150−CD27−
Pre-MEP Analogue: CD150+ CD27int
CMP/GMP Analogue: CD150−CD27+

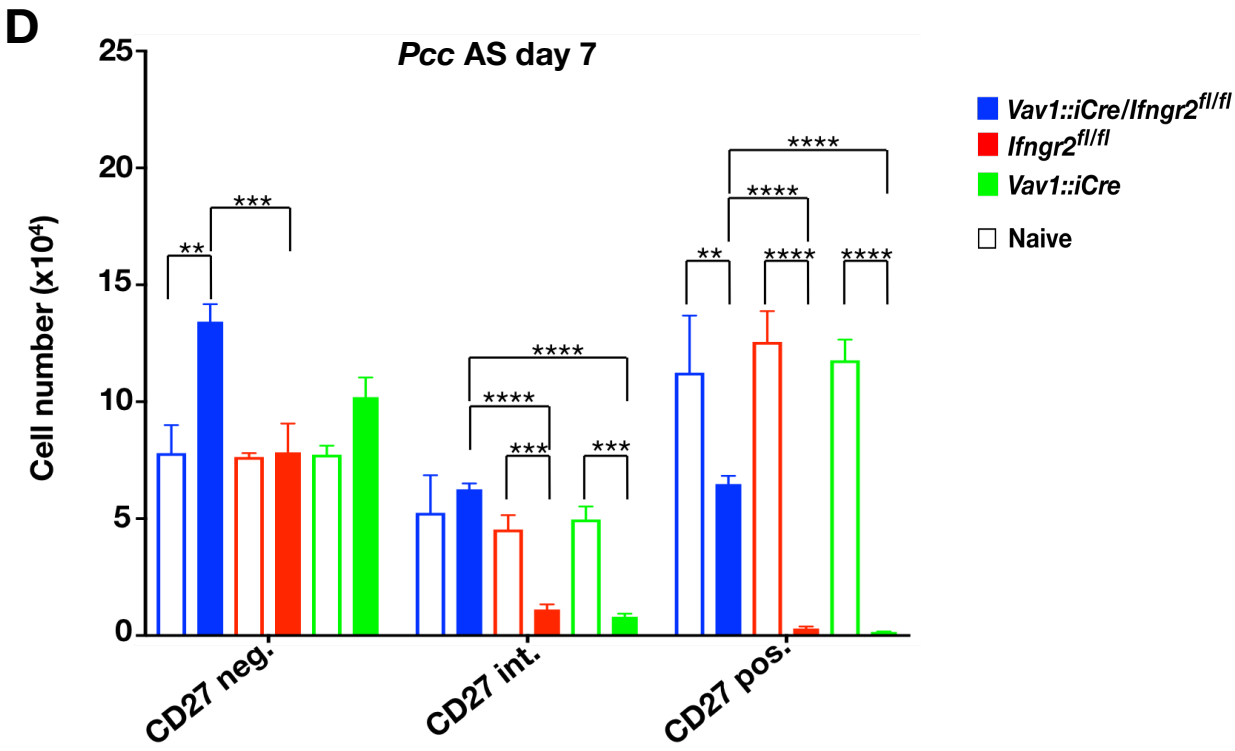

Figure 5.5 Suppression of erythroid progenitor expansion in the BM during malaria is dependent on IFN-γ signalling in haematopoietic cells

LIN⁻ BM cells from *Pcc* AS infected and naïve *Vav1::iCre/Ifngr2*$^{fl/fl}$, *Ifngr2*$^{fl/fl}$ and *Vav1::iCre* mice were labelled with monoclonal antibodies against CD117, Sca-1, CD150 and CD27. Frequency of MEP, Pre-MEP and CMP/GMP analogues at **(A)** day 5 and **(C)** day 7 post-infection. Absolute number per femur/tibia pair of MEP, Pre-MEP and CMP/GMP analogues at **(B)** day 5 and **(D)** day 7 post-infection. Data represents results from two independent experiments, values represent mean ± SEM, n=10 *Pcc* AS infected *Vav1::iCre/Ifngr2*$^{fl/fl}$ and *Ifngr2*$^{fl/fl}$ mice and 6 *Pcc* AS infected *Vav1::iCre mice* per time point. Significance was calculated using one-way ANOVA and Tukey multiple comparisons test. Asterisks represent statistically significant differences (*: $P \leq 0.05$, **: $P \leq 0.01$, ***: $P \leq 0.001$, ****: $P \leq 0.0001$).

BM erythroid precursors were identified as described in preceding chapters. At day 5 post-infection, the 1:2:4:8 ratio of erythroblast maturation was unperturbed with similar frequency of erythroid precursors in *Vav1::iCre/Ifngr2*$^{fl/fl}$, *Ifngr2*$^{fl/fl}$ and *Vav1::iCre* mice (Figure 5.6A). This reflected in the absolute number of erythroid precursors with no significant difference observed in infected *Vav1::iCre/Ifngr2*$^{fl/fl}$, *Ifngr2*$^{fl/fl}$, *Vav1::iCre* and naïve C57BL/6 mice (Figure 5.6B). At day 7 post-infection, there was a reduction in the frequency of erythroid precursors in control mice

whereas in IFN-γ signalling deficient mice the frequency of erythroid precursors remained stable (Figure 5.6C). Furthermore, I observed a significant reduction in the absolute number of erythroblasts at each stage of maturation in control mice in comparison to IFN-γ signalling deficient mice (Figure 5.6 D). Surprisingly, the absolute number of basophilic and polychromatic erythroblasts was significantly higher in infected *Vav1::iCre/Ifngr2*$^{fl/fl}$ mice than in naïve C57BL/6 mice, suggesting some degree of erythroid response in the absence of IFN-γ signalling in haematopoietic cells.

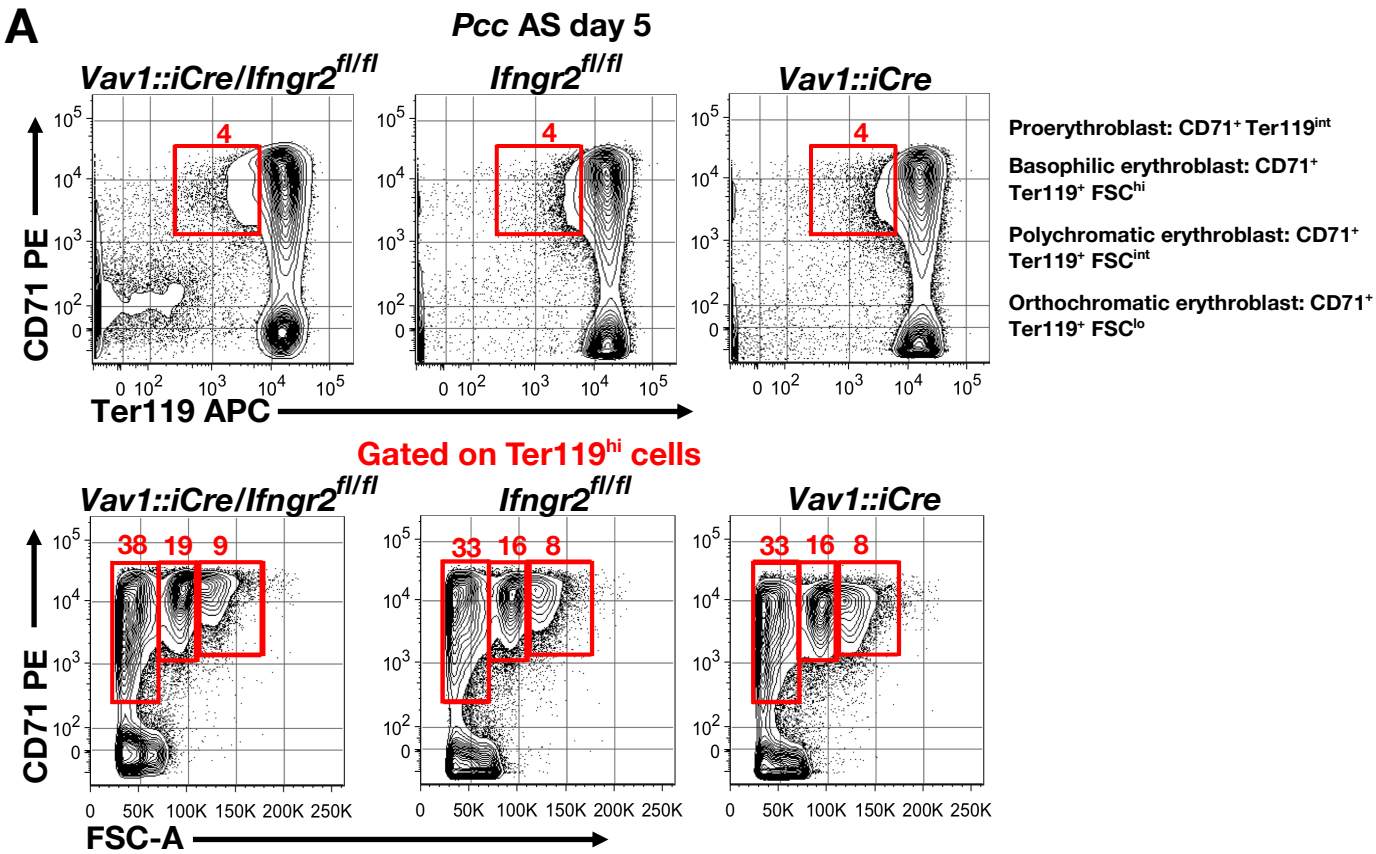

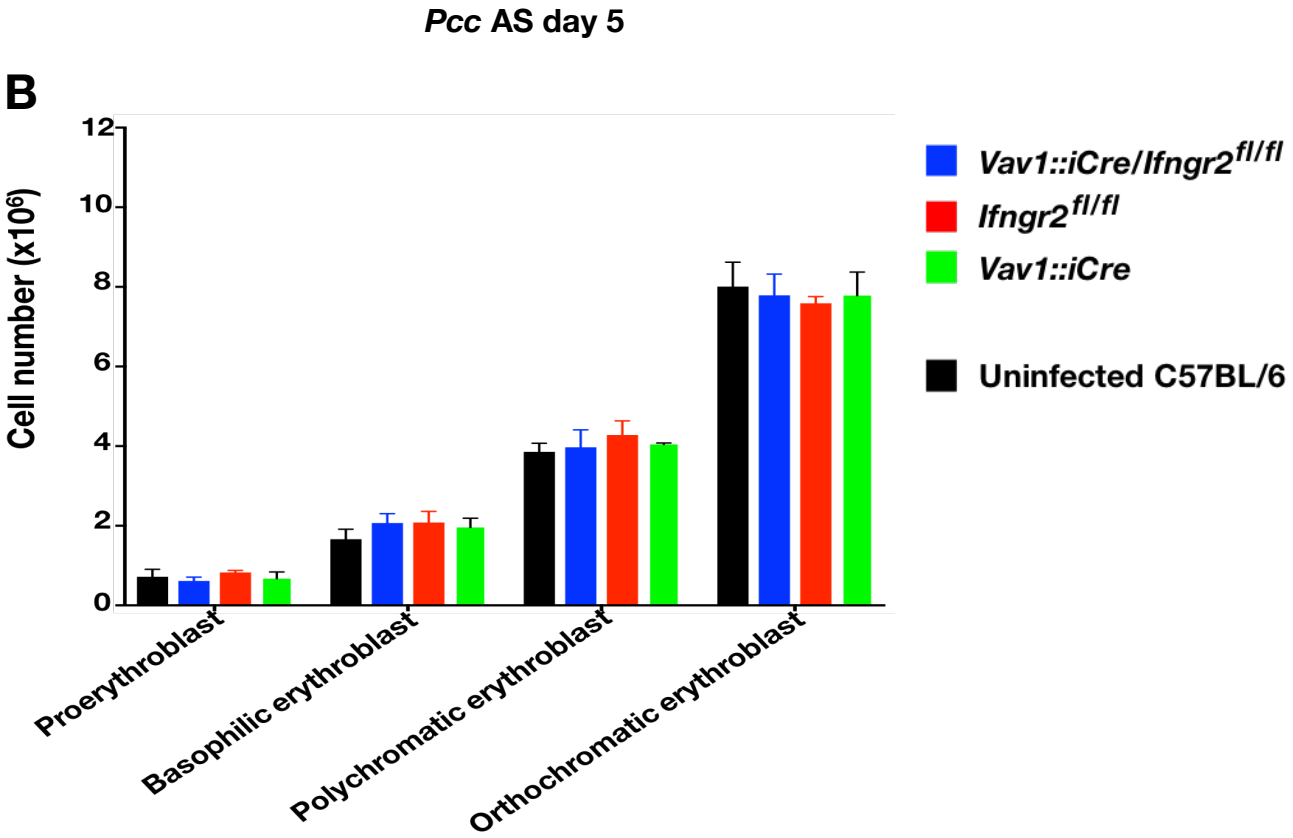
Pcc AS day 5
B
Cell number (x10⁶)
12
10
8
6
4
2
0
Vav1::iCre/Ifngr2fl/fl
Ifngr2fl/fl
Vav1::iCre
Uninfected C57BL/6
Proerythroblast
Basophilic erythroblast
Polychromatic erythroblast
Orthochromatic erythroblast

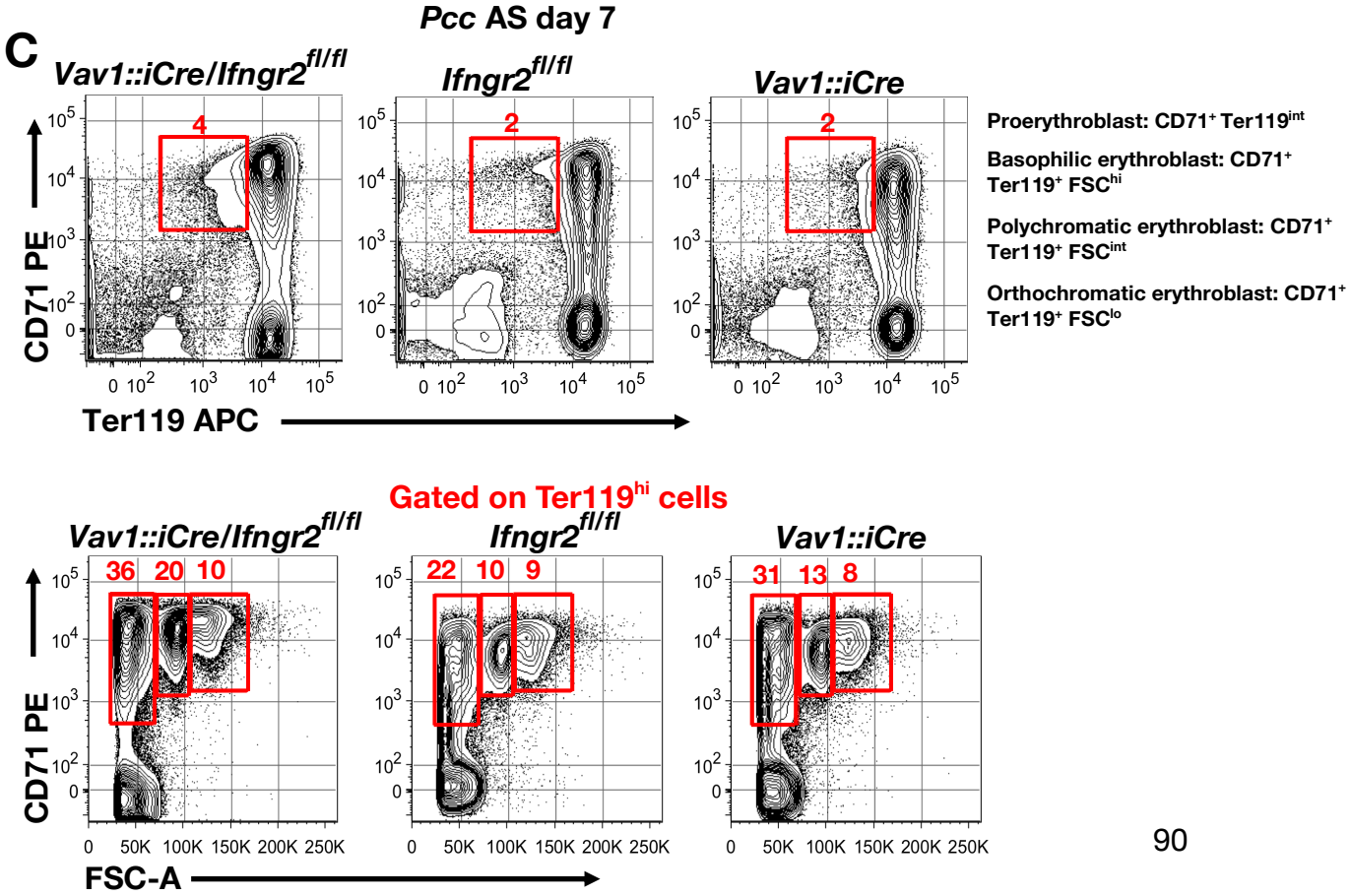
Pcc AS day 7
C
Vav1::iCre/Ifngr2fl/fl
Ifngr2fl/fl
Vav1::iCre
CD71 PE
Ter119 APC
4
2
2
Proerythroblast: CD71+ Ter119int
Basophilic erythroblast: CD71+ Ter119+ FSChi
Polychromatic erythroblast: CD71+ Ter119+ FSCint
Orthochromatic erythroblast: CD71+ Ter119+ FSClo
Gated on Ter119hi cells
36 20 10
22 10 9
31 13 8
FSC-A
0 50K 100K 150K 200K 250K

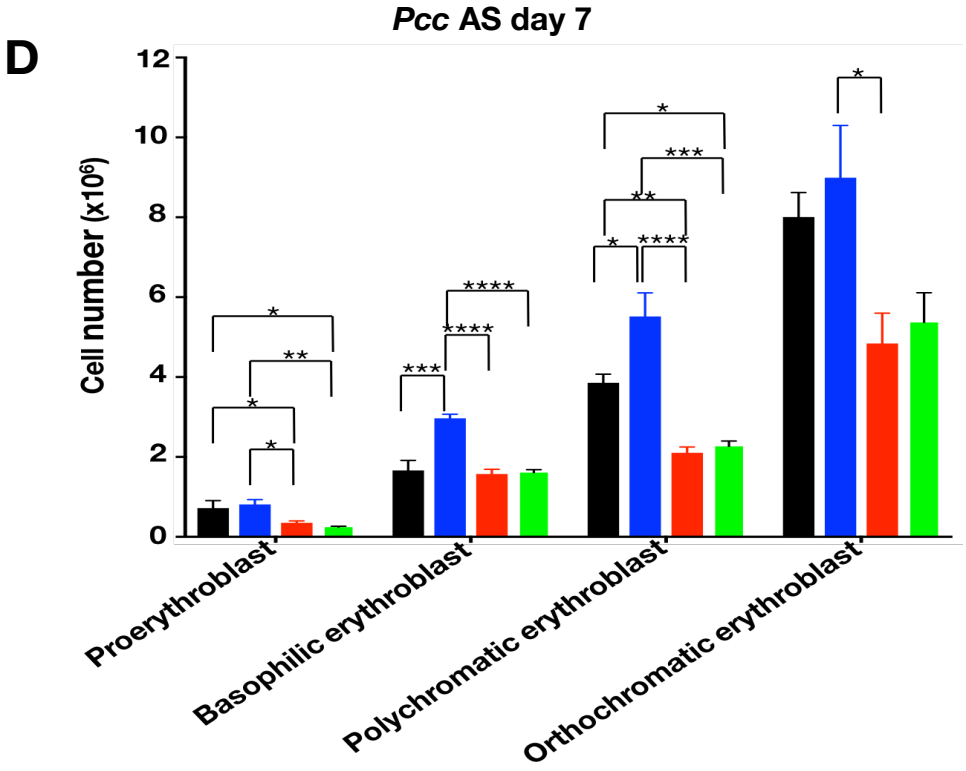

Figure 5.6 Contraction of erythroid precursors in the BM during malaria is dependent on IFN-γ signalling in haematopoietic cells

Frequency of BM erythroid precursors in *Vav1::iCre/Ifngr2*$^{fl/fl}$*, Ifngr2*$^{fl/fl}$ and *Vav1::iCre* mice at **(A)** day 5 and **(C)** day 7 post-infection. Absolute number per femur/tibia pair of BM erythroid precursors in naïve C57BL/6 and infected *Vav1::iCre/Ifngr2*$^{fl/fl}$*, Ifngr2*$^{fl/fl}$ and *Vav1::iCre* mice at **(B)** day 5 and **(D)** day 7 post-infection. Data represents results from two independent experiments, values represent mean ± SEM, n=10 *Pcc* AS infected *Vav1::iCre/Ifngr2*$^{fl/fl}$ and *Ifngr2*$^{fl/fl}$ mice and 6 *Pcc* AS infected *Vav1::iCre* and naïve C57BL/6 *mice* per time point. Significance was calculated using one-way ANOVA and Tukey multiple comparisons test. Asterisks represent statistically significant differences (*: $P \leq 0.05$, **: $P \leq 0.01$, ***: $P \leq 0.001$, ****: $P \leq 0.0001$)**.**

Next, spleens from infected *Vav1::iCre/Ifngr2*$^{fl/fl}$ *and Ifngr2*$^{fl/fl}$ mice were obtained and weighed then erythroid precursors in the spleen were identified as described in preceding chapters. At days 5, 7 and 9 post-infection, I observed that the spleens from *Vav1::iCre/Ifngr2*$^{fl/fl}$ mice weighed significantly less than infected control mice (Figure 5.7A) and were considerably smaller. (Figure 5.7B). The absence of IFN-γ signalling to mobilise myeloid progenitors from the BM to the spleen could have contributed to the smaller spleen size in *Vav1::iCre/Ifngr2*$^{fl/fl}$ mice. In addition, the spleens from infected *Vav1::iCre/Ifngr2*$^{fl/fl}$ mice were slightly larger than naïve

C57BL/6 mice. This suggests that other factors besides IFN-γ signalling in haematopoietic cells, such as accumulation of parasitised erythrocytes contribute to splenomegaly during malaria. At day 7 post-infection, the frequency of all erythroblasts was significantly higher in *Vav1::iCre/Ifngr2*$^{fl/fl}$ mice than in *Ifngr2*$^{fl/fl}$ mice (Figure 5.7C). This reflected in the absolute numbers, with a significantly higher absolute number of all erythroblasts in *Vav1::iCre/Ifngr2*$^{fl/fl}$ mice in comparison to control mice (Figure 5.7D). These observations suggest that the block in erythropoiesis in the spleen, described in Chapter 4 is ameliorated in the absence of IFN-γ signalling in haematopoietic cells.

Following binding of IFN-γ to its cognate receptor, there is a rapid internalisation of the cytokine-receptor complex (168). Unpublished data from our lab showed that T cells from *Vav1::iCre/Ifngr2*$^{fl/fl}$ mice stain positive for Ifngr1, indicating its presence in the mutant. To decipher whether the interactions between IFN-γ and the ligand binding component of the IFN-γ receptor affects serum levels of IFN-γ with respect to its internalisation and degradation in the absence of the β-chain, I measured circulating levels of IFN-γ in mice lacking the β-chain and those with the intact receptor. I hypothesised that the more this cytokine was internalised and degraded, the lesser would be its concentration in circulation. I observed no significant difference in the serum levels of IFN-γ in *Vav1::iCre/Ifngr2*$^{fl/fl}$ and control mice (Figure 5.7E) suggesting that IFN-γ internalisation, degradation and receptor recycling might not be dependent on the β-chain. The spike in serum concentration of IFN-γ was transient and could only be detected after day 3 post-infection by ELISA. I also determined the circulating levels of TNF-α and similar to earlier experiments in C57BL/6 mice, the peak was observed at day 7, much later than the peak of IFN-γ.

In this study, the serum concentration of TNF-α was much higher in *Vav1::iCre/Ifngr2*$^{fl/fl}$, *Ifngr2*$^{fl/fl}$ and *Vav1::iCre* mice than in C57BL/6 (discussed in Chapter 4) which might be due to differences in genetic background.

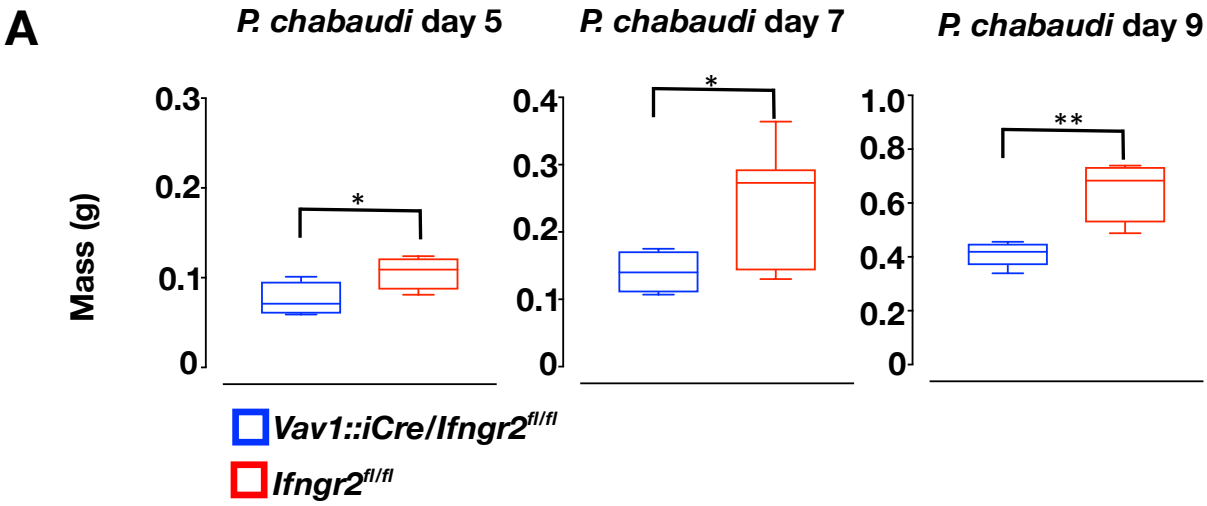

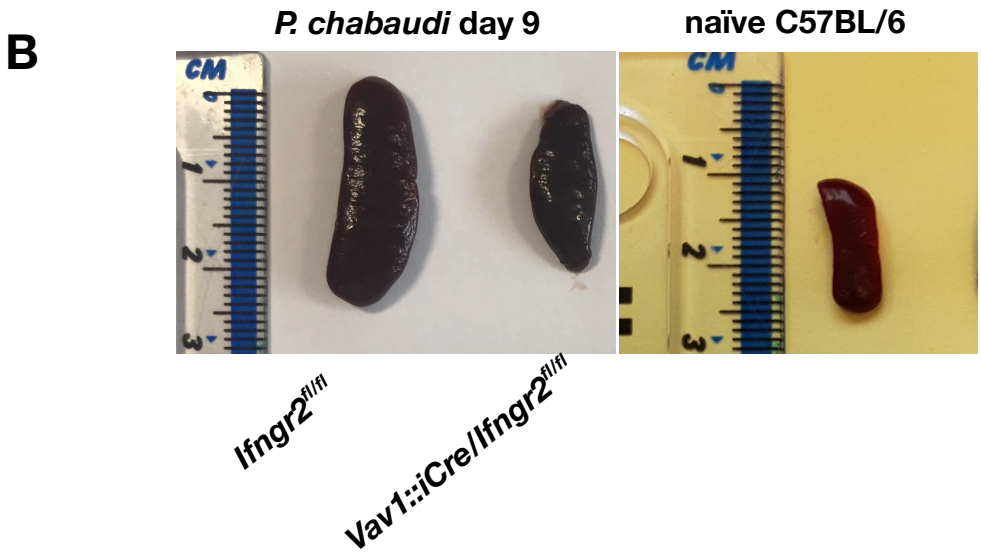

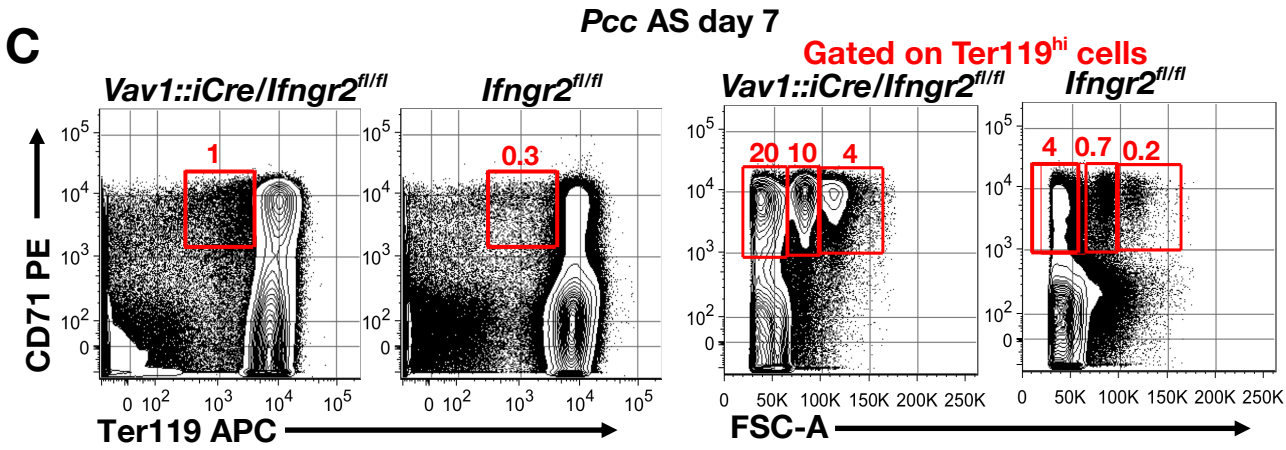

Proerythroblast: CD71⁺ Ter119^{int}

Polychromatic erythroblast: CD71⁺ Ter119⁺ FSC^{int}

Basophilic erythroblast: CD71⁺ Ter119⁺ FSC^{hi}

Orthochromatic erythroblast: CD71⁺ Ter119⁺ FSC^{lo}

D

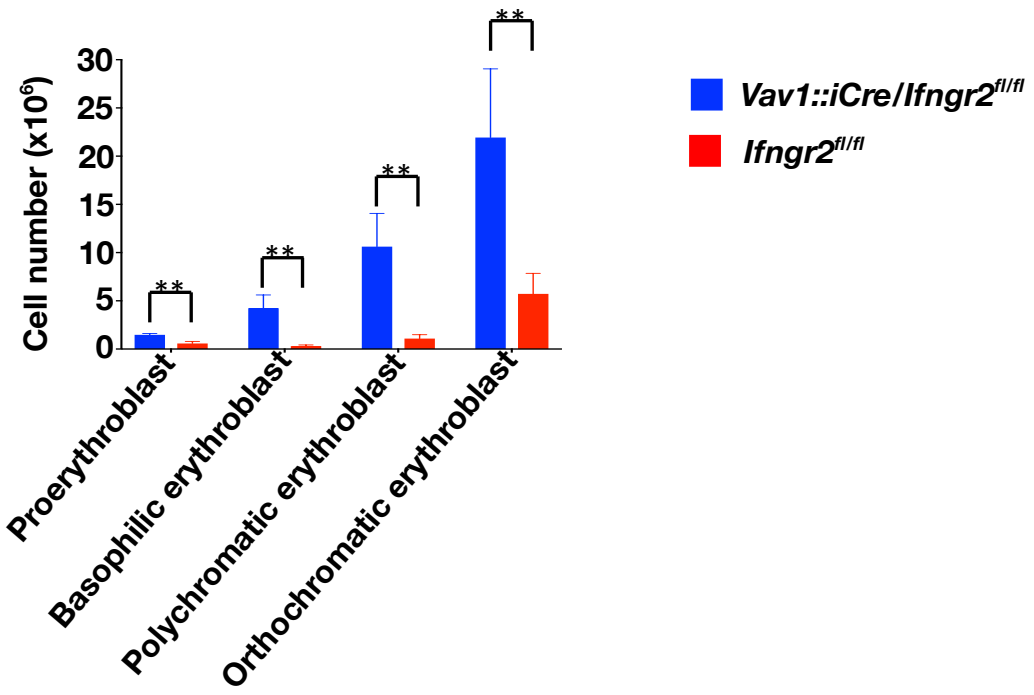
Cell number (x10^6)
30
25
20
15
10
5
0
**
**
**
**
Proerythroblast
Basophilic erythroblast
Polychromatic erythroblast
Orthochromatic erythroblast
Vav1::iCre/Ifngr2fl/fl
Ifngr2fl/fl

E

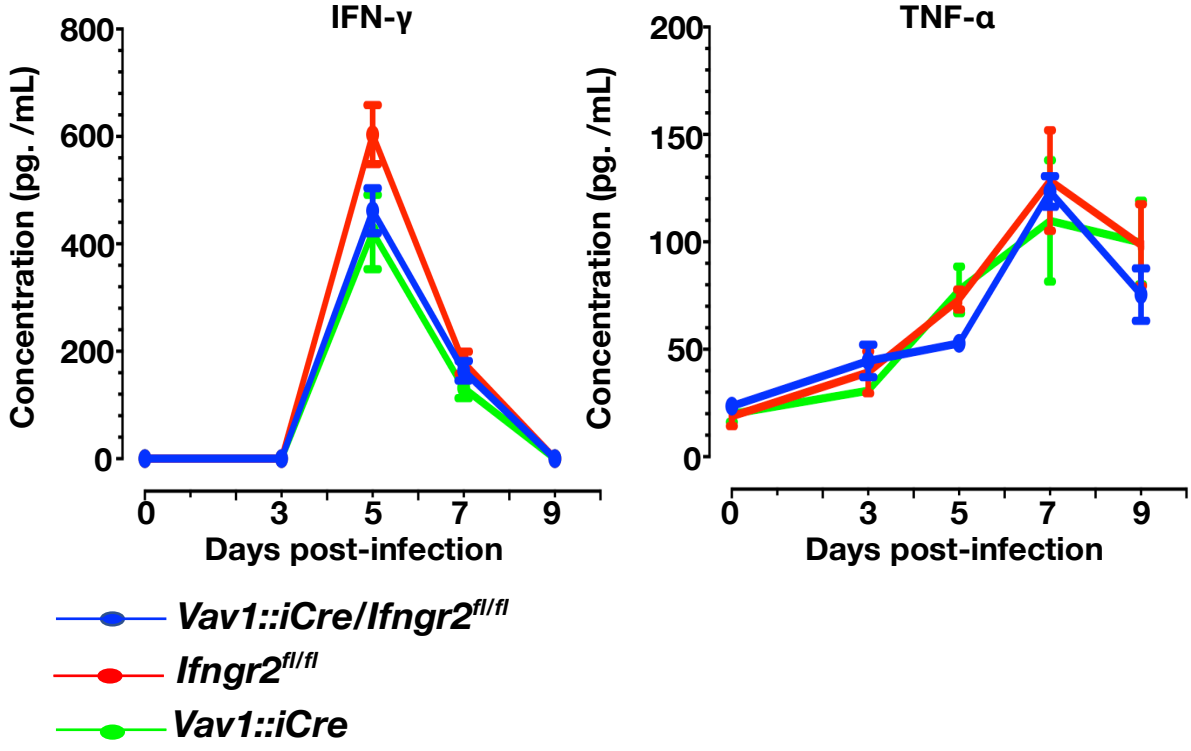
IFN-γ
TNF-α
Concentration (pg. /mL)
800
600
400
200
0
200
150
100
50
0
0
3
5
7
9
Days post-infection
Vav1::iCre/Ifngr2fl/fl
Ifngr2fl/fl
Vav1::iCre

Figure 5.7 Contraction of erythroid precursors in the spleen during malaria is dependent on IFN-γ signalling in haematopoietic cells

(A) Bar chart showing the mass per spleen of *Vav1::iCre/Ifngr2*$^{fl/fl}$ and *Ifngr2*$^{fl/fl}$ mice at days 5, 7 and 9 post-infection. **(B)** Representative image showing the spleens of *Vav1::iCre/Ifngr2*$^{fl/fl}$ and *Ifngr2*$^{fl/fl}$ mice at day 9 post-infection as well as spleen from naïve C57BL/6 mice. **(C)** Representative FACS plots illustrating the frequency of splenic erythroid precursors in *Vav1::iCre/Ifngr2*$^{fl/fl}$ *and Ifngr2*$^{fl/fl}$ mice at day 7 post-infection. (D) Absolute number per spleen of erythroid precursors in *Vav1::iCre/Ifngr2*$^{fl/fl}$ *and Ifngr2*$^{fl/fl}$ mice at day 7 post-infection. **(E)** Serum concentration of IFN-γ and TNF-α in *Vav1::iCre/Ifngr2*$^{fl/fl}$*, Ifngr2*$^{fl/fl}$ and *Vav1::iCre* mice throughout infection.
(A and E) Data represents results from two independent experiments, values represent mean ± SEM, n=10 *Pcc* AS infected *Vav1::iCre/Ifngr2*$^{fl/fl}$ and 6 *Ifngr2*$^{fl/fl}$ mice per time point. **(C and D)** Data represents results from one experiment, values represent mean ± SD, n=10 *Pcc* AS infected *Vav1::iCre/Ifngr2*$^{fl/fl}$ and 8 *Ifngr2*$^{fl/fl}$ mice per time point. **(A and D**) Significance was calculated using Student's t-test(*: $P \leq 0.05$, **: $P \leq 0.01$)**. (E)** Significance was calculated using one way ANOVA.

5.7 Discussion

It has been known mostly from *in vitro* studies that IFN-γ is a potent mediator of dyserythropoiesis. In malaria however, the role of IFN-γ in mediating erythroid suppression is still elusive and I attempted to dissect the role of IFN-γ *in vivo*. The availability of mice with a specifc ablation of IFN-γ signalling in the haematopoietic compartment was exploited to study the role of IFN-γ during acute malaria in a mouse model. The use of the genetically engineered strain eliminates the need for mixed BM chimaera thereby allowing the study of the infection-induced effect of IFN-γ.

I confirmed the absence of IFN-γ signalling using two independent means: Successful *Cre*-dependent ablation of *Ifngr2*, and using the upregulation of Sca-1 as a functional read-out of IFN-γ signalling. The proto-oncogene Vav1 is a protein encoded by the *Vav1* gene, whose expression is predominantly restricted to all haematopoietic cells regardless of stage of development and lineage (169). The upregulation of Sca-1 during infection is dependent on intact IFN-γ signalling (68), and this was used to confirm that the *Vav1::iCre/Ifngr2*$^{fl/fl}$ mice were deficient in IFN-γ signalling exclusively

in haematapoietic cells while both the *Ifngr2*$^{fl/fl}$ and *Vav1::iCre* mice had intact IFN-γ signalling.

The importance of IFN-γ in enhancing the phagocytic activity of myeloid cells to control parasite growth was clearly evident in this study, in that *Vav1::iCre/Ifngr2*$^{fl/fl}$ mice had significantly higher parasitaemia in comparison to mice with intact IFN-γ signalling. As I had previously demonstrated that erythroid suppression during malaria was independent of the degree of peripheral parasite density, this difference in parasitaemia between mice deficient in IFN-γ signalling and control mice would not have contributed to any observed difference in erythroid suppression in these mice.

I have shown for the first time in an *in vivo* setting, that at early time points during experimental malaria, IFN-γ signalling in haematopoietic cells is a crucial element in the infection-induced suppression of erythroid development in the BM and spleen. Applying a more refined phenotypic approach than has been defined previously (19), I demonstrated that the suppression of erythroid development during malaria afffects more primitive progenitor subsets than was previously thought, suggesting a functional impact already in HSCs and multipotent progenitors. In addition, I showed that the splenomegaly during malaria cannot be attributed exclusively to an increased erythropoiesis based on the key observation of absence of more differentiated erythroid precurors.

Using mixed BM chimaeras in which lethally irradiated C57BL/6 mice were transplanted with BM from *Ifngr1-null* mice, our laboratory previously showed that the mobilisation of the myeloid progenitors out of the BM into the spleen was an indirect consequence of IFN-γ signalling via the stromal compartment (68). Using a refined, genetically based system, which avoids transplantation, I have described a hitherto undetectable direct effect of IFN-γ on the myeloid progenitor compartment. This suggests that IFN-γ signalling via the haematopoietic and stromal compartments could both be playing a role in this egress of myeloid progenitors from the BM in the context of malaria. My findings are in agreement with MacNamara and colleagues (135) who demonstrated in a murine model of human monocytic ehrlichiosis that the mobilisation of myeloid progenitors from the BM is a direct consequence of IFN-γ signalling in haematopoietic cells. The efflux of myeloid progenitors from the BM to

the spleen as well as the contraction of the pre-MEP analogue in the *Ifngr2*$^{fl/fl}$ and *Vav1::iCre* control mice might account for the contraction of the LIN^{-} BM cells in these mice.

The unexpected significant increase in the basophilic and polychromatic erythroblast stages in the BM of *Pcc* AS infected *Vav1::iCre/Ifngr2*$^{fl/fl}$ mice, in comparison to naive C57BL/6 mice, suggests some degree of erythroid response to malaria in these populations. This implies that in the absence of IFN-γ signalling in haematopoietic cells, the expansion of the MEP in the BM and spleen reflects in the number of downstream erythroid precursors at both sites during malaria.

There was no significant change in the kinetics of IFN-γ in mice lacking Ifngr2 in comparison to control mice. To further investigate if IFN-γ internalisation, degradation and receptor recycling might be dependent on Ifngr2, a comparison of the intracellular concentration of IFN-γ between Ifngr2 deficient cells that do not synthesise the protein (to eliminate the need to distinguish internalised from newly synthesised protein) and Ifngr2 expressing cells after IFN-γ stimulation is required.

5.8 Conclusion

In summary, at early time points during experimental malaria, there is an IFN-γ dependent suppression of erythropoiesis in the BM and spleen that impacts multiple stages of erythroid development including the most primitive erythroid progenitor the Pre-MEP. The exact mechanism by which IFN-γ mediates this suppression is still unknown but might be due to lateral inhibition of erythropoietin signalling and/or apoptosis. This is discussed further in Chapter 6. My findings do not exclude the impact of other potential mediators of dyserythropoiesis during malaria such as TNF-α, however, they could be acting at much later time points.

Knowledge of the exact concentration of proinflammatory cytokines in particular, IFN-γ and TNF-α in the BM and spleen during malaria could provide useful insights into the spatial and temporal impact of these cytokines on erythroid development. To draw conclusions on the direct effect of *Pcc* AS on erythroid development, there is a need to measure the parasite density in the BM during the course of malaria.

In agreement to previous studies, I documented the importance of IFN-γ signalling in haematopoietic cells for the control of parasite growth. However, results might differ depending on the malaria model in use, and indeed there is a study showing that the early induction of IFN-γ in a murine model of *P. yoelii* malaria favoured the parasitaemia at early time points, but at later time points in this study, IFN-γ was crucial in efficiently clearing the blood stage parasite (170).

In this study I was unable to determine if the expansion of the MEP analogue in the spleen was as a result of the migration of BM MEP or upstream progenitors to the spleen, the proliferation of native splenic MEP and/or the increased differentiation of upstream splenic erythroid progenitors. Further research is required to decipher which of these processes might prevail during malaria.

Future work could focus on recent advances in single-cell RNA sequencing and transcriptomics to explore the molecular mechanism for IFN-γ dependent suppression of erythropoiesis during malaria . Changes that occur in key erythroid transcription factors such as GATA-1, GATA2, EKLF and FOG-1 in steady state and during malaria as well as transcriptional changes in pro-apoptotic genes such as *Bax*; and anti-apoptotic genes such as Bcl_{xl} could be determined. In this study I have restricted the ablation IFN-γ signalling to all haematopoietic cells, this can be improved upon by restricting the ablation of IFN-γ signalling to erythroid cells using the EpoR-Cre, $Ifngr2^{fl/fl}$ mice.

.

CHAPTER 6

GENERAL DISCUSSION

One of the most life-threatening complications of malaria is severe anaemia. In holo-endemic transmission areas, severe malarial anaemia (SMA) is the main clinical manifestation of severe childhood malaria. In these high transmission areas, mortality rates can exceed 30% in children (171). Management of patients with SMA is mainly by blood transfusion, however, in resource-poor settings in sub-Saharan Africa, there are several risks to life and health posed by blood transfusion. Rather than managing SMA, understanding the pathogenesis and devising measures to eliminate the drivers seems a much better approach.

One driver of SMA is suppressed erythropoiesis. Administration of erythropoietin and erythropoietin stimulating agents (ESAs) have been used in the treatment of anaemia of chronic kidney disease. However, they fail to stimulate erythropoiesis in individuals with SMA (172) because these individuals are not deficient in erythropoietin production. On the contrary, these patients have a robust erythropoietin response to malaria (139) but are nonresponsive to the hormone evidenced by the low RPI. Ferrous iron supplements have had the worse outcomes and had to be prematurely stopped. Of recent, triterpenes with pleiotropic (anti-inflammatory, anti-nociception, antioxidant) properties have been reported as having much potential in the treatment of SMA in murine models (172). Several proinflammatory cytokines such as TNF-α, IFN-γ and IL-6 have been implicated as mediators of dyserythropoiesis in multiple diseases. Considering the early spike in IFN-γ concentration in serum in murine models of malaria, and unpublished data from our lab that there is an expansion of erythroid progenitors in *Ifngr1-null* mice during malaria, I have focussed on IFN-γ in this study. I aimed to investigate the role of IFN-γ in mediating suppressed erythropoiesis during malaria.

The suppression of erythropoiesis during malaria has been demonstrated in several studies, however, there is a paucity of data on the *in-vivo* role of IFN-γ in mediating this erythroid suppression during malaria. Furthermore, there exists no published study that has utilised the most recent gating strategies to identify erythroid cells during malaria. Suppression of erythropoiesis is not unique to malaria, it occurs also in Leishmaniasis and has been attributed to cytokine mediated apoptosis of erythroblasts (173).

6.1 Steady state erythropoiesis

Studies on dyserythropoiesis in malaria have mainly focussed on the BFU-e, CFU-e and reticulocyte stages of erythropoiesis. Unfortunately, the transition from the HSC compartment into the most mature precursors of the erythroid lineage has not been comprehensively mapped. I set out to identify erythroid progenitors and precursors using the most recent gating strategies. Akashi *et al.*(12) pioneered the identification of the MEP using the surface markers CD16/32 and CD34. The MEP was previously thought to be the earliest erythroid progenitor downstream of the MPPs, but Pronk and colleagues (19) demonstrated using the surface marker CD150, that it is a heterogeneous population containing both $CD150^{+}$ and $CD150^{-}$ subsets. The $CD150^{+}$ subset was termed pre-MEP (precursor of MEP). CD150, a SLAM-family member, is a marker expressed on HSCs, and its expression on the pre-MEP suggested that it was more primitive than the MEP. Due to the poor resolution of cells within the HPC compartment by CD34, and considering that all the myeloid progenitors within this compartment express CD27, I used CD27 which provides a much better resolution, to distinguish the myeloid progenitors (CMP and GMP) from the MEP and pre-MEP. I also used CD150 to distinguish the pre-MEP from the MEP.

Next, I went further to confirm the erythroid potential of these populations *in vitro*. I demonstrated that the pre-MEP is a direct precursor of the MEP. Furthermore, MEPs cultured *in vitro* under erythroid conditions resulted in the acquisition of Ter119. The marker combination of CD150 and CD27 represents a significant advancement for the dissection of erythroid-committed progenitors and a yet unknown refinement in the study of erythropoiesis. In addition, antigen density of CD27 was found unchanged during infection as shown previously (68). Erythroid precursors were identified using a novel gating strategy in which the ratio of proerythroblast via basophilic erythroblast, polychromatic erythroblast to orthochromatic erythroblast, relate to each other in a 1:2:4:8 ratio during terminal differentiation in steady state. This ratio was found to be perturbed during malaria indicating either a cessation of proliferation and/or a defect in terminal differentiation.

6.2 Erythroid development during malaria

Using this novel gating strategy, I investigated the changes that occurred in erythroid progenitors and precursors during malaria. In three models of malaria namely the SBP model, the MT model and SI model which differ in the immune response elicited, cytokine induction, parasite density and parasite virulence, erythroid suppression was evident to similar degree. I observed an expansion of the BM MEP analogue and a contraction of downstream BM erythroid precursors. The contraction of $Ter119^{+}$ erythroblast populations during malaria has been well documented and my findings are in full agreement with previous studies (95,150,174,175). I extended my investigations to include erythroid-committed populations upstream of the MEP during malaria.

The failure of the increased number of BM MEPs to reflect in downstream stages could have been due to their translocation from the BM to the spleen, or as a result of a block in downstream differentiation. To further clarify this, a similar phenotypic approach to map erythroid development was employed for spleen-resident cells. There was approximately an 18-fold increase in the number of MEP analogue in the spleen of infected mice during malaria but similar to the BM, this highly significant expansion of MEPs was not reflected in the number of more distal erythroblast populations. Despite the possibility of MEP migration from the BM to spleen, there was a clear block in erythroid development which was independent of parasite density. These observations are similar to β-thalassemia dyserythropoiesis in humans which is characterised by expansion of early erythroid progenitors and a contraction of downstream stages (176).

While the BM MEP analogue expanded during malaria, there was no change in the $CD27^{int}$ fraction of the HPC, which contains the pre-MEP analogue, in two models of malaria, namely the SBP and SI, while in the MT model, there was a contraction of this population. Considering that this population is upstream of the MEP suggests that the suppressive effect on erythropoiesis during malaria could be occurring at multiple stages. As previously published (68,124), serum concentration of IFN-γ peaked at day 5 post infection. During malaria, specific $CD4^{+}$ T-cells are the main

cellular source of the transient IFN-γ production (177–179). The number of IFN-γ secreting T cells was significantly higher in the spleen compared to the BM (unpublished results, Belyaev *et al.*). In summary, this suggests a higher local concentration of IFN-γ in the spleen compared to the BM arguing for the higher degree of erythropoietic suppression observed in the spleen. Since no qualitative difference in erythroid suppression in all three murine models of malaria were recorded, I concentrated on the SBP model, since it exhibits a clear temporal dissociation in the peak levels of IFN-γ and TNF-α, whereas in the MT model, the kinetics overlap (124). This allows to dissect the distinct suppressive effect of IFN-γ versus TNF-α during acute malaria infection.

6.3 Erythroid development during malaria in tissue specific absence of IFN-γ signalling.

During experimental malaria infections, our laboratory demonstrated a dynamic remodelling of several developmental compartments in the BM which depended on IFN-γ signalling either directly (lymphoid and erythroid compartment) or indirectly (myeloid compartment). IFN-γ is a potent suppressor of haematopoiesis (180–182) and has been implicated in the pathology of several diseases. IFN-γ promotes experimental cerebral malaria in mice models by signalling in haematopoietic and non-haematopoietic compartments (183). Furthermore, IFN-γ-1616 C/T polymorphism in humans was associated with higher serum concentration of IFN-γ and susceptibility to *P. falciparum* malaria (184).

I investigated whether IFN-γ signalling in haematopoietic cells alone is responsible for the suppression of erythropoiesis during malaria. In this study, I made use of a refined genetically engineered mouse strain in which Ifngr2, the signalling component of the receptor, was deleted exclusively on haematopoietic cells. IFN-γ has been reported to modify the expression of Sca-1 on T-cells (185), B cells (186), GMPs, CMPs and MEPs (68). In this study, I demonstrate that IFN-γ signalling in haematopoietic cells is crucial for the upregulation of Sca-1 on HPCs, which correlates with previous findings in our lab in which HPCs in *Ifngr1-null* mice failed to upregulate Sca-1 on their surface.

It has been reported in several studies that IFN-γ is necessary for the control of malaria parasite (167,187), I observed that mice lacking IFN-γ signalling in haematopoietic cells had a significantly elevated parasitaemia in comparison to wildtype controls. This was not surprising as IFN-γ is a known activator of phagocytic cells enhancing their microbicidal activities (188,189)

At day 5 post-infection, there was a significant expansion in the MEPs in both IFN-γ signalling deficient mice and wild type controls in comparison to naive controls, at day-7 post infection however, the absolute number of MEPs in infected wild type mice contracted and was similar to naive controls. In contrast, in infected mice deficient in IFN-γ signalling, the MEPs were still significantly elevated. In the pre-MEP population, a significant contraction had already set in at day 5 post-infection, in infected wild type mice, with an even greater contraction at day 7 post-infection but in infected mice deficient in IFN-γ signalling, no contraction in the number of the pre-MEPs was observed and there was no difference in comparison to naive controls.

In addition, no difference in the absolute numbers of erythroid precursors was observed between infected and naive mice at day 5 post-infection, but at day 7 post-infection, there was a significant contraction in erythroblast populations in infected wild type mice, whereas, in infected mice deficient in IFN-γ signalling, no contraction was observed. In fact, there was a significant increase in the absolute numbers of basophilic erythroblasts and polychromatic erythroblasts in comparison to naive wild type mice. The lack of significant difference in the absolute numbers of the most mature erythroblast population, the orthochromatic erythroblast, in mice lacking IFN-γ signalling and wild type control, suggests that erythropoietic suppression in the BM might manifest first on the primitive erythroid populations and affects more differentiated populations only at later time-points. This might indicate a different level of IFN-γ susceptibility in different subsets. Similar to the BM, spleens of mice deficient in IFN-γ signalling, had significantly higher frequency and absolute number of erythroid precursors in comparison to wild type controls.

Putting all together, this study has demonstrated that IFN-γ signalling in haematopoietic cells alone is crucial for the early suppression of BM and splenic erythropoiesis during malaria in a cell-autonomous way. However, it does not rule out

the contribution of other mediators, such as TNF-α or haemozoin, at later time points in malaria. Furthermore, considering that the most primitive erythroid biased population within the HPC compartment, the pre-MEP, was suppressed by malaria, it raises the possibility that the earliest hit could be occurring in cells within the LSK pool. The amalgamation of the HPC and LSK pools during malaria clearly indicate the need for a further set of parameters to identify cells with impaired erythroid function.

The suppression of erythropoiesis and the expansion of myeloid progenitors during malaria might be an evolutionary strategy by the host to restrict the availability of cells that the pathogen can infect while producing more of those cells that are capable of eliminating the parasite. In this situation IFN-γ clearly would be the ideal mediator of both suppression and activation either directly or indirectly.

6.4 Future direction

As with most research, this study can be explored further. It is not clear if the striking expansion of the MEP analogue in the spleen is a consequence of their migration from the BM, a proliferation of native splenic erythroid progenitors or a combination of both, hence, this will be a subject for further research. In studies *in vitro*, IFN-γ mediated suppression of erythroid development through two main mechanisms; apoptosis and upregulation of antagonists of key erythroid transcription factors (113,117). Insight into the potential mechanisms by which IFN-γ mediates suppression of erythropoiesis during malaria can be gained by determining the changes that occur in key erythroid transcription factors such as GATA-1, GATA-2, EKLF and FOG-1 and their antagonists such as Pu.1. Transcriptional changes in pro-apoptotic genes such as *Bax*; and anti-apoptotic genes such as Bcl_{xl} in mice with tissue specific ablation of IFN-γ signalling could also be determined. Erythropoietin signalling in erythroid cells was demonstrated to be crucial for survival by inhibiting apoptosis in these cells (190). Furthermore, there is a joint requirement of Jak2 for downstream signalling by both EpoR and IFN-γR. Considering the elevated levels of IFN-γ during malaria, I hypothesise that there is a bias in the recruitment of Jak2 to the β chain of IFN-γR, thereby laterally inhibiting EpoR signalling. This hypothesis can be tested *in vitro.* Immunoprecipitation of EpoR and IFN-γR in MEPs stimulated with

Epo and increasing concentration of IFN-γ could be performed to detect the levels of phosphorylated Jak2 bound to each receptor. Mass spectrometry-based screening platforms could also be used to determine the protein interactome in this population during malaria. The findings might explain why erythroid cells in patients with dyserythropoiesis do not respond to erythropoietin stimulation despite the high serum levels of the growth factor in these individuals.

In this study the *Vav1::iCre* driver was used to abolish expression of IFN-γ signalling in all haematopoietic cells, this can be refined by restricting the absence of IFN-γ signalling to only erythroid cells using a Cre recombinase inserted in the erythropoietin receptor gene to ablate expression of IFN-γ receptor β-chain. This will provide further insights on the role of IFN-γ signalling exclusively in erythroid-committed cells and the impact of IFN-γ on malaria dyserythropoiesis. MEPs isolated from such a mouse could be useful in the *in vitro* experiment described above.

Appendix A: *Ifngr2*$^{wt/wt}$ locus

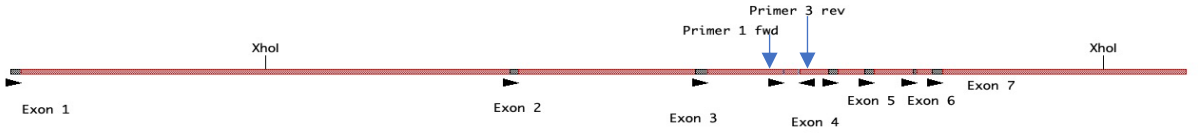

Ifngr2$^{wt/wt}$
(18552bp)

Primer 1 (5'-TGA GTT CCA AGC AAG ACA GA-3') anneals at positions 12189bp to 12208bp, while primer 3 (5'-CAG GGT AGA AAA GAT GTG CA-3') anneals at 12445bp to 12464. The sequence from 12189bp to 12464bp is amplified to yield a 276bp PCR product

Appendix B: *Ifngr2*$^{fl/fl}$ locus

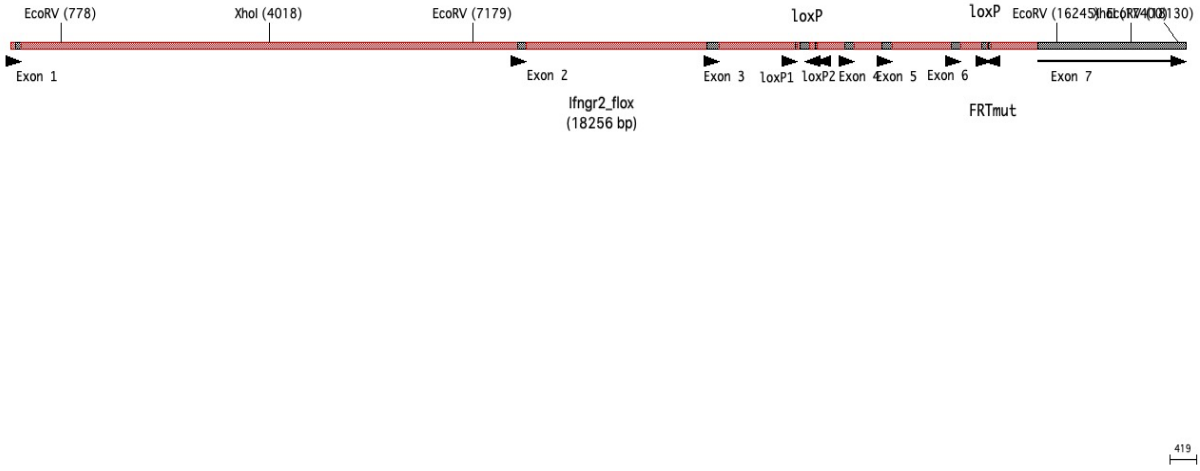

The *lox-p*1 (5'-TGA GTT CCA AGC AAG ACA GA-3'), *lox-p* 2 (5'-CAG GGT AGA AAA GAT GTG CA-3') and *lox-p* site (5'-AAG TTA TGG TCT GAG CTC GC-3') primers anneal such that PCR products of 191bp and 392bp are generated.

Bibliography

1. WHO. World Malaria Report 2019. Geneva. World Malar Rep. 2019;

2. Jacobsen SEW, Nerlov C. Haematopoiesis in the era of advanced single-cell technologies. Nat Cell Biol. 2019;21(1):2–8.

3. Orkin SH, Zon LI. Hematopoiesis: an evolving paradigm for stem cell biology. Cell. 2008;132(4):631–44.

4. Jagannathan-Bogdan M, Zon LI. Hematopoiesis - At A Glance. Development. 2013;140(12):2463–7.

5. Ivanovs A, Rybtsov S, Welch L, Anderson RA, Turner ML, Medvinsky A. Highly potent human hematopoietic stem cells first emerge in the intraembryonic aorta-gonad-mesonephros region. J Exp Med. 2011;208(12):2417–27.

6. Zaretsky AG, Engiles JB, Hunter CA. Infection-Induced Changes in Hematopoiesis. J Immunol. 2014;192(1):27–33.

7. Orford KW, Scadden DT. Deconstructing stem cell self-renewal: Genetic insights into cell-cycle regulation. Nat Rev Genet. 2008;9(2):115–28.

8. Wilson A, Laurenti E, Oser G, van der Wath RC. Hematopoietic Stem Cells Reversibly Switch from Dormancy to Self-Renewal during Homeostasis and Repair. Cell. 2008;135(6):1118–29.

9. MacNamara KC, Jones M, Martin O, Winslow GM. Transient activation of hematopoietic stem and progenitor cells by IFNγ during acute Bacterial infection. PLoS One. 2011;6(12):e28669.

10. Oguro H, Ding L, Morrison SJ. SLAM family markers resolve functionally distinct subpopulations of hematopoietic stem cells and multipotent progenitors. Cell Stem Cell. 2013;13(1):102–16.

11. Wang, C.Y. & Dick J. Cancer stem cells: Lessons from leukaemia. Trends Cell

Biol. 2005;15(9):494–501.

12. Akashi K, Traver D, Miyamoto T, Weissman IL. A clonogenic common myeloid progenitor that gives rise to all myeloid lineages. Nature. 2000;404(6774):193–7.

13. Osawa M, Hanada KI, Hamada H, Nakauchi H. Long-term lymphohematopoietic reconstitution by a single CD34- low/negative hematopoietic stem cell. Science (80-). 1996;273(5272):242–5.

14. Kiel MJ, Yilmaz ÖH, Iwashita T, Yilmaz OH, Terhorst C, Morrison SJ. SLAM family receptors distinguish hematopoietic stem and progenitor cells and reveal endothelial niches for stem cells. Cell. 2005;121(7):1109–21.

15. Pietras EM, Reynaud D, Kang YA, Carlin D, Calero-Nieto FJ, Leavitt AD, et al. Functionally Distinct Subsets of Lineage-Biased Multipotent Progenitors Control Blood Production in Normal and Regenerative Conditions. Cell Stem Cell. 2015;17(1):35–46.

16. Adolfsson J, Borge OJ, Bryder D, Theilgaard-Mönch K, Åstrand-Grundström I, Sitnicka E, et al. Upregulation of Flt3 expression within the bone marrow Lin-Sca1+c-kit+ stem cell compartment is accompanied by loss of self-renewal capacity. Immunity. 2001;15(4):659–69.

17. Forman SJ, Negrin RS, Antin JH, Appelbaum FR. Thomas' Hematopoietic Cell Transplantation: Fifth Edition. Thomas' Hematopoietic Cell Transplantation: Fifth Edition. 2016.

18. Adolfsson J, Månsson R, Buza-Vidas N, Hultquist A, Liuba K, Jensen CT, et al. Identification of Flt3 + lympho-myeloid stem cells lacking erythro-megakaryocytic potential: A revised road map for adult blood lineage commitment. Cell. 2005;121(2):295–306.

19. Pronk CJH, Rossi DJ, Månsson R, Attema JL, Norddahl GL, Chan CKF, et al. Elucidation of the Phenotypic, Functional, and Molecular Topography of a Myeloerythroid Progenitor Cell Hierarchy. Cell Stem Cell. 2007;1(4):428–42.

20. Psaila B, Barkas N, Iskander D, Roy A, Anderson S, Ashley N, et al. Single-cell profiling of human megakaryocyte-erythroid progenitors identifies distinct megakaryocyte and erythroid differentiation pathways. Genome Biol. 2016;17(83):doi: 10.1186/s13059-016-0939-7.

21. Mori Y, Chen JY, Pluvinage J V., Seita J, Weissman IL. Prospective isolation of human erythroid lineage-committed progenitors. Proc Natl Acad Sci. 2015;112(31):9638–43.

22. Chasis JA, Mohandas N. Erythroblastic islands: Niches for erythropoiesis. Blood. 2008;112(3):470–8.

23. Giger KM, Kalfa TA. Phylogenetic and Ontogenetic View of Erythroblastic Islands. Biomed Res Int. 2015;2015:87362:doi: 10.1155/2015/87362.

24. Hom J, Dulmovits BM, Mohandas N, Blanc L. The erythroblastic island as an emerging paradigm in the anemia of inflammation. Immunol Res. 2015;63(1–3):75–89.

25. Stephenson JR, Axelrad AA, McLeod DL, Shreeve MM. Induction of Colonies of Hemoglobin-Synthesizing Cells by Erythropoietin In Vitro. Proc Natl Acad Sci. 1971;68(7):1542–6.

26. Iscove NN, Sieber F, Winterhalter KH. Erythroid colony formation in cultures of mouse and human bone marrow: Analysis of the requirement for erythropoietin by gel filtration and affinity chromatography on agarose-concanavalin A. J Cell Physiol. 1974;83(2):309–20.

27. Moriyama Y, Fisher JW. Effects of testosterone and erythropoietin on erythroid colony formation in rabbit bone marrow cultures. Life Sci. 1974;15(6):1181–8.

28. Gregory C, Eaves A. Human marrow cells capable of erythropoietic differentiation in vitro: definition of three erythroid colony responses. Blood. 1977;49(6):855–64.

29. Gregory J, Eaves C. Three stages of erythropoietic progenitor cell

differentiation distinguished by a number of physical and biologic properties. Blood. 1978;51(3):527–37.

30. Socolovsky M, Nam HS, Fleming MD, Haase VH, Brugnara C, Lodish HF. Ineffective erythropoiesis in Stat5a-/-5b-/- mice due to decreased survival of early erythroblasts. Blood. 2001;98(12):3261–73.

31. Zhang J, Socolovsky M, Gross AW, Lodish HF. Role of Ras signaling in erythroid differentiation of mouse fetal liver cells: Functional analysis by a flow cytometry-based novel culture system. Blood. 2003;102(12):3938–46.

32. Liu Y, Pop R, Sadegh C, Brugnara C, Haase VH, Socolovsky M. Suppression of Fas-FasL coexpression by erythropoietin mediates erythroblast expansion during the erythropoietic stress response in vivo. Blood. 2006;108(1):123–33.

33. Chen K, Liu J, Heck S, Chasis JA, An X, Mohandas N. Resolving the distinct stages in erythroid differentiation based on dynamic changes in membrane protein expression during erythropoiesis. Proc Natl Acad Sci. 2009;106(41):17413–8.

34. Liu J, Zhang J, Ginzburg Y, Li H, Xue F, De Franceschi L, et al. Quantitative analysis of murine terminal erythroid differentiation in vivo: novel method to study normal and disordered erythropoiesis. Blood. 2013;121(8):e43-9.

35. Nuez B, Michalovich D, Bygrave A, Ploemacher R, Grosveld F. Defective haematopoiesis in fetal liver resulting from inactivation of the EKLF gene. Nature. 1995;375(6529):316–8.

36. Coghill E, Eccleston S, Fox V, Cerruti L, Brown C, Cunningham J, et al. Erythroid Kruppel-like factor (EKLF) coordinates erythroid cell proliferation and hemoglobinization in cell lines derived from EKLF null mice. Blood. 2001;97(6):1861–8.

37. Drissen R, von Lindern M, Kolbus A, Driegen S, Steinlein P, Beug H, et al. The Erythroid Phenotype of EKLF-Null Mice: Defects in Hemoglobin Metabolism and Membrane Stability. Mol Cell Biol. 2005;25(12):5205–14.

38. Parkins AC, Sharpe AH, Orkin SH. Lethal β-thalassaemia in mice lacking the erythroid CACCC-transcription factor EKLF. Nature. 1995;375(6529):318–22.

39. Gnanapragasam MN, McGrath KE, Catherman S, Xue L, Palis J, Bieker JJ. EKLF/KLF1-regulated cell cycle exit is essential for erythroblast enucleation. Blood. 2016;128(12):1631–44.

40. Zhou D, Liu K, Sun CW, Pawlik KM, Townes TM. KLF1 regulates BCL11A expression and γ- to β-globin gene switching. Nat Genet. 2010;42(9):742–4.

41. Borg J, Papadopoulos P, Georgitsi M, Gutiérrez L, Grech G, Fanis P, et al. Haploinsufficiency for the erythroid transcription factor KLF1 causes hereditary persistence of fetal hemoglobin. Nat Genet. 2010;42(9):801–5.

42. Pilon AM, Arcasoy MO, Dressman HK, Vayda SE, Maksimova YD, Sangerman JI, et al. Failure of Terminal Erythroid Differentiation in EKLF-Deficient Mice Is Associated with Cell Cycle Perturbation and Reduced Expression of E2F2. Mol Cell Biol. 2008;28(24):7394–401.

43. Tallack MR, Keys JR, Humbert PO, Perkins AC. EKLF/KLF1 controls cell cycle entry via direct regulation of E2f2. J Biol Chem. 2009;284(31):20966–74.

44. Hodge D, Coghill E, Keys J, Maguire T, Hartmann B, McDowall A, et al. A global role for EKLF in definitive and primitive erythropoiesis. Blood. 2006;107(8):3359–70.

45. Ko LJ, Engel JD. DNA-binding specificities of the GATA transcription factor family. Mol Cell Biol. 1993;13(7):4011–22.

46. Merika M, Orkin SH. DNA-binding specificity of GATA family transcription factors. Mol Cell Biol. 1993;13(7):3999–4010.

47. Fujiwara Y, Browne CP, Cunniff K, Goff SC, Orkin SH. Arrested development of embryonic red cell precursors in mouse embryos lacking transcription factor GATA-1. Proc Natl Acad Sci. 1996;93(22):12355–8.

48. Martin DIK, Zon LI, Mutter G, Orkin SH. Expression of an erythroid transcription

factor in megakaryocytic and mast cell lineages. Nature. 1990;344(6265):444–7.

49. Zon LI, Yamaguchi Y, Yee K, Albee EA, Kimura A, Bennett JC, et al. Expression of mRNA for the GATA-binding proteins in human eosinophils and basophils: potential role in gene transcription. Blood. 1993;81(12):3234–41.

50. Pevny L, Lin CS, D'Agati V, Simon MC, Orkin SH, Costantini F. Development of hematopoietic cells lacking transcription factor GATA-1. Development. 1995;121(1):163–72.

51. Weiss MJ, Orkin SH. Transcription factor GATA-1 permits survival and maturation of erythroid precursors by preventing apoptosis. Proc Natl Acad Sci. 1995;92(21):9623–7.

52. Gregory T, Yu C, Ma A, Orkin SH, Blobel G a, Weiss MJ. GATA-1 and erythropoietin cooperate to promote erythroid cell survival by regulating bcl-xL expression. Blood. 1999;94(1):87–96.

53. Ohneda K, Yamamoto M. Roles of hematopoietic transcription factors GATA-1 and GATA-2 in the development of red blood cell lineage. Acta Haematol. 2002;108(4):237–45.

54. Ikonomi P, Rivera CE, Riordan M, Washington G, Schechter AN, Noguchi CT. Overexpression of GATA-2 inhibits erythroid and promotes megakaryocyte differentiation. Exp Hematol. 2000;28(2):1423–31.

55. Mancini E, Sanjuan-Pla A, Luciani L, Moore S, Grover A, Zay A, et al. FOG-1 and GATA-1 act sequentially to specify definitive megakaryocytic and erythroid progenitors. EMBO J. 2012;31(2):351–65.

56. Klemsz MJ, McKercher SR, Celada A, Van Beveren C, Maki RA. The macrophage and B cell-specific transcription factor PU.1 is related to the ets oncogene. Cell. 1990;61(1):113–24.

57. Galson DL, Hensold JO, Bishop TR, Schalling M, D'Andrea AD, Jones C, et al.

Mouse beta-globin DNA-binding protein B1 is identical to a proto-oncogene, the transcription factor Spi-1/PU.1, and is restricted in expression to hematopoietic cells and the testis. Mol Cell Biol. 1993;13(5):2929–41.

58. Hromas R, Orazi A, Neiman RS, Maki R, Van Beveran C, Moore J, et al. Hematopoietic lineage- and stage-restricted expression of the ETS oncogene family member PU.1. Blood. 1993;82(10):2998–3004.

59. McKercher SR, Torbett BE, Anderson KL, Henkel GW, Vestal DJ, Baribault H, et al. Targeted disruption of the PU.1 gene results in multiple hematopoietic abnormalities. EMBO J. 1996;15(20):5647–58.

60. Scott EW, Simon MC, Anastasi J, Singh H. Requirement of transcription factor PU.1 in the development of multiple hematopoietic lineages. Science (80-). 1994;265(5178):1573–7.

61. Fisher RC, Scott EW. Role of PU.1 in hematopoiesis. Stem Cells. 1998;16(1):25–37.

62. Back J, Dierich A, Bronn C, Kastner P, Chan S. PU.1 determines the self-renewal capacity of erythroid progenitor cells. Blood. 2004;103(10):3615–23.

63. Doré LC, Crispino JD. Transcription factor networks in erythroid cell and megakaryocyte development. Blood. 2011;118(2):231–9.

64. Villeval J-LL, Lew A, Metcalf D, Gearing A, Metcalf D. Changes in hemopoietic and regulator levels in mice during fatal or nonfatal malarial infections. Exp Parasitol. 1990;71(4):375–85.

65. Petakov M, Stojanovic N, Jovcic G, Bugarski D, Todorovic V, Djurkovic-Djakovic O. Hematopoiesis during acute Toxoplasma gondii infection in mice. Haematol. 2002;32(4):439–55.

66. Chou DB, Sworder B, Bouladoux N, Roy CN, Uchida AM, Grigg M, et al. Stromal-derived IL-6 alters the balance of myeloerythroid progenitors during Toxoplasma gondii infection. J Leukoc Biol. 2012;92(1):123–31.

67. Belyaev NN, Brown DE, Diaz A-IG, Rae A, Jarra W, Thompson J, et al. Induction of an IL7-R(+)c-Kit(hi) myelolymphoid progenitor critically dependent on IFN-gamma signaling during acute malaria. Nat Immunol [Internet]. 2010;11(6):477–85. Available from: http://dx.doi.org/10.1038/ni.1869

68. Belyaev NN, Biro J, Langhorne J, Potocnik AJ. Extramedullary Myelopoiesis in Malaria Depends on Mobilization of Myeloid-Restricted Progenitors by IFN-g Induced Chemokines. PLoS Pathog. 2013;9(6):doi: 10.1371/journal.ppat.1003406.

69. MacNamara KC, Racine R, Chatterjee M, Borjesson D, Winslow GM. Diminished hematopoietic activity associated with alterations in innate and adaptive immunity in a mouse model of human monocytic ehrlichiosis. Infect Immun. 2009;77(9):4061–9.

70. Aguilar R, Moraleda C, Achtman AH, Mayor A, Quintó L, Cisteró P, et al. Severity of anaemia is associated with bone marrow haemozoin in children exposed to Plasmodium falciparum. Br J Haematol. 2014;164(6):877–87.

71. Fendel R, Brandts C, Rudat A, Kreidenweiss A, Steur C, Appelmann I, et al. Hemolysis is associated with low reticulocyte production index and predicts blood transfusion in severe malarial anemia. PLoS One. 2010;5(4):e10038.

72. Wang Z, Zhang DX, Zhao Q. Infection-stimulated anemia results primarily from interferon gamma-dependent, signal transducer and activator of transcription 1-independent red cell loss. Chin Med J (Engl). 2015;128(7):948–55.

73. De Bruin AM, Libregts SF, Valkhof M, Boon L, Touw IP, Nolte MA. IFNγ induces monopoiesis and inhibits neutrophil development during inflammation. Blood. 2012;119(6):1543–54.

74. de Bruin AM, Demirel Ö, Hooibrink B, Brandts CH, Nolte MA. Interferon-γ impairs proliferation of hematopoietic stem cells in mice. Blood [Internet]. 2013;121(18):3578–86. Available from: http://www.bloodjournal.org/content/121/18/3578.abstract

75. Baldridge MT, King KY, Boles NC, Weksberg DC, Goodell MA. Quiescent haematopoietic stem cells are activated by IFN-γ in response to chronic infection. Nature. 2010;465(7299):793–7.

76. White NJ, Pukrittayakamee S, Hien TT, Faiz MA, Mokuolu OA, Dondorp AM. Seminar: Malaria. Lancet. 2014;383:723–35.

77. David A. Warrell HMG. Bruce-Chwatt's essential malariology. In 1993.

78. Prudêncio M, Rodriguez A, Mota MM. The silent path to thousands of merozoites: The Plasmodium liver stage. Nat Rev Microbiol. 2006;4(11):849–56.

79. Amino R, Thiberge S, Martin B, Celli S, Shorte S, Frischknecht F, et al. Quantitative imaging of Plasmodium transmission from mosquito to mammal. Nat Med. 2006;12(2):220–4.

80. Medica DL, Sinnis P. Quantitative dynamics of Plasmodium yoelii sporozoite transmission by infected anopheline mosquitoes. Infect Immun. 2005;73(7):4363–9.

81. Rosenberg R, Burge R, Schneider I. An estimation of the number of malaria sporozoites ejected by a feeding mosquito. Trans R Soc Trop Med Hyg. 1990;84(2):209–12.

82. Hellriegel B. Modelling the immune response to malaria with ecological concepts: Short-term behaviour against long-term equilibrium. Proc R Soc B Biol Sci. 1992;250(1329):249–56.

83. Kurup SP, Butler NS, Harty JT. T cell-mediated immunity to malaria. Nat Rev Immunol. 2019;19(7):457–71.

84. Baird JK. Severe and fatal vivax malaria challenges "benign tertian malaria" dogma. Ann Trop Paediatr. 2009;29(4):251–2.

85. Cox-Singh J, Hiu J, Lucas SB, Divis PC, Zulkarnaen M, Chandran P, et al. Severe malaria - A case of fatal Plasmodium knowlesi infection with post-

mortem findings: A case report. Malar J. 2010;9(10):doi: 10.1186/1475-2875-9-10.

86. Gonçalves BP, Huang CY, Morrison R, Holte S, Kabyemela E, Prevots DR, et al. Parasite burden and severity of malaria in Tanzanian children. N Engl J Med. 2014;370(19):1799–808.

87. Snow RW, Omumbo JA, Lowe B, Molyneux CS, Obiero JO, Palmer A, et al. Relation between severe malaria morbidity in children and level of Plasmodium falciparum transmission in Africa. Lancet. 1997;349(9066):1450–4.

88. Doolan DL, Dobaño C, Baird JK. Acquired immunity to Malaria. Clin Microbiol Rev. 2009;22(1):13–36.

89. Gupta S, Snow RW, Donnelly CA, Marsh K, Newbold C. Immunity to non-cerebral severe malaria is acquired after one or two infections. Nat Med. 1999;5(3):340–3.

90. Achidi EA, Apinjoh TO, Anchang-Kimbi JK, Mugri RN, Ngwai AN, Yafi CN. Severe and uncomplicated falciparum malaria in children from three regions and three ethnic groups in Cameroon: Prospective study. Malar J. 2012;24(11):215.

91. Obonyo CO, Vulule J, Akhwale WS, Grobbee DE. In-hospital morbidity and mortality due to severe malarial anemia in western Kenya. Am J Trop Med Hyg. 2007;77(6):23–8.

92. Brickley EB, Kabyemela E, Kurtis JD, Fried M, Wood AM, Duffy PE. Developing a novel risk prediction model for severe malarial anemia. Glob Heal Epidemiol genomics. 2017;2:e14.

93. Fleming AF. HIV and blood transfusion in sub-Saharan Africa. Transfus Sci. 1997;18(2):167–79.

94. Burchard GD, Radloff P, Philipps J, Nkeyi M, Knobloch J, Kremsner PG. Increased erythropoietin production in children with severe malarial anemia. Am

J Trop Med Hyg. 1995;53(5):547–51.

95. Dörmer P, Dietrich M, Kern P, Horstmann RD. Ineffective erythropoiesis in acute human P. falciparum malaria. Blut. 1983;46(5):279–88.

96. Lamikanra AA, Brown D, Potocnik A, Casals-pascual C, Langhorne J, Roberts DJ, et al. Malarial anemia : of mice and men Review in translational hematology Malarial anemia : of mice and men. Blood. 2014;110(1):18–28.

97. Stephens R, Culleton RL, Lamb TJ. The contribution of Plasmodium chabaudi to our understanding of malaria. Trends Parasitol [Internet]. 2012;28(2):73–82. Available from: http://dx.doi.org/10.1016/j.pt.2011.10.006

98. Lamikanra AA, Brown D, Potocnik A, Casals-pascual C, Langhorne J, Roberts DJ, et al. Malarial anemia: Of mice and men. Blood [Internet]. 2007;110(1):18–28. Available from: http://www.bloodjournal.org/content/110/1/18.abstract

99. Chang KH, Stevenson MM. Effect of anemia and renal cytokine production on erythropoietin production during blood-stage malaria. Kidney Int. 2004;65(5):1640–6.

100. Wickramasinghe SN, Abdalla SH. Blood and bone marrow changes in malaria. Bailliere's Best Pract Res Clin Haematol. 2000;13(2):277–99.

101. Yap GS, Stevenson MM. Plasmodium chabaudi AS: Erythropoietic responses during infection in resistant and susceptible mice. Exp Parasitol. 1992;75(3):340–52.

102. Belyaev NN, Brown DE, Diaz AIG, Rae A, Jarra W, Thompson J, et al. Induction of an IL7-R+ c-Kithi myelolymphoid progenitor critically dependent on IFN-γ signaling during acute malaria. Nat Immunol. 2010;11(6):477–85.

103. Casals-Pascual C, Kai O, Cheung JOP, Williams S, Lowe B, Nyanoti M, et al. Suppression of erythropoiesis in malarial anemia is associated with hemozoin in vitro and in vivo. Blood. 2006;108(8):2569–77.

104. Lamikanra AA, Theron M, Kooij TWAA, Roberts DJ. Hemozoin (Malarial

pigment) directly promotes apoptosis of erythroid precursors. PLoS One. 2009;4(12):e8446.

105. Miller KL, Schooley JC, Smith KL, Kullgren B, Mahlmann LJ, Silverman PH. Inhibition of erythropoiesis by a soluble factor in murine malaria. Exp Hematol. 1989;17(4):379–85.

106. Were T, Hittner JB, Ouma C, Otieno RO, Orago AS, Ong'echa JM, et al. Suppression of RANTES in children with Plasmodium falciparum malaria. Haematologica. 2006;91(10):1396–9.

107. Clark IA, Chaudhri G. Tumour necrosis factor may contribute to the anaemia of malaria by causing dyserythropoiesis and erythrophagocytosis. Br J Haematol. 1988;70(1):99–103.

108. McDevitt MA, Xie J, Shanmugasundaram G, Griffith J, Liu A, McDonald C, et al. A critical role for the host mediator macrophage migration inhibitory factor in the pathogenesis of malarial anemia. J Exp Med [Internet]. 2006;203(5):1185–96. Available from: http://www.pubmedcentral.nih.gov/articlerender.fcgi?artid=2121202&tool=pmcentrez&rendertype=abstract

109. Bao Y, Liu X, Han C, Xu S, Xie B, Zhang Q, et al. Identification of IFN-γ-producing innate B cells. Cell Res. 2014;24(2):161–76.

110. Zeng B, Shi S, Ashworth G, Dong C, Liu J, Xing F. ILC3 function as a double-edged sword in inflammatory bowel diseases. Cell Death Dis. 2019;10(4):315.

111. Darwich L, Coma G, Peña R, Bellido R, Blanco EJJ, Este JA, et al. Secretion of interferon-γ by human macrophages demonstrated at the single-cell level after costimulation with interleukin (IL)-12 plus IL-18. Immunology. 2009;126(3):386–93.

112. McCall MBB, Sauerwein RW. Interferon-γ-central mediator of protective immune responses against the pre-erythrocytic and blood stage of malaria. J Leukoc Biol. 2010;88(6):1131–43.

113. Libregts SF, Gutiérrez L, De Bruin AM, Wensveen FM, Papadopoulos P, Van Ijcken W, et al. Chronic IFN-γ production in mice induces anemia by reducing erythrocyte life span and inhibiting erythropoiesis through an IRF-1/PU.1 axis. Blood. 2011;118(9):2578–88.

114. Rekhtman N, Radparvar F, Evans T, Skoultchi AI. Direct interaction of hematopoietic transcription factors PU.1 and GATA- 1: Functional antagonism in erythroid cells. Genes Dev. 1999;13(11):1398–411.

115. Dai CH, Price JO, Brunner T, Krantz SB. Fas ligand is present in human erythroid colony-forming cells and interacts with Fas induced by interferon gamma to produce erythroid cell apoptosis. Blood. 1998;91(4):1235–42.

116. Taniguchi S, Dai CH, Price JO, Krantz SB. Interferon gamma downregulates stem cell factor and erythropoietin receptors but not insulin-like growth factor-I receptors in human erythroid colony-forming cells. Blood. 1997;90(6):2244–52.

117. Felli N, Pedini F, Zeuner A, Petrucci E, Testa U, Conticello C, et al. Multiple Members of the TNF Superfamily Contribute to IFN-γ Mediated Inhibition of Erythropoiesis. J Immunol. 2005;175(3):1464–72.

118. Zaidi MR, Merlino G. The two faces of interferon-γ in cancer. Clin Cancer Res. 2011;17(19):6118–24.

119. Xu X, Xu J, Wu J, Hu Y, Han Y, Gu Y, et al. Phosphorylation-Mediated IFN-γR2 Membrane Translocation Is Required to Activate Macrophage Innate Response. Cell. 2018;175(5):1336–51.

120. Shimshek DR, Kim J, Hübner MR, Spergel DJ, Buchholz F, Casanova E, et al. Codon-improved Cre recombinase (iCre) expression in the mouse. Genesis. 2002;32(1):19–26.

121. de Boer J, Williams A, Skavdis G, Harker N, Coles M, Tolaini M, et al. Transgenic mice with hematopoietic and lymphoid specific expression of Cre. Eur J Immunol. 2003;33(2):314–25.

122. Lee HM, Fleige A, Forman R, Cho S, Khan AA, Lin LL, et al. IFNγ Signaling Endows DCs with the Capacity to Control Type I Inflammation during Parasitic Infection through Promoting T-bet+ Regulatory T Cells. PLoS Pathog. 2015;11(2):e1004635.

123. Spence PJ, Cunningham D, Jarra W, Lawton J, Langhorne J, Thompson J. Transformation of the rodent malaria parasite plasmodium chabaudi. Nat Protoc. 2011;6(4):553–61.

124. Spence PJ, Jarra W, Lévy P, Reid AJ, Chappell L, Brugat T, et al. Vector transmission regulates immune control of Plasmodium virulence. Nature. 2013;498(7453):228–31.

125. Joseph C, Quach JM, Walkley CR, Lane SW, Lo Celso C, Purton LE. Deciphering Hematopoietic Stem Cells in Their Niches: A Critical Appraisal of Genetic Models, Lineage Tracing, and Imaging Strategies. Cell Stem Cell. 2013;13(5):520–33.

126. Mooney CJ, Cunningham A, Tsapogas P, Toellner KM, Brown G. Selective expression of Flt3 within the mouse hematopoietic stem cell compartment. Int J Mol Sci. 2017;18(5):1037.

127. Kim KT, Levis M, Small D. Constitutively activated FLT3 phosphorylates BAD partially through Pim-1. Br J Haematol. 2006;134(5):500–9.

128. Kikushige Y, Yoshimoto G, Miyamoto T, Iino T, Mori Y, Iwasaki H, et al. Human Flt3 is expressed at the hematopoietic stem cell and the granulocyte/macrophage progenitor stages to maintain cell survival. J Immunol. 2008;180(11):7358–67.

129. Yang M, Büsche G, Ganser A, Li Z. Morphology and quantitative composition of hematopoietic cells in murine bone marrow and spleen of healthy subjects. Ann Hematol. 2013;92(5):587–94.

130. Martín-Jaular L, Elizalde-Torrent A, Thomson-Luque R, Ferrer M, Segovia JC, Herreros-Aviles E, et al. Reticulocyte-prone malaria parasites predominantly

invade CD71§ssup§hi§esup§ immature cells: Implications for the development of an in vitro culture for Plasmodium vivax. Malar J. 2013;12(434).

131. Malleret B, Li A, Zhang R, Tan KSW, Suwanarusk R, Claser C, et al. Plasmodium vivax: Restricted tropism and rapid remodeling of CD71-positive reticulocytes. Blood. 2015;125(8):1314–24.

132. Srichaikul T, Siriasawakul T, Poshyachinda M, Poshyachinda V. Ferrokinetics in patients with malaria: normoblasts and iron incorporation in vitro. Am J Clin Pathol. 1973;60(1):166–74.

133. Achtman AH, Khan M, MacLennan ICM, Langhorne J. Plasmodium chabaudi chabaudi Infection in Mice Induces Strong B Cell Responses and Striking But Temporary Changes in Splenic Cell Distribution. J Immunol. 2003;171(1):317–24.

134. Weiss, L. Johnson J and W. Mechanisms of splenic control of murine malaria: Cellular reactions of the spleen in lethal (strain 17XL) Plasmodium yoelii malaria in BALB/c mice, and the consequences of pre-infective splenectomy. Am J Trop Med Hyg. 1989;1(2):135–43.

135. MacNamara KC, Oduro K, Martin O, Jones DD, McLaughlin M, Choi K, et al. Infection-Induced Myelopoiesis during Intracellular Bacterial Infection Is Critically Dependent upon IFN-γ Signaling. J Immunol. 2011;186(2):1032–43.

136. Zhang P, Nelson S, Bagby GJ, Siggins R, Shellito JE, Welsh DA. The Lineage−c-Kit+Sca-1+ Cell Response to Escherichia coli Bacteremia in Balb/c Mice. Stem Cells. 2008;26(7):1778–86.

137. Dumont FJ, Boltz RC. The augmentation of surface Ly-6A/E molecules in activated T cells is mediated by endogenous interferon-γ. J Immunol. 1987;139(2):4088–95.

138. Chang KH, Tam M, Stevenson MM. Inappropriately low reticulocytosis in severe malarial anemia correlates with suppression in the development of late erythroid precursors. Blood. 2004;103(10):3727–35.

139. Kurtzhals JAL, Rodrigues O, Addae M, Commey JOO, Nkrumah FK, Hviid L. Reversible suppression of bone marrow response to erythropoietin in Plasmodium falciparum malaria. Br J Haematol. 1997;97(1):169–74.

140. Poshyachinda M, Siriasawakul T. Ferrokinetics in patients with malaria: Haemoglobin synthesis and normoblasts in vitro. Trans R Soc Trop Med Hyg. 1976;70(3):244–6.

141. Pathak VA, Ghosh K. Erythropoiesis in malaria infections and factors modifying the erythropoietic response. Anemia. 2016;10:1–8.

142. Phillips RE, Looareesuwan S, Warrell DA, Lee SH, Karbwang J, Warrell MJ, et al. The importance of anaemia in cerebral and uncomplicated falciparum malaria: Role of complications, dyserythropoiesis and iron sequestration. QJM. 1986;58(227):305–223.

143. Camacho LH, Gordeuk VR, Wilairatana P, Pootrakul P, Brittenham GM, Looareesuwan S. The course of anaemia after the treatment of acute, falciparum malaria. Ann Trop Med Parasitol. 1998;92(5):525–37.

144. M. H, B.Q. G, B.D. A, G. O-A, O. R, J.A.L. K. Bone marrow suppression and severe anaemia associated with persistent Plasmodium falciparum infection in African children with microscopically undetectable parasitaemia. Malar J. 2005;1(4):56.

145. Engwerda CR, Beattie L, Amante FH. The importance of the spleen in malaria. Trends Parasitol. 2005;21(2):75–80.

146. del Portillo HA, Ferrer M, Brugat T, Martin-Jaular L, Langhorne J, Lacerda MVG. The role of the spleen in malaria. Cell Microbiol. 2012;14(3):343–55.

147. del Portillo HA, Ferrer M, Brugat T, Martin-Jaular L, Langhorne J, Lacerda MVG. The role of the spleen in malaria. Cell Microbiol. 2012;14(3):343–55.

148. Wickramasinghe SN, Looareesuwan S, Nagachinta B, White NJ. Dyserythropoiesis and ineffective erythropoiesis in Plasmodium vivax malaria.

Br J Haematol. 1989;72(1):91–9.

149. Maggio-Price L, Brookoff D, Weiss L. Changes in hematopoietic stem cells in bone marrow of mice with Plasmodium berghei malaria. Blood. 1985;66(5):1080–5.

150. Thawani N, Tam M, Bellemare M-J, Bohle DS, Olivier M, de Souza JB, et al. Plasmodium products contribute to severe malarial anemia by inhibiting erythropoietin-induced proliferation of erythroid precursors. J Infect Dis [Internet]. 2014;209(1):140–9. Available from: http://www.ncbi.nlm.nih.gov/pubmed/23922378

151. Rusten LS, Jacobsen SE. Tumor necrosis factor (TNF)-alpha directly inhibits human erythropoiesis in vitro: role of p55 and p75 TNF receptors. Blood [Internet]. 1995;85(4):989–96. Available from: http://www.ncbi.nlm.nih.gov/pubmed/7849320

152. Means RT, Krantz SB. Inhibition of human erythroid colony-forming units by gamma interferon can be corrected by recombinant human erythropoietin. Blood. 1991;78(10):2564–7.

153. Means RT, Dessypris EN, Krantz SB. Inhibition of human erythroid colony-forming units by interleukin-1 is mediated by gamma interferon. J Cell Physiol. 1992;150(1):59–64.

154. Buck I, Morceau F, Cristofanon S, Heintz C, Chateauvieux S, Reuter S, et al. Tumor necrosis factor α inhibits erythroid differentiation in human erythropoietin-dependent cells involving p38 MAPK pathway, GATA-1 and FOG-1 downregulation and GATA-2 upregulation. Biochem Pharmacol. 2008;76(10):1229–39.

155. Johnson RA, Waddelow TA, Caro J, Oliff A, Roodman GD. Chronic exposure to tumor necrosis factor in vivo preferentially inhibits erythropoiesis in nude mice. Blood. 1989;74(1):130–8.

156. Sherwin SA, Gutterman J. Phase I study of recombinant tumor necrosis factor

in cancer patients. Cancer Res. 1987;47(11):2986–9.

157. Macciò A, Madeddu C, Massa D, Mudu MC, Lusso MR, Gramignano G, et al. Hemoglobin levels correlate with interleukin-6 levels in patients with advanced untreated epithelial ovarian cancer: Role of inflammation in cancer-related anemia. Blood. 2005;106(1):362–7.

158. YAP GS, STEVENSON MM. Production of Soluble Inhibitor of Erythropoiesis during Plasmodium chabaudi AS Infection in Resistant and Susceptible Mice. Ann N Y Acad Sci. 1991;628(1):279–81.

159. McDevitt MA, Xie J, Gordeuk V, Bucala R. The anemia of malaria infection: role of inflammatory cytokines. Curr Hematol Rep. 2004;3(2):97–106.

160. Nagy A. Cre recombinase: The universal reagent for genome tailoring. Genesis. 2000;26(2):99–109.

161. Jung V, Rashidbaigi A, Jones C, Tischfield JA, Shows TB, Pestka S. Human chromosomes 6 and 21 are required for sensitivity to human interferon gamma. Proc Natl Acad Sci. 1987;84(12):4151–5.

162. Ma X, Ling KW, Dzierzak E. Cloning of the Ly-6A (Sca-1) gene locus and identification of a 3′ distal fragment responsible for high-level γ-interferon-induced expression in vitro. Br J Haematol. 2001;114(3):724–30.

163. Ferreira A, Schofield L, Enea V, Schellekens H, van der Meide P, Collins W, et al. Inhibition of development of exoerythrocytic forms of malaria parasites by gamma-interferon. Science (80-). 2006;232(4752):881–4.

164. Mellouk S, Green SJ, Nacy CA, Hoffman SL. IFN-γ inhibits development of Plasmodium berghei exoerythrocytic stages in hepatocytes by an L-arginine-dependent effector mechanism. J Immunol. 1991;146(11):3971–6.

165. da Silva HB, de Salles ÉM, Panatieri RH, Boscardin SB, Rodríguez-Málaga SM, Álvarez JM, et al. IFN-γ–Induced Priming Maintains Long-Term Strain-Transcending Immunity against Blood-Stage Plasmodium chabaudi Malaria. J

Immunol. 2013;191(19):5160–9.

166. McCall MBB, Hopman J, Daou M, Maiga B, Dara V, Ploemen I, et al. Early Interferon-γ Response against Plasmodium falciparum Correlates with Interethnic Differences in Susceptibility to Parasitemia between Sympatric Fulani and Dogon in Mali. J Infect Dis. 2009;201(1):142–52.

167. Van Der Heyde HC, Pepper B, Batchelder J, Cigel F, Weidanz WP. The time course of selected malarial infections in cytokine-deficient mice. Exp Parasitol. 1997;85(2):206–13.

168. Sadir R, Lortat-Jacob H, Morel G. Internalization and nuclear translocation of IFN-γ and IFN-γR: An ultrastructural approach. Cytokine. 2000;12(6):711–4.

169. Katzav S, Martin-Zanca D, Barbacid M. vav, a novel human oncogene derived from a locus ubiquitously expressed in hematopoietic cells. EMBO J. 1989;8(8):2283–90.

170. Soulard V, Roland J, Gorgette O, Barbier E, Cazenave P-AA, Pied S. An early burst of IFN- induced by the pre-erythrocytic stage favours Plasmodium yoelii parasitaemia in B6 mice. Malar J [Internet]. 2009;8(128):doi:10.1186/1475-2875-8-128. Available from: http://www.pubmedcentral.nih.gov/articlerender.fcgi?artid=2699347&tool=pmcentrez&rendertype=abstract

171. Perkins DJ, Were T, Davenport GC, Kempaiah P, Hittner JB, Ong'echa JM. Severe malarial anemia: innate immunity and pathogenesis. Int J Biol Sci. 2011;7(9):1427–42.

172. Mavondo GA, Mzingwane ML. Severe Malarial Anemia (SMA) Pathophysiology and the Use of Phytotherapeutics as Treatment Options. In: Current Topics in Anemia. 2018. p. DOI: 10.5772/intechopen.70411.

173. Lafuse WP, Story R, Mahylis J, Gupta G, Varikuti S, Steinkamp H, et al. Leishmania donovani Infection Induces Anemia in Hamsters by Differentially Altering Erythropoiesis in Bone Marrow and Spleen. PLoS One.

2013;8(3):e59509.

174. Awandare GA, Kempaiah P, Ochiel DO, Piazza P, Keller CC, Perkins DJ. Mechanisms of erythropoiesis inhibition by malarial pigment and malaria-induced proinflammatory mediators in an in vitro model. Am J Hematol [Internet]. 2011;86(2):155–62. Available from: http://www.ncbi.nlm.nih.gov/pubmed/21264897

175. Poshyachinda V, Wasanasomsithi M, Panikbutr N, Rabieb T. Ferrokinetic Studies and Erythropoiesis in Malaria. Arch Intern Med. 1969;124(5):623–8.

176. Ribeil JA, Arlet JB, Dussiot M, Cruz Moura I, Courtois G, Hermine O. Ineffective erythropoiesis in β-thalassemia. Sci World J. 2013;394295:10.1155/2013/394295.

177. Meding SJ, Cheng SC, Simon-Haarhaus B, Langhorne J. Role of gamma interferon during infection with Plasmodium chabaudi chabaudi. Infect Immun. 1990;58(11):3671–8.

178. Stevenson MM, Wolf SF, Sher A. IL-12-induced protection against blood-stage Plasmodium chabaudi AS requires IFN-γ and TNF-α and occurs via a nitric oxide-dependent mechanism. J Immunol. 1995;555(5):2545–56.

179. Snowden FM, Bucala R. The Global Challenge of Malaria. The Global Challenge of Malaria. 2014. 203 p.

180. Rottman M, Soudais C, Vogt G, Renia L, Emile JF, Decaluwe H, et al. IFN-γ mediates the rejection of haematopoietic stem cells in IFN-γR1-deficient hosts. PLoS Med. 2008;5(1):e26.

181. Qin Y, Fang K, Lu N, Hu Y, Tian Z, Zhang C. Interferon gamma inhibits the differentiation of mouse adult liver and bone marrow hematopoietic stem cells by inhibiting the activation of notch signaling. Stem Cell Res Ther. 2019;10(1):210.

182. de Bruin AM, Voermans C, Nolte MA. Impact of interferon-γ on hematopoiesis.

Blood [Internet]. 2014;124(16):2479–86. Available from: http://www.bloodjournal.org/content/124/16/2479.abstract

183. Villegas-Mendez A, Strangward P, Shaw TN, Rajkovic I, Tosevski V, Forman R, et al. Gamma interferon mediates experimental cerebral malaria by signaling within both the hematopoietic and nonhematopoietic compartments. Infect Immun. 2017;85(11):e01035-16.

184. Nasr A, Allam G, Hamid O, Al-Ghamdi A. IFN-gamma and TNF associated with severe falciparum malaria infection in Saudi pregnant women. Malar J. 2014;314:doi: 10.1186/1475-2875-13-314.

185. Dumont FJ, Boltz RC. The augmentation of surface Ly-6A/E molecules in activated T cells is mediated by endogenous interferon-γ. J Immunol. 1987;139(12):4088–95.

186. Chen HC, Frissora F, Durbin JE, Muthusamy N. Activation induced differential regulation of stem cell antigen-1 (Ly-6A/E) expression in murine B cells. Cell Immunol. 2003;225(1):42–52.

187. Su Z, Stevenson MM. Central role of endogenous gamma interferon in protective immunity against blood-stage Plasmodium chabaudi AS infection. Infect Immun. 2000;68(8):4399–406.

188. Lees JR. Interferon gamma in autoimmunity: A complicated player on a complex stage. Cytokine. 2015;74(1):18–26.

189. Dallagi A, Girouard J, Hamelin-Morrissette J, Dadzie R, Laurent L, Vaillancourt C, et al. The activating effect of IFN-γ on monocytes/macrophages is regulated by the LIF-trophoblast-IL-10 axis via Stat1 inhibition and Stat3 activation. Cell Mol Immunol. 2015;12(3):326–41.

190. Sui X, Krantz SB, Zhao ZJ. Stem cell factor and erythropoietin inhibit apoptosis of human erythroid progenitor cells through different signalling pathways. Br J Haematol. 2000;110(1):63–70.